



Universidad de Navarra

Facultad de Ciencias

**Characterization of a mouse model for the study
of hepatitis delta virus infection**

Carla Usai



Universidad de Navarra

Facultad de Ciencias

Characterization of a mouse model for the study of hepatitis delta virus infection

Memoria presentada por D^a Carla Usai para aspirar al grado de Doctor por la Universidad de Navarra

El presente trabajo ha sido realizado bajo nuestra dirección en el Departamento de Terapia Génica y Regulación de la Expresión Génica del Centro de Investigación Médica Aplicada (CIMA) y autorizamos su presentación ante el Tribunal que lo ha de juzgar.

Pamplona, 2 de Julio de 2018

Dr. Gloria González Aseguinolaza

Dr. Rafael Aldabe Arregui

This doctoral research has been funded by the Spanish
Ministry of Economy and Competitiveness (MINECO)

Ci sono soltanto due possibili conclusioni: se il risultato conferma le ipotesi, allora hai appena fatto una misura; se il risultato è contrario alle ipotesi, allora hai fatto una scoperta.

(Enrico Fermi)

ACKNOWLEDGMENTS

First and foremost I would like to earnestly thank my supervisors Dr. Gloria González Aseguinolaza and Dr. Rafael Aldabe Arregui, great mentors and wonderful people, for teaching, supporting and motivating me during these four intense years.

I am genuinely grateful to all the members of both groups for the daily support and collaboration, and to the Department of Gene Therapy and Regulation of Gene Expression for the fruitful discussions during seminars and informal conversations.

Thanks to the technology platforms of CIMA and UNAV: Bioinformatics Service, Animal Experimentation, Imaging, Morphology, and Cytometry, whose contributions have been essential for the development of this work.

I would like to express my gratitude to Dr. Urtzi Garaigorta for accepting me in his laboratory at the Scripps Research Institute (San Diego, California), and to his staff for their kindness and invaluable assistance during my stay.

I am also hugely appreciative of Prof. Francis V. Chisari and his kind availability in discussing my experiments and ideas.

Last but not least, I am truly thankful to Prof. Isabel Mérida and her group at the Spanish National Centre for Biotechnology (Madrid, Spain) for encouraging me to undertake a Ph.D. program.

INDEX

ABBREVIATIONS	1
GENERAL INTRODUCTION	9
1. Hepatitis delta virus infection	11
1.1 Hepatitis delta virus	11
1.1.1 Genome structure and replication	12
1.1.2 Viral entry and infection	14
1.1.3 Hepatitis delta antigens	15
1.1.4 Viral particle formation	16
1.2 Pathogenesis and clinical virology of hepatitis delta infection	17
1.2.1 HBV-HDV coinfection and superinfection	17
1.2.2 Chronic and acute hepatitis delta	18
1.2.3 Histopathology	19
1.2.4 Inhibitory effect of HDV on HBV	20
1.3 Current treatments	22
1.4 Novel antiviral therapy	23
1.4.1 Entry inhibitors	23
1.4.2 Farnesylation inhibitors	24
1.4.3 Nucleic acid polymers	25
2. Cellular and animal models	25
2.1 Cell culture models	26
2.2 Animal models	26
3. Adeno-associated vectors for gene transfer	28
3.1 Adeno-associated viruses	28
3.2 Adeno-associated vectors	30
3.2.1 The use of rAAVs to transfer replication-competent HBV genomes	31
4. Immune response against viral infections	32
4.1. The innate immune response	33
4.1.1 Toll-like receptors	35
4.1.2 C-lectin-like receptors	37
4.1.3 RIG-I-like receptors	37
4.1.4 NOD-like receptors	40
4.1.5 AIM-2-like receptors	40

4.1.6 Innate immune cells	41
4.2 The adaptive immune response.....	42
4.2.1 Cross-talk between innate and adaptive immune system: antigen presenting cells	43
4.2.2 Cellular and humoral immunity	43
4.2.3 Immune tolerance	45
4.3 Liver immunology	46
4.3.1 Hepatotropic infections.....	51
OBJECTIVES	57
MANUSCRIPTS	61
Manuscript 1	63
Manuscript 2	85
GENERAL DISCUSSION	113
CONCLUSIONS.....	121
GENERAL BIBLIOGRAPHY	125
Annex 1	145

ABBREVIATIONS

A	adenine
aa	aminoacid
AAP	assembly activating protein
AAV	adeno-associated virus
ADAR1	adenosine deaminase that acts on RNA 1
AGL	antigenic loop
AIM2	absent in melanoma 2
APC	antigen presenting cell
ALR	AIM2-like receptor
ALT	alanine aminotransferase
AST	aspartate aminotransferase
BAFF/BlyS	B lymphocyte stimulator
BCR	B cell receptor
BEC	bile endothelial cells
C	cytosine
CARD	caspase recruitment domain
Cardiff	CARD-containing adapter protein
cccDNA	circular covalently closed DNA of HBV
CCD	coil-coiled domain
CD	cluster of differentiation
CHB	chronic hepatitis B
CHD	chronic hepatitis delta
CRD	carbohydrate recognition domain
CTL	cytotoxic T lymphocyte
CTLA4	cytotoxic T lymphocyte antigen 4
CYP3A4	cytochrome P450 3A4
DAMP	damage-associated molecular pattern
DC	dendritic cell
DHBV	duck hepatitis B virus

DNA	deoxyribonucleic acid
dsRNA	double-stranded RNA
EMA	European Medicines Agency
Enh1	enhancer 1 of HBV
Enh2	enhancer 2 of HBV
ER	endoplasmic reticulum
FADD	Fas-associated protein with death domain
FasL	Fas ligand
FDA	Food and Drug Administration
G	guanine
GPC5	glypican5
HAV	Hepatitis A virus
HBV	Hepatitis B virus
HBcAg	Hepatitis B core antigen
HBeAg	Hepatitis B e antigen
HBsAg	hepatitis B surface antigen
HCC	hepatocellular carcinoma
HDAg	Hepatitis delta antigen
HDV	Hepatitis delta virus
HEV	Hepatitis E virus
HIN	hematopoietic interferon-inducible
HIV	human immunodeficiency virus
HLA	human leukocyte antigen
hNTCP	human Na ⁺ /taurocholate cotransporting polypeptide
HSC	hepatic stellate cells
HSP	heat-shock protein
HSPG	heparin sulfate proteoglycan
I	inosine
IDP	intrinsic disordered protein

IFN	interferon
IgG	immunoglobulin isotype G
IgM	immunoglobulin isotype M
IHC	immunohistochemistry
IKK	inhibitor of nuclear factor kappa-B
IL	interleukin
ILC	innate lymphoid cell
IL-1R	interleukin 1 receptor
IPS-1	IFN β promoter stimulator 1
IRF	IFN regulatory factor
ISG	IFN stimulated gene
ISGF	IFN stimulated gene factor
ISRE	IFN stimulated response element
ITR	inverted terminal repeat
Jak	Janus kinase
kb	kilobase
KC	Kupffer cell
LGP2	laboratory of genetics and physiology 2
L-HBsAg	large hepatitis B surface antigen
L-HDAg	large hepatitis delta antigen
LPS	lipopolysaccharide
LRR	leucine-rich repeated
LSEC	liver sinusoidal endothelial cell
MAVS	mitochondrial antiviral signaling protein
MDA5	melanoma differentiation-associated gene 5
mDC	myeloid dendritic cell
M-HBsAg	medium hepatitis B surface antigen
MHC	major histocompatibility complex
MxA	human myxovirus resistance gene A

NAP	nucleic acid polymer
NES	nuclear export signal
NFκ-B	nuclear factor kappa-B
NK	natural killer cell
NKT	natural killer T cell
NLR	NOD-like receptor
NLS	nuclear localization signal
NOD	nucleotide-binding oligomerization domain
NTCP	Na ⁺ /taurocholate cotransporting polypeptide
NUC	nucleot(s)ide analogues
OAS	2'-5'-oligoadenylate synthase
PAMP	pathogen-associated molecular pattern
PBMC	peripheral blood mononuclear cells
pDC	plasmacytoid dendritic cell
PD-1	programmed death 1
PD-L1	programmed death 1 ligand 1
PEGIFNα-2a	pegylated interferon alpha
PFA	paraformaldehyde
PGN	peptidoglycan
PHH	primary human hepatocytes
PTM	post-translational modification
PRR	pattern-recognition receptor
rAAV	recombinant adeno-associated virus
RBD	RNA binding domain
RIG-I	retinoic acid-inducible gene I
RIP1	receptor-interacting protein 1
RLR	RIG-I-like receptor
RNA	ribonucleic acid
RNP	ribonucleoprotein

RSV	respiratory syncytial virus
S-HBsAg	small hepatitis B surface antigen
S-HDAg	small hepatitis delta antigen
siRNA	small interfering RNA
ssRNA	single-stranded RNA
STAT	Signal transducers and activators of transcription
T	thymidine
TANK	TRAF family member-associated NF-kappa-B activator
TBF	TRAF-binding motif
TBK1	TANK-binding kinase 1
TCR	T cell receptor
T _{FH}	follicular T helper cell
T _H	T helper cell
TIR	Toll/IL-1R homology domain
TNF	tumor necrosis factor
TRADD	tumor necrosis factor receptor type-1-associated death domain protein
TRAF	tumor necrosis factor receptor-associated factor
T _{reg}	regulatory T cell
U	uracil
UTR	untranslated region
VISA	virus-induced signaling adapter
WMHBV	woolly monkey hepatitis B virus
WHV	woodchuck hepatitis virus
5'-ppp	5'- triphosphate

GENERAL INTRODUCTION

1. Hepatitis delta virus infection

1.1 Hepatitis delta virus

Hepatitis delta Virus (HDV) is a negative sense single-stranded RNA (ssRNA) virus¹ that belongs to the *Deltaviridae* family, genus Deltavirus. It is a defective virus depending on its helper hepatitis B virus (HBV) for virion assembly².

The first breakthrough in HDV was the observation of a new antigen-antibody system associated with HBV infection (delta antigen, δ) in 1977 by the group of Dr. Rizzetto³.

Later on, the same group reported the association of a low molecular weight RNA, smaller than the genomes of any known RNA virus but larger than plant viroids (1.7 kb), advancing the hypothesis of a new infective agent requiring helper functions from HBV^{4,5}. Only a decade after these initial observations, the hepatitis delta antigen (HDAg) was identified as the expression product of a RNA virus^{6,7}.

Eight different genotypes of the hepatitis delta virus have been characterized to date, each of them showing a specific geographic distribution with the exception of the ubiquitous clade HDV-1 [**Fig. 1**]. HDV-2 is found in Japan, Taiwan and Russia, HDV-3 in the Amazonian region of South America, HDV-4 in Taiwan and Japan, HDV-5, HDV-6, HDV-7 in Africa and HDV-8 in Africa and in Europe (in this latter case limited to African origin patients)^{8,9}.

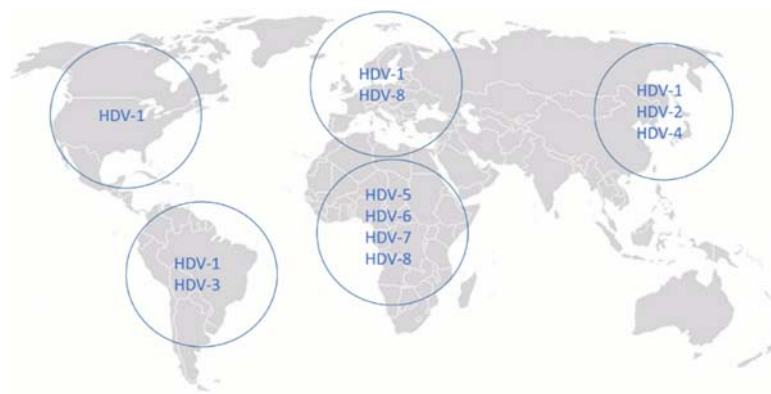


Fig. 1 Geographic distribution of HDV genotypes.

1.1.1 Genome structure and replication

The hepatitis delta virion is an enveloped 36 nm spherical particle⁴. The outer coating contains the three surface antigens of HBV (small, S-, medium, M-, and large, L-HBsAg), and host membrane-derived lipids. The inner ribonucleoprotein (RNP) consists of the negative circular genomic RNA and about 200 molecules of two different isoforms of the delta antigen (small, S-, and large L-HDAg) per genome^{4,10} [Fig. 2]. In the infected cell, it is also possible to detect a low amount of a complementary circular RNA molecule (called anti-genome) and a smaller linear positive-sense polyadenylated RNA of 0.8 kb in length. Intracellularly, most of the monomeric RNAs are in a circular conformation, while only about 5% is linear^{6,11}.

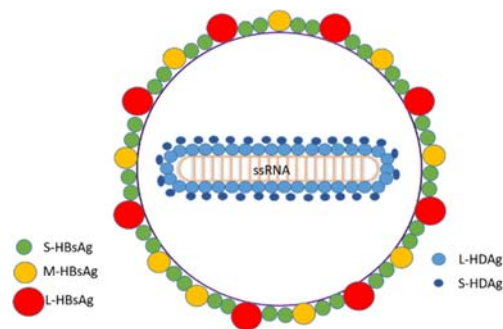


Fig. 2 Schematic representation of HDV viral particle and its components¹²

The genomic RNA is about 1680 nucleotides long with a high guanine (G) and cytosine (C) content (60%) that allows the formation of a stable secondary rod-like structure, in which 71% of the nucleotides are base-paired. These characteristics make HDV more similar to viroids that cause pathologies in plants than to animal viruses⁶. However, HDV RNA is longer than viroid RNA and encodes structural proteins, whereas viroid RNA does not encode any protein.

Like plant viroids, HDV replicates through a rolling circle mechanism carried out by the host RNA polymerase/s and it requires the processing of the longer-than-one-genome replicative intermediates into unit-length molecules. The first step in HDV replication is

the synthesis of multimeric copies of the anti-genomic RNA by the DNA-dependent RNA-polymerase II in the nucleus^{13,14}. Subsequent cycles of this reaction generate multiple copies of both genomic and anti-genomic multimers. An autocatalytic cleavage mediated by ribozymes that are included in both the genomic and anti-genomic strands produces monomeric molecules of either polarity¹⁵⁻¹⁸. A yet uncharacterized ligation factor converts linear monomers to circular genomes and antigenomes.

The only functioning open reading frame resides in the anti-genome. It encodes the smaller isoform of the delta antigen (S-HDAg); this sequence is copied in the nucleus into a 5'-capped 3'-polyadenylated 0.8 kb long RNA molecule, that is transported in the cytosol and transcribed into a protein of 195 amino acids⁷. In later stages of the infection, the viral antigenome is edited in position 1012 by the host adenosine deaminase that acts on RNA (ADAR1) within the nucleus. The adenosine (A) in this position is deaminated into an inosine (I), which in turn is transcribed as a guanosine. Such transition transforms the original stop codon UAG in a tryptophan codon UGG. The result of editing is the extension of the open reading frame and the transcription and translation of a 214 amino acid-long form of the hepatitis delta antigen (L-HDAg)¹⁹⁻²¹ [Fig. 3]. Edited forms accumulate during infection to a maximum of 30% of the total amount of genome and antigenome²¹.

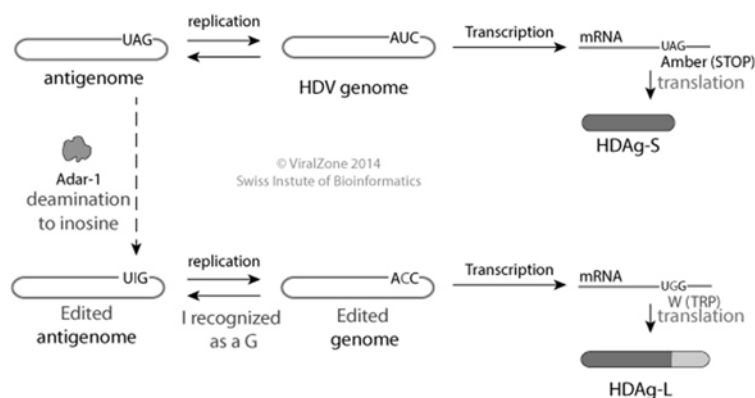


Fig. 3 Schematic representation of HDV RNA editing by the host enzyme ADAR1 (taken from viralzone.expasy.org)

Virions can contain either unedited or edited genome molecules, but the latter produces an ineffective infection since the S-HDAg is necessary for viral replication.

1.1.2 Viral entry and infection

As the HDV envelope is composed of the HBV surface proteins (HBsAg), the two viruses share the same hepatotropism and species-specificity by exploiting the same entry mechanisms. The three HBsAg share the C-terminal portion (corresponding to the S protein) and differ in their N-termini²² [Fig. 4]. The pre-S1 domain of the L-HBsAg specifically interacts with the Na⁺/taurocholate cotransporting polypeptide (NTCP)²³, encoded by the *SLC10A1* gene [Fig. 5], a bile salt transporter expressed in the basolateral membrane of the hepatocytes^{24,25}, and the residues 157 to 165 were identified to be critical for binding and entry for both HBV and HDV infection. Differences in residues within this motif between homologous NTCP in mammals account for the human specificity of these pathogens²³.

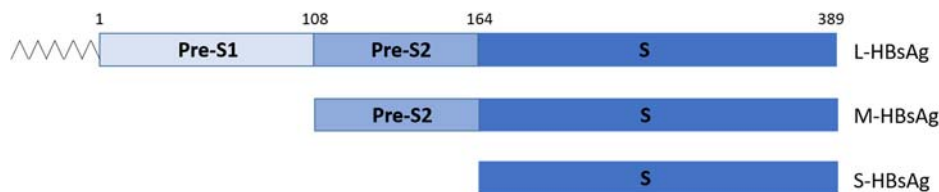


Fig. 4 Schematic representation of HBV envelope proteins.

HBV and HDV entry in the hepatocyte is mediated by a multistep process [Fig. 5]. The first event is the “attachment” of the viral particle to the surface of the target cell. It has been demonstrated *in vivo* and *in vitro* that HSPGs (heparan sulfate proteoglycans) bind to the preS2 domain of the L-HBsAg and to the antigenic loop (AGL) in the S domain^{26–29}. In particular, GPC5, a member of the glypican family, a group of six HSPGs highly expressed in the liver, has been recently identified as the major common

entry factor of HBV and HDV, being responsible for the initial attachment of both viruses at the cellular surface and contributing to their hepatotropism³⁰. Attachment is followed by the highly specific step in which the myristoylated N-terminal domain of preS1 interacts with human NTCP (hNTCP).

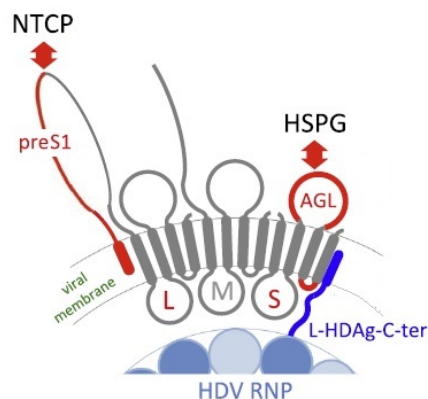


Fig. 5 Schematic representation of the interactions between HDV RNP, HBsAgs and host cellular surface components (modified from³¹).

1.1.3 Hepatitis delta antigens

S-HDAg and L-HDAg share several functional domains within the common amino acid sequence, nevertheless they play different roles in the viral cycle.

S-HDAg is produced in the first stages of the viral cycle and is necessary for the initiation of viral replication and for HDV RNA accumulation. L-HDAg is synthesized later during infection and its 19 extra amino acids confer unique functional properties, such as inhibition of viral replication and viral assembly^{32,33}.

Both isoforms contain a nuclear localization signal (NLS) (aa 66-75)³⁴, a coil-coiled domain (CCD) or dimerization domain (aa 12-60), and an RNA binding domain (RBD) (aa 97-146)³⁵. The L-HDAg also contains a nuclear export signal (NES) within its extra sequence³³[Fig. 6].

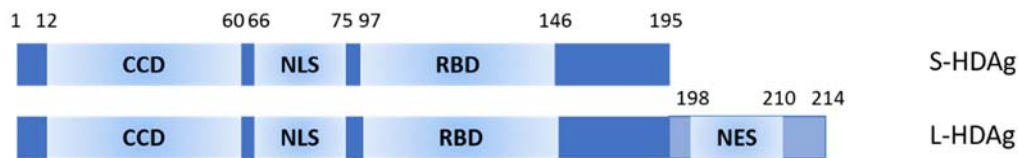


Fig. 6 Schematic representation of S- and L-HDAg and their functional domains.

Both delta antigens undergo post-translational modifications (PTMs) catalyzed by host enzymes (phosphorylation, methylation, and sumoylation). Some of them are shared between S- and L-HDAg, however different patterns of phosphorylation have been observed for the two isoforms, accounting for their different biological functions³⁶. On the other hand, prenylation on a Cxxx motif embodied in the 19 C-terminal aa of L-HDAg (Cys211) is unique for this isoform and necessary for its interaction with HBsAg^{37,38}. Moreover, it has been shown that this PTM enhances the dominant negative activity of L-HDAg on HDV replication^{39,40}.

S-HDAg belongs to the intrinsically disordered protein (IDP) class, characterized by a broad spectrum of interaction and functional versatility. IDPs are mainly nucleic acid binding proteins with high multimerization capability, features present in S-HDAg. So far, more than 100 human proteins have been shown to interact to a various extent with S-HDAg⁴¹.

1.1.4 Viral particle formation

HDV RNA and HDAGs interact with each other to form the RNP; it has a diameter of about 20 nm, and its rod shape is mediated by the dimerization of HDAGs through their CCD, followed by oligomerization^{42,43}. The NES on L-HDAg allows RNP export to the cytoplasm and viral envelope formation [**Fig. 7**]. The HDV-interacting motif consists on W196, W199, Y200 and W201 in the S domain of HBsAg (residues conserved among all *Orthohepadnaviruses*)⁴⁴; nevertheless, L-HBsAg is necessary for infectivity since it is the myristoylated pre-S1 domain that interacts with hNTCP.

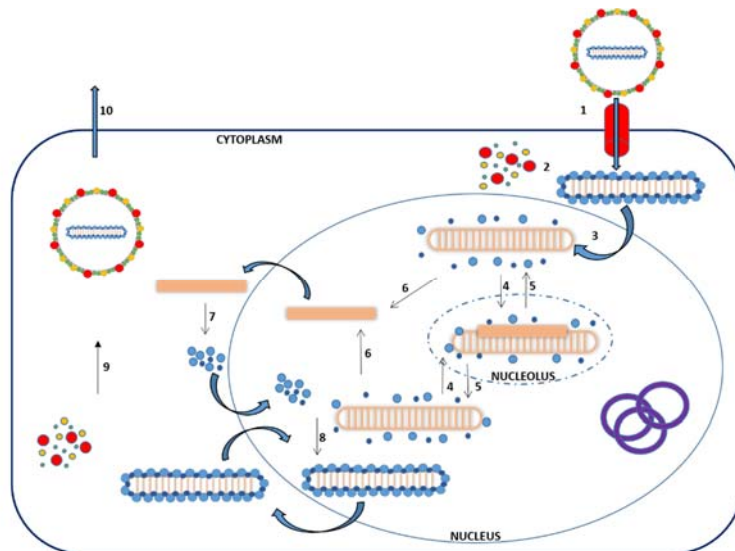


Fig. 7 Schematic representation of HDV replication cycle¹². (1) Binding to NTCP on human hepatocyte; (2) uncoating; (3) translocation of the ribonucleoprotein into the nucleus; (4) transcription of the anti-genome in the nucleolus; (5) production of genomic RNA in the nucleoplasm; (6) transcription of the mRNA; (7) translation of HDsAg; (8) ribonucleoparticle assembly; (9) association of HBsAg and virion production in the cytoplasm; (10) virion release.

1.2 Pathogenesis and clinical virology of hepatitis delta infection

1.2.1 HBV-HDV coinfection and superinfection

Even though HDV genome replication and RNP formation are HBV independent, HDV can though productively complete its infective cycles only in hepatocytes expressing HBV envelope proteins. In natural infection, this occurs in HBV infected cells, in which the circular covalently closed DNA (cccDNA) is synthesized. HDV is, therefore, an obligated HBV satellite virus that can either infect naïve patients simultaneously with HBV (coinfection), or chronically infected HBV carriers (superinfection). In these scenarios, HDV causes the most severe form of viral hepatitis with a twofold higher risk of developing cirrhosis, a threefold higher risk of developing hepatocellular carcinoma (HCC), and a twofold increased mortality in comparison with HBV monoinfection⁴⁵⁻⁴⁷. 350 million people worldwide are HBV carrier, and approximately de 5% of them have been exposed to HDV, with a total of 15-20 million patients. In the 95% of cases, HBV-

HDV coinfection is self-limiting, as in HBV acute monoinfection, although a more severe clinical course is possible. Superinfection causes severe acute hepatitis and often proceeds to chronicity (80% of patients). The severity of the pathology is influenced by the HDV serotype⁴⁸.

1.2.2 Chronic and acute hepatitis delta

Acute hepatitis delta is commonly caused by HBV-HDV coinfection and often clinically indistinguishable from acute HBV infection, with the appearance of the characteristic serum alanine aminotransferase (ALT) and aspartate aminotransferase (AST) elevation; frequently two peaks of serum ALT and AST are observed. It is usually transient and self-limiting (>95% of cases), but a more severe clinical course is possible with an increased risk of liver failure and massive hepatocyte necrosis, leading to death in 80% of patients. Diagnostic markers are the presence of HBsAg in serum, HDV genomic RNA and a high-titer of α -HBcAg IgM; the latter is absent in chronic hepatitis B (CHB), thus allowing to distinguish between acute coinfection and superinfection of a chronic HBV carrier⁴⁵ [**Table 1**].

Chronic hepatitis delta (CHD) follows superinfection in 80% of cases, with a broad range of clinical manifestations, from asymptomatic cases to rapidly progressive hepatitis, but it usually exacerbates the preexisting liver disease. Diagnostic markers are elevated ALT and AST in serum, persistent HDV RNA in serum and α -HDAg IgM (non specific). α -HBcAg IgM is absent, and α -HDAg IgG increases in the late phase of infection. Persistent HDV replication enhances the progression of liver disease to cirrhosis and increases the risk of HCC and mortality. Therefore, data about the exact impact of HDV infection on the rate of these outcomes though controversial⁴⁵.

	Coinfection	Superinfection
HBV infection	Acute	Chronic
Outcome	Usually self-limiting (>95% of cases)	Usually persistent
α-HBcAg IgM	Positive, high-titer	Negative
α-HBsAg	Positive (convalescence phase)	Negative
HDV infection	Acute	Acute or chronic
Outcome	Usually self-limiting (>95% of cases)	Usually persistent (~80% of cases)
Serum HDAg	Early and short-lived	Transient (undetectable because of complexing with antibodies)
Liver HDAg	Positive and short-lived	Positive
Serum HDV RNA	Early positive and transient	Early positive and persistent
α-HDAg IgG	Late and low-titer	Rapidly increasing titers and persistent
α-HDAg IgM	Positive, transient	Positive, high titer

*Table 1 Comparison between the clinical and diagnostic features of HDV coinfection and superinfection*⁴⁵.

1.2.3 Histopathology

Chronic hepatitis, either infectious or not, is characterized by typical lesions, such as interface hepatitis, which is also referred as to lymphocytic piecemeal necrosis (characterized by the replacement of the limiting plate by inflammatory infiltrate) [**Fig. 8 A**], cytoplasmic dissociation (swelling of the hepatocytes with cytoplasmic rarefaction) [**Fig. 8 B**], bridging necrosis (linking the portal and the lobular areas) [**Fig. 8 C**] often followed by fibrosis, and apoptosis.⁴⁹

Specific markers of HBV infection are the presence of “ground-glass” cells containing HBsAg, and of “sanded” nuclei with granular inclusions due to the accumulation of HBcAg [**Fig. 8 D**]. Both HBsAg and HBcAg can be detected by immunohistochemistry (IHC) and show different patterns: the first being cytoplasmic and the latter having a

nuclear distribution. The presence of HBcAg in the cytoplasm correlates with liver inflammation, membrane staining of HBsAg indicates active viral replication⁵⁰ [Fig. 8 E]. Chronic HDV is indistinguishable from CHB; HDAg location can be determined by IHC, being generally nuclear and occasionally cytoplasmic⁵¹ [Fig. 8 F].

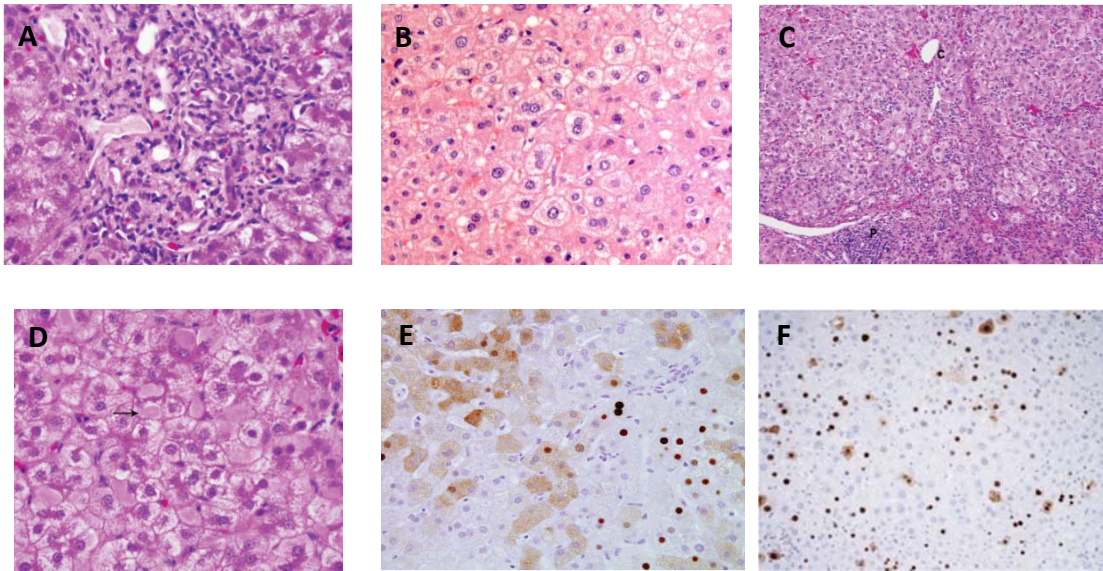


Fig. 8 Histopathological features of hepatitis delta infection. A: lymphocyte piecemeal necrosis (600X); B: cytoplasmic swelling (400X); C: Bridging necrosis (200X); D: sanded nuclei (600X); E: HBsAg staining (200X)⁵⁰; F: HDAg staining (20x)⁵².

1.2.4 Inhibitory effect of HDV on HBV

It is known that in patients HBV replication is inhibited during the acute phase of HDV infection, and that the two viruses can have fluctuating patterns of predominance over time⁵³⁻⁵⁵. The exact mechanisms of the inhibitory effect of HDV on HBV is still unknown, but it is thought to be independent of the adaptive immune system since the phenomenon is reproducible *in vitro*⁵⁶⁻⁵⁸.

Inhibition of HBV replication can be due to a direct interaction between the two viruses inside the cells: HDV needs HBsAg for packaging and release, and it has been speculated that HDV is able to repress HBV replication maintaining surface proteins production, for instance competing for RNA pol-II recruitment (necessary for cccDNA replication)⁵⁹. Both L- and S- HDAG are able to repress the function of the two HBV enhancers (Enh1 and Enh2) that, along with four promoters, regulate HBV replication⁵⁷

[Fig. 9]

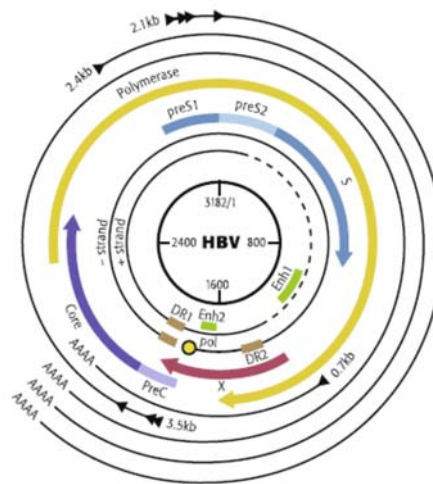


Fig. 9 Schematic representation of HBV genome, transcripts, and proteins⁶⁰.

Furthermore, HDV can indirectly hinder HBV replication by inducing interferon-stimulated genes (ISG) and the SRE pathway, that regulates numerous genes involved in cell growth and differentiation among other things⁶¹. Moreover, HDAGs induce MxA expression, reverting the inhibitory effect of HBV on the same gene^{62,63} [Table 2].

Direct interactions between HBV and HDV	
Interaction	Effect
HDAg – HBV Enh1/2	HBV suppression
HDV interaction with host factors	
Interaction	Effect
L-HDAg- RNA-polymerase II	HBV suppression
HDV-interferon stimulated genes	Innate immune response, HBV suppression
S- and L-HDAg – MxA	Innate immune response, HBV suppression
L-HDAg – SRE pathway	HBV suppression

Table 2 Interactions between HDV and HBV or the host cell machinery responsible for HBV inhibition. Adapted from⁵⁹.

1.3 Current treatments

Due to the peculiar life cycle of HDV and its strong dependence on host cell factors, the development of direct antiviral treatment is challenging.

Since HDV does not encode any viral RNA polymerase, the only viral targets available are the HDAGs and the ribozyme. Inhibitors of the cellular DNA-dependent RNA-polymerase would lead to severe adverse effects, and thus cannot be taken into consideration as therapeutic agents. Specific inhibition of the ribozyme activity has been achieved *in vitro* with small molecules as well as with small interfering RNA (siRNA) strategies, avoiding multimeric RNA cleavage and functional genomic and anti-genomic RNA production^{64,65}.

One of the strategies used to date is the suppression of HBV replication and the induction of a strong immune response against the helper virus, with the aim of developing a protective titer of α -HBsAg antibodies. Treatments against HBV infection are based on the pegylated form of IFN α (PEGIFN α -2a) and nucleos(t)ide analogs (NUC). Unfortunately, these treatments are effective only in a small percentage of HDV patients, with adverse effects and relapse after the end of the treatment^{66,67}. No approved

treatment specific for HDV infection is available. New antiviral therapies under development target either viral or cellular factors, trying to inhibit the attachment and entry of the virus, its replication or the assembly and release of virions.

1.4 Novel antiviral therapy

1.4.1 Entry inhibitors

The discovery of hNTCP as a specific receptor for HBV and HDV opened the door to the development of entry inhibitors. Myrcludex B is a myristoylated synthetic peptide of 47 aa derived from the S1 domain of HBsAg, that inhibits viral entry by interfering with binding to hNTCP, thus avoiding reinfection of regenerating hepatocytes and, hopefully, leading to the elimination of the virus with time. This molecule showed efficiency at IC₅₀ ~8 nM *in vitro*⁶⁸ and in humanized mice^{69,70}, and it is currently tested in a phase Ib/IIa clinical trial for the treatment of CHD patients, alone or in combination with PEGIFN α -2a, and in comparison to the approved treatment with PEGIFN α -2a⁷¹. Preliminary results show that Myrcludex B is able to decrease HDV viremia and that the antiviral effect is enhanced in the combination with PEGIFN α -2a. Moreover, treatment with Myrcludex B alone induced a normalization of ALT serum levels, indicating a probable reduction of the *de novo* infection rate and of the subsequent turnover of the hepatocytes. Interestingly, this molecule is showing antiviral efficiency at concentrations that do not interfere with the physiological role of hNTCP as a bile salt transporter⁷¹.

Recently, other NTCP inhibitors able to reduce HBV and HDV entry have been identified in an *in vitro* screening of 1280 clinically applied compounds⁷². Two cyclosporin A-derived compounds with no immunosuppressive activity also showed the ability to block HBV entry *in vitro* in a dose-dependent manner without affecting bile

acid uptake; moreover, other NTCP ligands capable to inhibit bile acids transport cannot block HBV infection, indicating that the molecular determinants of the two functions do not overlap⁷³. The same group also identified plant-derived molecules of the proanthocyanin family, that act as entry inhibitors for HBV by directly binding to L-HBsAg rather than to the host cells, thus not interfering with NTCP transporter function⁷⁴. These compounds have been tested only on HBV *in vitro*, and results may be possibly extended to similar HDV infection models.

1.4.2 Farnesylation inhibitors

Compounds able to directly inhibit HDAg functions are still unknown, mainly due to the scarcity of suitable model systems able to reproduce the complete viral cycle. Prenylation of the last four C-terminal aa of L-HDAg is known to be necessary for the interaction with HBsAg and virion assembly^{37,38}. That is why prenylation inhibitors, initially selected for their antineoplastic activity, are being tested as antiviral agents. First, *in vitro* efficacy of farnesyltransferase inhibitors was assessed on HDV-like particle-producing cell lines, in which post-translational modification of L-HDAg, but not its translation, was prevented, with a significant reduction of virus-like particle production⁷⁵.

A proof-of-concept study has assessed the safety, tolerability, and efficacy of the farnesyltransferase inhibitor Lonafarnib, previously used as an anticancer drug, during four weeks of treatment. Preliminary results show a significant reduction of HDV viremia that correlates to Lonafarnib serum concentration, even though virological rebound was observed after stopping the treatment. No mutation of L-HDAg was detected in the nonresponders, and gastrointestinal side effects, already observed in Lonafarnib treatment for other purposes, were recorded⁷⁶. A more recent clinical trial investigated optimal Lonafarnib regimens, exploring different doses, combination with

PEGIFN α -2a or inhibitors of CYP3A4 (the predominant mediator of Lonafarnib metabolism⁷⁷), and different treatment durations. Low doses of Lonafarnib in combination with a CYP3A4 inhibitor show a greater antiviral activity with less gastrointestinal effects than Lonafarnib monotherapy, and similar results were obtained in combination with PEGIFN α -2a⁷⁸.

The added value of these molecules is that they do not exert selective pressure on the virus, since their effect is on a post-transcriptional modification; on the other hand, the fact that they target cellular enzyme can induce adverse effects in the patients.

MyrcludexB and Lonafarnib received orphan drug status from FDA and EMA.

1.4.3 Nucleic acid polymers

Nucleic acid polymers (NAPs) have been demonstrated to inhibit HIV-1 and HCV entry in a sequence-independent and size-dependent manner⁷⁹. Antiviral activity of this class of compound was shown with duck hepatitis B virus (DHBV) both *in vitro* and *in vivo*, having entry- and post-entry-inhibitor properties^{80,81}. Recent studies have assessed the safety and efficacy of NAPs in CHB patients, and preliminary results are available about their antiviral activity against HDV, even though the molecular mechanism is still unknown⁸²⁻⁸⁴.

2. Cellular and animal models

The host range of HDV is limited to organisms that support the replication of HBV or related Hepadnavirus that can act as a helper, such as the woolly monkey hepatitis B virus (WMHBV) and the woodchuck hepatitis virus (WHV)⁸⁵. Chimpanzees, woodchucks and *Tupaia bulangeri* have been used to develop *in vitro* and *in vivo* infection systems.

2.1 Cell culture models

The most physiological *in vitro* system for the study of HBV and HDV infection are primary human hepatocytes (PHH) since the human is the exclusive natural host of both viruses, and because they maintain cell polarization and have a competent cell-intrinsic innate immune system⁸⁶. However, scarce availability, short lifespan and rapid *in vitro* dedifferentiation with the subsequent loss of hNTCP expression, strongly limit their application.

Alternative systems are provided by hepatoma cell lines: HepaRG, Huh7, and HepG2 are the most commonly used. HepaRG is a cell line derived from a tumor of a patient with HCC associated with HCV infection, maintaining hepatic functions and a transcriptomic profile very similar to that of PHH; moreover, after a differentiation process, HepaRG cells can be differentiated into hepatocyte-like cells and support HBV and HDV infection⁸⁷. Nevertheless, infectivity is low, and the long differentiation process required can lead to high variability between experiments.

Huh7 and HepG2 are immortalized cell lines that have lost most of the hepatocyte-specific function; they support replication of HBV and HDV but not virus entry, because of low NTCP expression levels⁸⁸. Cell lines over-expressing hNTCP derived from Huh7 and HepG2 have been used to test entry inhibitors⁸⁹.

2.2 Animal models

Humans are the only natural host for HDV; however, all the species that support HBV (e.g. chimpanzee⁹⁰) or related viruses of the Hepadnaviridae family, able to supply helper functions, are susceptible to HDV infection and propagation⁹¹. This has permitted to extend the host range of HDV to woodchucks (natural hosts for the woodchuck hepatitis virus, WHV)^{92,93}, woolly monkeys (natural hosts for the woolly

monkey hepatitis B virus, WMHV), and the tree shrew *Tupaia bulangeri* (experimentally infected with both HBV and WMHV)^{85,94}. These natural models of HDV infection, however, have limitations including their large size and difficult handling, genetic variability and ethical considerations.

The mouse is the most commonly used animal model for the study of human diseases, and several attempts of experimental HDV infection have been performed.

Transgenic mice expressing L- and S-HDAg⁹⁵ or carrying a replication-competent HDV genome dimer⁹⁶ were developed in the early nineties in order to unveil the basis of the exacerbation of the liver pathology associated to HDV. In the first model, no liver damage was observed, while in the second one genomic and antigenomic RNA, as well as S- (but not L-) HDAg, were detected in several tissues (with a strong prevalence in muscle) without any evidence of liver damage or inflammation. However, in these animals, the liver cells that expressed the most HDAg were epithelial cells of bile ducts, and only a few hepatocytes expressed a high level of HDAg. The replication of HDV in other organs suggested for the first time that the tissue-specificity of HDV was dependent on the HBV-derived envelope. Interestingly, the tissue in which maximal HDV replication and HDAg expression occurred was the muscle, and mild muscle atrophy was observed.

Humanized mice are another useful tool for the study of HDV: liver damage is induced in immune-deficient mice followed by engrafting of human hepatocytes, susceptible to HBV and HDV infection^{97,98}. Different groups have taken advantage of this model to study HDV entry, replication and spreading *in vivo*, and the suppression of HBV replication during HDV coinfection or superinfection was also detected, as already observed in patients^{99,100}.

Transgenic and humanized mouse have helped to elucidate some of the aspects of HDV virology, however, none of these models permits the study of the interaction between the virus and the host immune system. (The animal models mentioned above, described before 2015, are extensively reviewed in **Annex 1.**)

More recently, based on the identification of hNTCP as the receptor for HBV and HDV, a mouse model expressing the human version of the transporter was developed. hNTCP-transgenic mice are able to support a transient single-round HDV infection of about 3% of hepatocytes in an age-dependent manner¹⁰¹. The same group was able to make both neonate and adult mice susceptible to HDV infection by modifying three residues of the mouse NTCP, replacing them with the corresponding human aa (H84R, T86K, and S87N)¹⁰². Interestingly, mice with the modified receptor are not able to support HBV infection, so that co-infection or super-infection cannot be studied. Moreover, the short-term transient infection achieved in these two models does not lead to liver damage, representing an important limitation to study HDV-related liver pathology.

3. Adeno-associated vectors for gene transfer

3.1 Adeno-associated viruses

Adeno-associated virus (AAV) is a small non-enveloped icosahedral virus, member of the *Parvovirus* family. It was detected for the first time as a contaminant in adenovirus preparations and it is ascribed to the *Dependovirus* genus because it relies on a helper virus (adenovirus, herpes virus) to complete its replication cycle. AAV has a single-stranded DNA genome of approximately 4,6 kb composed of only two genes (*rep* and *cap*), which are flanked by two 145 nucleotide-long inverted terminal repeats (ITR), that allow correct encapsidation of the genetic material^{103,104}.

The *rep* gene encodes the structural proteins rep78, rep68, rep 52 and rep40 necessary for viral replication, packaging, transcriptional replication and site-specific integration. The *cap* gene encodes the three capsid proteins VP1, VP2, and VP3, which form the viral capsid at a ratio of 1:1:10, respectively^{105–108}. An alternative open reading frame inside the *cap* gene and with a non-conventional CUG start codon, encodes an assembly activating protein (AAP), which is necessary for viral assembly but that is not present in the mature capsid¹⁰⁹ [Fig. 10].

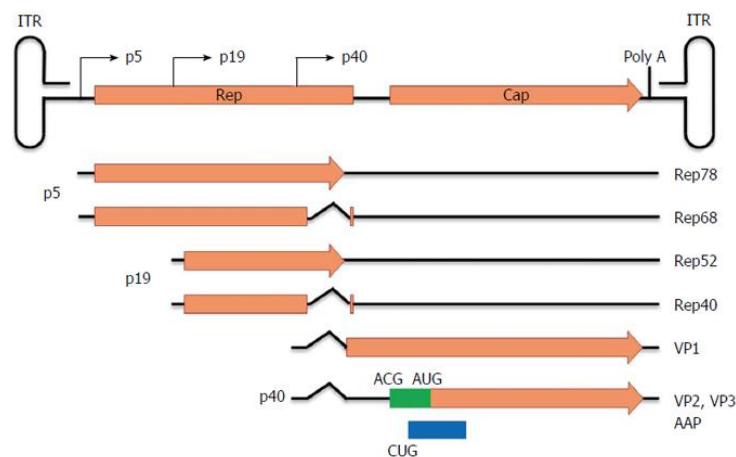


Fig. 10 AAV genome organization. Gene expression is driven by the p5, p19 or p40 promoters. VP2 translation starts from a weaker start codon (ACG) to maintain low proteins levels while a highly efficient start codon (AUG) drives VP3 translation. ITR: inverted terminal repeat, poly(A): poly-adenylation signal¹⁰⁹.

After infection of the host cell, AAV can enter either a lytic or a lysogenic phase of its life cycle. In the presence of a helper virus, the lytic phase is established, which allows productive infection and virion production¹¹⁰. If AAV infects the host cell alone, it enters a lysogenic stage integrating into the AAVS1 locus in human chromosome 19 (q13.4)^{103,111}. If a latently AAV-infected cell is super-infected by a helper virus, de provirus can be rescued from the host genome and the lytic phase can initiate¹⁰³. AAV replication can be induced by a variety of genotoxic agents or cell cycle perturbations¹¹²; however, it has been demonstrated that, at least *in vitro*, AAV replication in the absence of a helper virus cannot occur a significant levels¹¹³.

AAV is not associated with any pathology in humans, and to date, 12 natural serotypes have been isolated (AAV1 to AAV12). Serotypes are determined by variation in their capsid structures that cause different antigenicity and tropism¹¹⁴.

3.2 Adeno-associated vectors

Viral vectors have been used for *in vivo* gene transfer by replacing the viral genes, responsible for replication and pathogenicity, with exogenous sequences of interest [Fig. 11]. The process called “transduction” is a non-replicative infection exploited to delivery heterologous genetic information to the target cell¹¹⁵.

Recombinant adeno-associated viral vectors (rAAV) are generated replacing the *rep* and *cap* genes between the ITRs with the exogenous sequence [Fig. 11] that must not exceed 5 kb in length. rAAVs are produced by co-transfection in mammalian cells of a plasmid carrying the *rep* and *cap* genes of the chosen serotype (helper plasmid), and a plasmid carrying the sequence of interest flanked by the ITRs. The helper plasmid lacks the ITRs to avoid the packaging of replication-competent viruses^{103,114,116}.

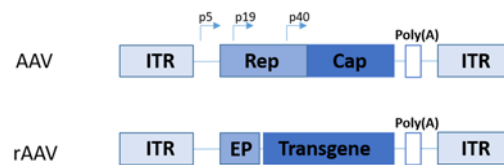


Fig. 11 Schematic representation of an adeno-associated virus (AAV) and an adeno-associated viral vector (rAAV). ITR: inverted terminal repeat, poly(A): poly-adenylation signal; EP: eukaryotic promoter.

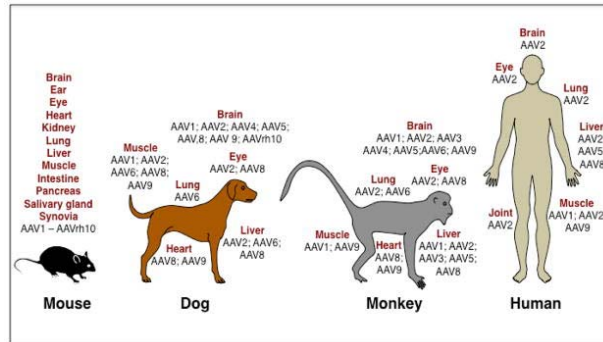


Fig. 12 Use of natural and recombinant AAV serotypes in humans and animal models²⁰⁰.

Integration of rAAV after administration is very infrequent due to the absence of the Rep78 protein, which is necessary for the process, and the transferred DNA is maintained as an episome^{103,117,118}. rAAVs, are available as different serotypes with tissue-specificity, and are able to efficiently transduce dividing and non-dividing cell-types; moreover, new engineered serotypes have been developed to reach a broad range of tissue and to avoid pre-existing immunity^{119,120}. For these reasons, and because of their only low to mild immunogenicity, rAAVs are currently successfully used in gene therapy¹²¹ [Fig. 12].

3.2.1 The use of rAAVs to transfer replication-competent HBV genomes

During the last decade, rAAVs have been used to develop mouse models of HBV infection, in which the viral vector acts as a shuttle to deliver the genome of HBV into the mouse hepatocytes^{122,123}.

The first immunocompetent model of HBV infection was achieved by co-injecting intravenously in adult mice two rAAVs each one carrying approximately half of HBV genome flanked by ITRs from AAV serotype 2 and packaged in a serotype 8 capsid. Co-administration of the two vectors resulted in liver-specific transduction, and tail-to-tail recombination of the rAAVs allowed the formation of HBV genomes, and the production of HBV antigens in four different strains of immunocompetent mice (Balb/c,

C57BL/6, FVB, ICR). HBV viremia, HBsAg and HBeAg were detectable in the sera of injected mice, and hepatocytes stained positive for both HBcAg and HBsAg during 16 weeks. At the end of the experimental period C57BL/6 mice developed liver tumors and histological features similar to those of HCC human patients¹²².

Another mouse model took advantage of adult mice transgenic for the human leukocyte antigen (HLA) A2/DR1, which received intravenously a rAAV carrying 1.2 copies of HBV genome flanked by ITRs from AAV serotype 2 and encapsidated in a serotype 8 capsid. This procedure allowed a liver-specific transduction, which resulted in persistent levels of HBsAg and HBeAg in the serum of injected mice associated with detectable HBV viremia (at least during 56 weeks post-infection), a pattern similar to persistent HBV infection in humans. Moreover, HBcAg as well as HBV transcripts and DNA intermediates were detectable in the liver of injected animals. In this mouse model, however, cccDNA was not detectable in the nucleus of infected hepatocytes¹²³. More recently, cccDNA was detected in the liver of C57BL/6 mice injected with the same vector¹²⁴.

4. Immune response against viral infections

The immune system is a complex organization of cells and molecules with the function of protecting the organism from pathogens or the development of cancer. The invading pathogens (fungi, bacteria, viruses and microorganisms) have to overcome anatomic and physiologic barriers (keratin, enzymes, mucus, ciliary movement, controlled pH), and to face two different levels of defense: innate immunity and adaptive immunity. Innate immunity is an early non-specific mechanism put into effect immediately after encountering the pathogen, and it does not have immunological memory. On the other hand, adaptive (acquired) immunity is a late antigen-specific mechanism characterized

by immunological memory that enables the host to mount a specific, faster and stronger response upon repeated exposures to the same antigen. Innate and adaptive immunity are complementary, and failure of one of the three defense levels described above hinders an efficient protection of the organism^{125,126}.

4.1. The innate immune response

The innate immune response begins with the detection of the pathogen by a limited number of pattern-recognition receptors (PRRs) that discriminate self from foreign molecules. PRRs are constitutively expressed in the host and can detect invariable microbial components known as pathogen-associated molecular patterns (PAMPs), usually necessary for the survival of the pathogen. Different PRRs recognize specific PAMPs and activate specific signaling pathways, culminating in the production and release of cytokines, a family of low-molecular weight soluble proteins involved in the regulation of cellular activities^{126,127}. Mediators produced by innate immune cells after PRRs triggering act by directly leading to destruction of invading microbes, or they act on other cells by propagating the immune response.

Type-I interferons (IFNs), namely IFN- α and IFN- β , constitute an important class of cytokines with antiviral activities. They can act in both autocrine and paracrine manners by binding to their cognate receptor (IFN α/β R) and activating the Janus kinase/signal transducers and activators of transcription (Jak/STAT) pathway, resulting in the phosphorylation of the heterodimer STAT1/STAT2 and its translocation to the nucleus. Once in the nucleus, they assemble with interferon regulating factor 9 (IRF9) forming a trimeric complex called “IFN-stimulated gene factor 3” (ISGF3) that binds to the interferon-stimulated response elements (ISRE) in the promoter sequence of interferon

stimulated genes (ISGs), inducing their expression^{128,129}. Interestingly, both STAT1 and IRF9 are ISGs themselves¹³⁰.

Different cell types express various STAT family members at different concentrations, influencing the type of complex that can be generated after an IFN stimulus, activating distinct gene expression programs, as summarized in **Fig. 13**¹²⁹.

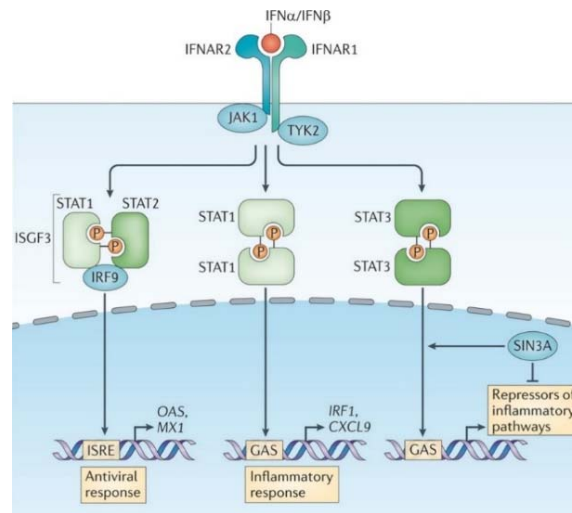


Fig. 13 Gene expression pathways induced by type-I IFNs: antiviral response, inflammatory response, repressors of inflammatory pathways¹²⁹.

Innate immunity can be cell-intrinsic when elicited by infected cells, or cell-extrinsic when PAMPs are recognized by surface PRRs of uninfected cells.

The first molecule with PRR function to have been discovered was the *Drosophila* receptor Toll, which was shown to increase fruit-fly susceptibility to fungal infection when mutated¹³¹. The subsequent discovery of homologous proteins in human and mouse led to the identification of the membrane-bound Toll-like receptor (TLR) family. The C-lectin-like receptors (CLRs) are another family of surface PRRs. Cytosolic PRRs include members of the retinoic acid-inducible gene-I (RIG-I)-like receptor (RLR), of the nucleotide-binding oligomerization domain (NOD)-like receptor (NLR) and of the absent in melanoma 2 (AIM2)-like receptor (ALRs) families¹³².

Cellular components of the innate immune systems are hematopoietic cells such as monocytes, macrophages and neutrophils (all with phagocytic function), dendritic cells (DCs), mast cells, eosinophils, basophils, natural killers (NKs) and NKT cells, but also epithelial cells lining the outer and inner surface of the body. Recognition and effector functions are enhanced by humoral components such as LPS- and mannose-binding proteins, C-reactive protein, acute phase mediators, complement proteins and cytokines¹²⁷.

4.1.1 Toll-like receptors

The human TLR family consists of 10 receptors, while 13 members of this family have been identified in mouse¹³³. They are type-I transmembrane proteins with numerous leucine-rich-repeats (LRRs) in the extracellular domain, which mediate the recognition of PAMPs, and a cytoplasmic signaling domain homologous to that of the interleukin-1 receptor (IL-1R), called Toll/IL-1R homology domain (TIR)¹³⁴. There are different subfamilies, whose members share similar primary structure and detect related PAMPs:

- (i) TLR1, TLR2 and TLR6 recognize lipids,
- (ii) TLR3, TLR7, TLR8 and TLR9 recognize nucleic acids^{135–138},
- (iii) TLR5 recognizes bacterial flagellin¹³⁹,
- (iv) TLR4 recognizes different molecules such as bacterial lipopolysaccharide (LPS)¹⁴⁰, the fusion protein of the respiratory syncytial virus (RSV), fibronectin and endogenous heat-shock proteins (HSPs)¹³².

TLR1 to 9 are conserved between human and mouse; TLR10 is not functional in mouse and its ligand specificity is unknown, while TLR11, TLR12 and TLR13 (recognizing bacterial and parasite molecules) are lost in human genomes^{126,132,141}

TLRs can be divided into two subgroups according to their localization: TLR1, TLR2, TLR4, TLR5 and TLR6 are expressed on the cell surface, while TLR3, TLR8 and TLR9 are localized mainly in the membrane of intracellular organelles (endosomes, lysosomes, endoplasmic reticulum (ER)), where they detect nucleic acids^{132,142,143}. In resting cells, they are located on the ER membrane and then trafficked to the endosomal compartment upon PAMP-mediated stimulation, via a mechanism controlled by the ER transmembrane protein UNC93B^{132,144}.

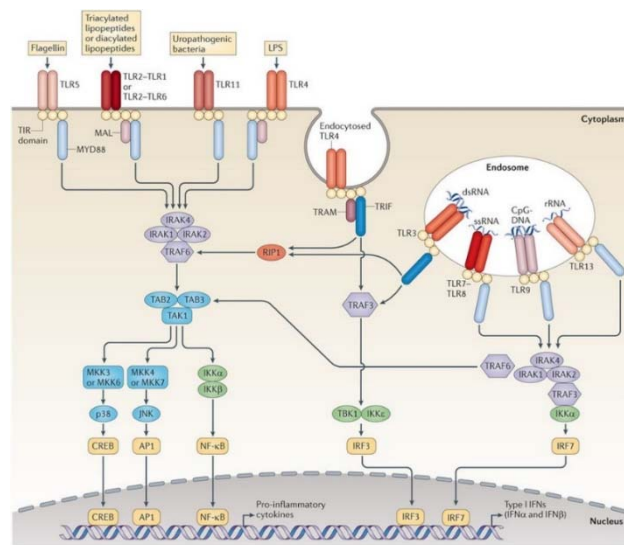


Fig. 14 The TLR family sensors and their signaling pathways²⁰¹.

In general, after ligand binding, TLRs dimerize and recruit TIR-containing proteins that function as adapters for the activation of different pathways leading to the production of pro-inflammatory cytokines and interferons (IFNs). There are four adaptor molecules known to date: myeloid differentiation factor 88 (MyD88), TIR-associated protein (TIRAP) also called MyD88 adaptor-like (MAL), TIR-domain-containing adaptor protein-inducing IFN- β (TRIF), and TRIF-related adaptor molecule (TRAM) [Fig. 14]

4.1.2 C-lectin-like receptors

CLRs belong to a large family of transmembrane proteins that bind to carbohydrates. They are characterized by a carbohydrate recognition domain (CRD) and a calcium-binding site in the extracellular domain. Upon binding with carbohydrate derived from microbes or tissue damage, they induce signaling cascades culminating in the activation of several transcription factors and the triggering of an inflammatory response¹⁴⁵.

4.1.3 RIG-I-like receptors

The RLR family of cytoplasmic nucleic acid sensors consists of three members: RIG-I, melanoma differentiation-associated gene 5 (MDA5), and laboratory of genetics and physiology 2 (LGP2)¹⁴⁶. These proteins share central DExD/H-box RNA helicase domains and a C-terminal domain implicated in RNA detection. RIG-I and MDA5 but not LGP2, have two N-terminal caspase recruitment domains (CARDs) necessary for the interaction with other CARD-containing proteins. These proteins have the ability to stimulate type-I IFNs and cytokine expression in response to RNA virus infection¹³².

RIG-I is activated by a variety of RNA viruses, such as hepatitis C virus (HCV), influenza A virus (IAV) and vesicular stomatitis virus (VSV). The non-self signature of these viruses is a 5'-triphosphate (5'-ppp) single-stranded end of a short dsRNA molecule with homopolymeric nucleotide motifs (like the poly(U) of HCV), a feature of the untranslated regions (UTRs) of several negative-stranded RNA viruses¹⁴⁷. In eukaryotic cells, the 5'-ppp end is cleaved during RNA processing in the nucleus, thus allowing discrimination between self and non-self RNA¹⁴⁸ [Fig. 15]. It has been recently shown that RIG-I is able to induce the expression of a subset of ISGs in the context of *in vitro* hepatitis E virus (HEV) and influenza virus infection in a Jak/STAT-independent manner. This ISG subset is different from that induced by type-I IFN signaling^{149,150}.

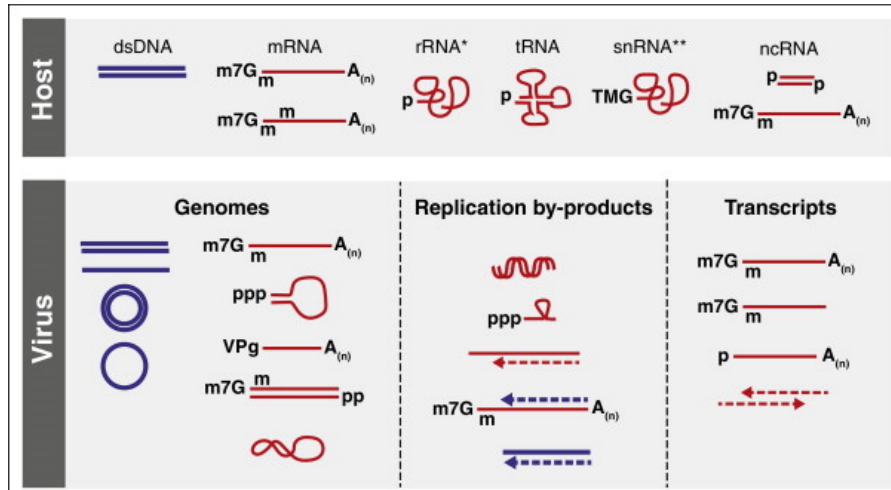


*Fig. 15 Features of eukaryotic and viral RNA molecules*¹⁴⁸.

MDA5 detects infection by other classes of RNA viruses, like picornavirus, recognizing long dsRNA molecules (1-2 kb). Some viruses can be recognized by both RIG-I and MDA5, such as Dengue virus and West Nile virus among others¹⁴⁶. LPG2, lacking the CARD domain, is a regulator of RIG-I and MDA5, associating with certain RNA species and facilitating the activation of the other RLRs¹⁵¹.

Viral RNAs activate RLRs that shift from an autoinhibitory conformation to an open one, and expose their CARD domains in order to interact with the downstream adapter known as mitochondrial antiviral-signaling protein (MAVS), IFN- β promoter stimulator 1 (IPS-1), virus-induced signalling adapter (VISA) or CARD-containing adapter protein (Cardiff)¹⁵².

MAVS is composed of an N-terminal single CARD, three tumor necrosis factor receptor-associated factor (TRAF)-binding motifs (TBFs) and a transmembrane domain, which determines its mitochondrial and peroxisomal localization. The oligomerization of MAVS with RIG-I or MDA5 leads to the recruitment of other downstream signaling molecules such as members of the TRAF family, the tumor necrosis factor receptor type-1 associated death domain protein (TRADD), the receptor-interacting protein 1 (RIP-1) and the Fas-associated protein with death domain (FADD). Eventually, the TRAF family member-associated NF κ -B activator (TANK)-binding kinase 1/inhibitor of nuclear factor kappa-B subunit ϵ (TBK1/ IKK ϵ) and inhibitor of nuclear factor kappa-B (NF κ -B) subunits α and β (IKK α /IKK β) complexes are recruited and in turn activate NF κ -B and IFN regulatory factors 3 and 7 (IRF3, IRF7). The activated transcription factors translocate to the nucleus where they induce the transcription of pro-inflammatory cytokines, type-I IFNs and ISGs¹⁴⁶ [Fig. 16].

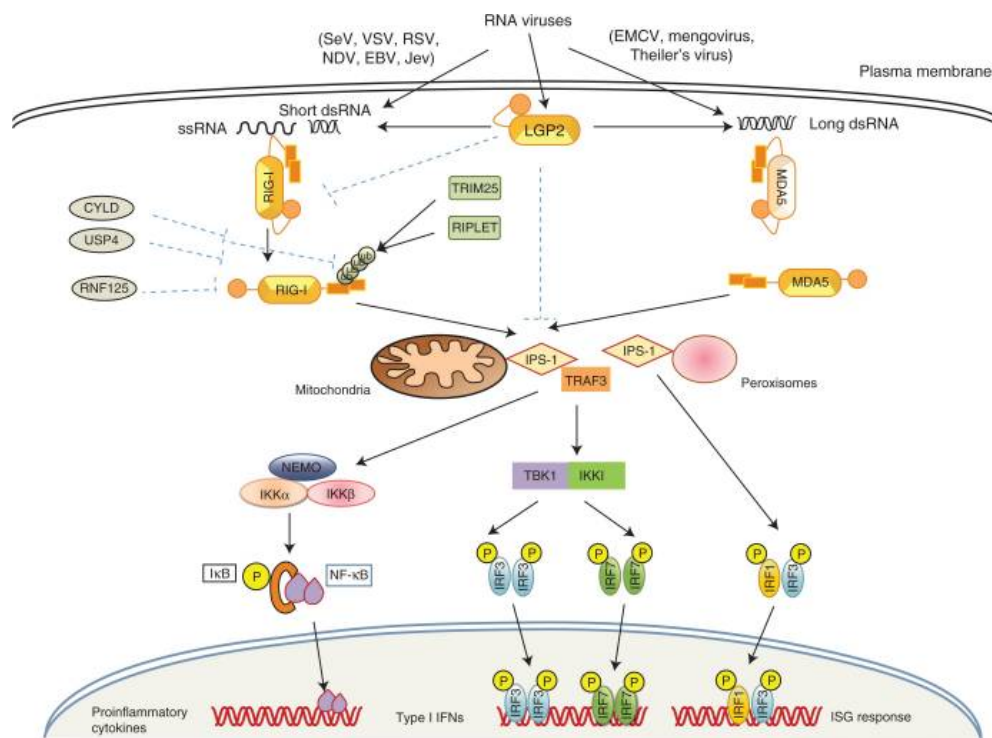


Fig. 16 The RLR family of ds-RNA sensors and their signaling pathways²⁰².

4.1.4 NOD-like receptors

NLRs are intracellular sensors of PAMPs and endogenous DAMPs. Members of this family present an N-terminal protein interaction domain, a central NOD-like domain, and a C-terminal LRR motif. Based on their N-terminal domain, NLRs are divided into four subfamilies: NLRA, NLRB, NLRC and NLRX. Their activation elicits downstream signaling culminating in the NF κ B-dependent expression of pro-inflammatory cytokines, inflammasome assembly, signal transduction and autophagy^{153,154}. So far 22 members of the NLR family have been described in humans; they mainly recognize PAMPs of bacterial and fungal origin, but NOD2 has been recently identified as a sensor for viral ssRNA, which results in MAVS-mediated induction of IFN- β expression^{153,155}.

4.1.5 AIM-2-like receptors

ALRs are characterized by two structural domains: an N-terminal pyrin domain, and a HIN domain (hematopoietic interferon inducible) at the C-terminal region. They are known to bind to cytosolic DNA and to activate inflammasomes, high-weight molecular complexes able to recruit and activate inflammatory caspases. AIM2 and most ALRs are induced by type-I IFN signaling¹⁵⁶.

The best-characterized nucleic acid sensors and their pattern of expression are summarized in **Table 3**.

PRR	PAMP	Expression pattern
TLR3	dsRNA	Endosomes of DCs, macrophages, fibroblasts and epithelial cells, CD8 α^+ DCs with high phagocytic activity
TLR7	ssRNA	Endosomes of plasmacytoid dendritic cells (pDCs), unique in their capacity to rapidly secrete vast amounts of type-I IFN in response to viral infection
TLR8	ssRNA	Endosomes of various cell types with the highest expression in monocytes; up-regulated upon bacterial infection
RLRs	5'-pppRNA, dsRNA,	Cytosolic; ubiquitous; expressed at low levels; their expression is induced by IFNs or upon viral infection
NOD2	Viral ssRNA	Cytosolic; ubiquitous, although different tissues predominantly express distinct members of the family; their expression is induced by IFNs or upon viral infection
ALRs	DNA	Cytosol of macrophages, DCs, B cells

Table 3 Nucleic acid sensors and their characteristics.

4.1.6 Innate immune cells

Most cell types of the innate immune system belong to the myeloid lineage. Their functions are listed in **Table 4**.

Cell type	Lineage	Function
Monocytes	Myeloid	Circulating precursors of macrophages; phagocytic activity.
Macrophages	Myeloid	Resident in almost every tissue or circulating. Phagocyte microbes or infected cells targeted by the adaptive immune response; produce inflammatory mediators; scavengers.
Neutrophils	Myeloid	Granulocytes; are the most abundant innate immune cells. Phagocyte microbes and destroy them in intracellular vesicles by degradative enzymes and antimicrobial substances stored in their granules.
Basophils and eosinophils	Myeloid	Granulocytes. Involved in immunity against parasites and in allergic reactions.

Cell type	Lineage	Function
Mast cells	Myeloid	Resident in mucosal and epithelial tissues. Release inflammatory mediators, histamine and proteases; involved in allergic reactions.
Dendritic cells	Myeloid	Phagocytic cells that take up microbes and extracellular fluid (micropinocytosis); their role is not pathogen clearance but rather the secretion of mediators to activate other innate and adaptive immune cells, and antigen presentation to B and T cells.
Natural killer	Lymphoid	Cells with a characteristic granular cytoplasm able to kill tumoral and infected cells. They exert cytotoxic functions playing a very important role in innate immunity against viral infections.
Natural killer T cells	Lymphoid	Cells coexpressing the NK cell receptor and the T cell receptor (TCR); activated by lipid agonists, modulate both innate and adaptive immune cells
Innate lymphoid cells (ILCs)	Lymphoid	NK-related cells resident in peripheral tissues; source of mediators of the inflammatory response.

Table 4 Innate immune cells, characteristics and functions. Adapted from ^{157,158}.

4.2 The adaptive immune response

In parallel with the innate immune response, an adaptive antigen-specific immune response is initiated; however, its effects are delayed. In contrast to the limited PRRs of the innate immune cells, lymphocytes express a vast repertoire of highly specific antigen receptors, enabling them to respond to virtually any pathogen. There are two main classes of lymphocytes: B and T cells; they are small circulating cells with a reduced cytoplasm and a condensed chromatin. Lymphocytes are in an inactive state until specifically activated through their surface receptors (the B cell receptor (BCR)

and the T cell receptor (TCR), respectively). In this quiescent state, they are called naïve lymphocytes, while when activated they are known as effector lymphocytes^{125,157,159}.

4.2.1 Cross-talk between innate and adaptive immune system: antigen presenting cells

Inflammation, induced by cytokines released by the innate immune response, increases the flow of lymph, which carries pathogens or cells bearing their antigens to the lymphoid tissue (spleen, lymph nodes, mucosal lymphoid tissues) where the adaptive immune response is initiated. A pivotal role in this phenomenon is played by antigen presenting cells (APCs) such as DCs, macrophages and B cells. In the case of T cells, activation requires interaction with an activated DC that previously phagocytosed and degraded a pathogen and presents peptide antigens on major histocompatibility complex (MHC) molecules. Interactions between MHC-antigen complex together with co-stimulatory molecules expressed on activated DCs with the TCR, lead to T cell differentiation and proliferation. The activation and induction of clonal expansion of T cells upon the first encounter with antigens is called priming. Free circulating antigens (polysaccharides or other molecules carrying repeated epitopes) can directly activate specific B cells, but in most cases B lymphocytes need to interact with helper T cells in order to start an effective antibody response. These processes can take about 4-6 days, so that the effector phase of the adaptive immunity starts about a week after the infection^{157,159}.

4.2.2 Cellular and humoral immunity

T cells are usually involved in the reaction against intracellular pathogens. Some activated T cells can directly kill the infected cell (cytotoxic T lymphocytes, CTLs), while others can differentiate into helper T (T_H) or regulatory T (T_{reg}) cells. Cytotoxic T

cells are responsible for the cell-mediated immune response of adaptive immunity and are characterized by the expression of the surface molecule cluster of differentiation 8 (CD8), while T_H cells contribute to the humoral immune response, and are characterized by the expression of the surface molecule CD4. CD8 and CD4 recognize two different classes of MHC molecules. CD8 interacts with MHC class 1 (MHC-I) and CD4 interacts with MHC-II¹⁵⁷.

MHC-I molecules are expressed on the surface of most cell types, and present antigens derived from intracellular pathogens such as viruses and intracellular proteins, including misfolded ones. Infected cells that display viral epitopes through their MHC-I are targeted by $CD8^+$ T cells that can kill them via two different pathways:

- (i) by introducing perforins into the cell membrane to create pores through which granzymes are transferred and induce apoptosis;
- (ii) by binding the Fas protein on the surface of the target cell using their Fas ligand (FasL) eventually inducing apoptosis¹⁵⁹.

MHC-II is expressed only by APCs and display peptides derived by antigens taken up by phagocytosis from the extracellular environment. $CD4^+$ T cells differentiate into different subsets of T_H . T_H1 produce and secrete IL-2 and IFN- γ , both of which enhance the phagocytic activity of macrophages and are important for the initial $CD8^+$ response. In the lymphoid tissues, follicular T_H cells (T_{FH}) interact with antigen-specific naïve B cells to induce their activation and proliferation. T_H2 produce IL-2, IL-4 and IL-5 that stimulate B cell activation. Antigens recognized by a specific BCR are internalized and presented by MHC-II molecules; a bystander $CD4^+$ T lymphocyte able to recognize the peptide/MHC-II complex becomes activated and expresses the ligand for the CD40 surface molecule (CD40L), that binds the CD40 on the B cells inducing activation; moreover, bystander $CD4^+$ T produce cytokines like IL-4 and IL-10. Peptides generated

by B cell antigen processing are usually conformational and may be different from those generated by macrophages and DCs, increasing the diversity of T cell responses against the same pathogen¹⁵⁹.

During B cell proliferation, the genes encoding the BCR undergo a rearrangement called somatic hypermutation; this event, followed by clonal selection, results in a population of B cells with high-affinity BCR. Fully activated B cells differentiate into plasma cells able to produce high levels of antibodies. Antibodies can directly inhibit soluble antigens or toxins or can act in combination with other cellular or soluble components of the immune system to eliminate the invading pathogen. Since there are only a few B cells specific for each epitope, the activated B cells need to proliferate in order to guarantee an adequate response. Usually, the humoral response against a pathogen is polyclonal, that means it involves the proliferation of different clones bearing a specific BCR for distinct epitopes of the same antigen^{125,159}.

The proliferation of activated T and B cells in the lymphoid tissues gives rise to effector as well as memory cells; memory cells enable a quantitatively and qualitatively superior secondary response after a subsequent encounter with the same antigen.

4.2.3 Immune tolerance

Autoreactive B and T cells are negatively selected in the bone marrow and in the thymus (central tolerance). This mechanism of selection is incomplete since not all self-antigens are presented in the central lymphoid organs, and some self-reacting lymphocytes can reach the peripheral lymphoid tissues^{160,161}.

Self-reacting T cells that escape central tolerance can undergo programmed cell death or functional tolerance when they encounter self-antigens presented by non-activated APC; incomplete priming renders T cells unable to proliferate in response to antigen

stimulation. A similar unresponsive state is achieved after suboptimal stimulation, leading to anergy or adaptive tolerance. Chronic antigen stimulation in the context of chronic viral infection and persistent inflammation can lead to T cell exhaustion, a phenomenon in which proliferative capacity and cytokine production are lost, accompanied by the expression of inhibitory receptors. All these dysfunctional T cell states are reversible and each one is characterized by a specific epigenetic landscape¹⁶⁰. In the bone marrow, B cells with a high-affinity BCR for self-antigens undergo clonal deletion, while those with low-affinity BCR enter an unresponsive state that does not avoid migration; anergic B cells have a reduced life-span. One rescue mechanism adopted by self-reactive B cells is the so-called “receptor editing”: a rearrangement of the light chain loci in order to generate a new, non-autoreactive BCR. Self-reactive B cells that reach the peripheral lymphoid tissues undergo peripheral tolerance, regulated by the balance between BCR-dependent signaling and the B cell survival factor BAFF/BlyS (B lymphocyte stimulator)¹⁶¹.

4.3 Liver immunology

The liver is the largest organ of the human body, accounting for almost 2% of adult body weight. The main roles of the liver are protein synthesis and metabolism of lipids, carbohydrates and vitamins, bile production and secretion, but also the removal of pathogens and toxins from the incoming blood. It has always been considered as a metabolic organ however, the concept of the liver as a lymphoid organ is becoming established.

The liver has a double blood supply, receiving the 80% of its blood from the gastrointestinal tract through the portal vein, while the remaining 20% is oxygenated blood from the systemic circulation coming through the hepatic artery. The liver is thus constantly exposed to harmless non-self antigens derived from food and commensal

microbiota, and has developed specialized mechanisms to prevent unnecessary immune activation, maintaining the ability to switch from a tolerant to an activated state in case of pathogen infections^{162,163}.

The peculiar anatomy of the hepatic vascularization allows a rigorous scanning of the bloodstream by immune cells, rendering the liver a physical barrier for blood borne pathogens and metastatic cells. Venous and arterial blood enters the liver via the blood vessels of the portal triad and pass at low speed through very narrow capillaries called hepatic sinusoids. Sinusoids are lined by a fenestrated epithelium composed of liver sinusoidal endothelial cells (LSECs), which lack a basal membrane, and are patrolled by blood monocytes and resident macrophages called Kupffer cells (KCs)¹⁶⁴.

Eighty % of cells constituting the liver are hepatocytes, while the remaining 20% are composed of innate and adaptive immune cells and other parenchymal cells able to carry out immune functions [Fig. 17].

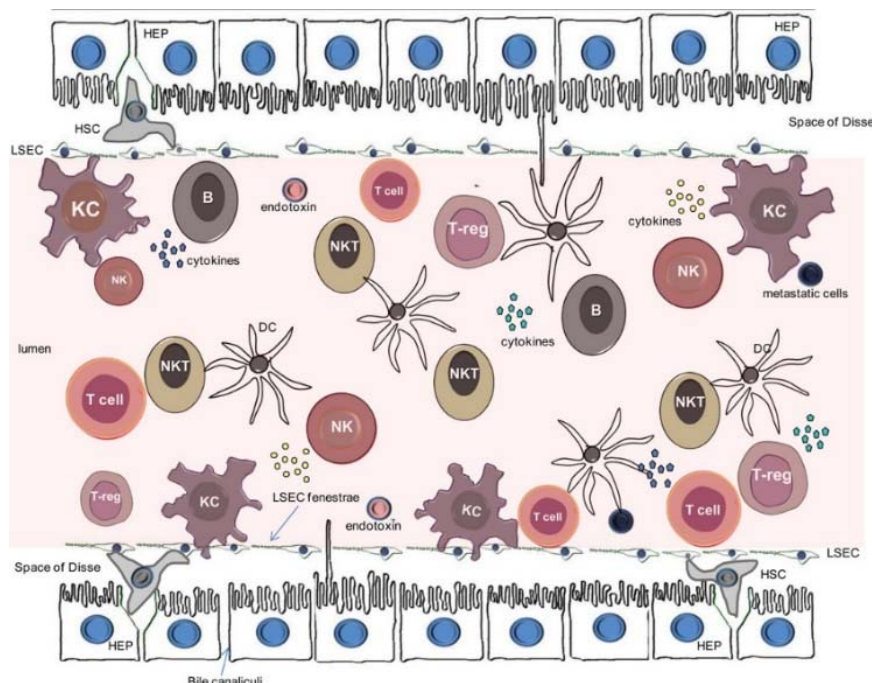


Fig. 17 Parenchymal and non-parenchymal cells of the liver. HEP: hepatocyte, HSC: hepatic stellate cell, KC: Kupffer cell, NK: natural killer cell, NKT: natural killer T cell, B: B lymphocyte, T-reg: regulatory T cell, DC: dendritic cell¹³³.

DCs, KCs and LSECs are classical APCs, while hepatocytes and the endothelial cells of the bile ducts express MHC-I and can directly present antigens to the local T cell populations^{162,163}.

KCs constitute 80% of the whole body macrophages and 15% of all liver cells; they are a self-renewing pool, independent of the circulating myeloid compartment. Their strategic position in the sinusoids allows the sensing and clearance of antigens, endotoxins, cell debris, apoptotic cells and microbes by phagocytosis. KCs are able to activate T cells and release pro-inflammatory cytokines in the presence of a pathogen, and they are responsible for tolerance and homeostasis in the non-infected liver. Continuous exposure to LPS derived from commensal bacteria causes the release of TNF- α , IL-10 and prostaglandin E2, that downregulate CD4⁺ T cell activation. Moreover, the constant presence of LPS and dietary antigens induces low levels of activation markers and downregulation of costimulatory molecules in KCs and LSECs, resulting in inefficient antigen presentation to CD8⁺ T cells. KCs also express co-inhibitory molecules such the programmed death ligand 1 (PD-L1) inducing regulatory T cells under homeostatic conditions^{163,164}.

DCs are present as a heterogenic population mainly concentrated near the portal triad; liver DCs are more phagocytic but less immunogenic than those found in other tissues, since they express lower levels of MHC-II and do not express costimulatory molecules. They play an important role in the establishment of oral and portal tolerance^{163,164}. The main subpopulations found in the mouse liver are conventional myeloid dendritic cells (mDCs), CD8 α ⁺ DCs and pDCs. pDCs originate in the bone marrow from myeloid and lymphoid progenitors, they sense viral DNA and RNA and secrete type-I IFNs, IL-6 and TNF- α . Their relative amount in the liver is higher than in other secondary lymphoid

organs. Murine liver pDCs promote *in vivo* tolerance by inducing T cell anergy or clonal deletion¹⁶⁵.

Granulocytes are rarely found in healthy liver, where neutrophils count for <1% of non-parenchymal cells in mouse. During acute hepatitis, chemoattractant released by KCs recruit large numbers of neutrophils into the liver¹⁶⁴.

NK cells are more abundant in the liver than in any other organ, accounting for the 30-50% of the intrahepatic lymphocytes in human and 5-10% in mouse. They have a limited interaction with the healthy liver, but play a relevant role in immunity against HCV by killing infected cells, and they are also antitumoral agents. IL-10 secreted by KCs downregulates hepatic NKs, while IL-18 and IL-1 β induce their activation^{163,164}.

NKT cells are also important in the mouse liver (in some mouse strains such as C57BL/6 they make up ~30% of total intrahepatic lymphocytes), while they are less frequent in humans. They can produce both pro- (IFN- γ) and anti-inflammatory (IL-4) cytokines upon activation and play a role in different models of liver injury, autoimmunity, cancer and infection^{163,164}.

LSECs constitutively express MHC-II and costimulatory molecules, so they can act as APCs. Antigen presentation by LSECs to naïve T cell induces T_H2 and T_{reg} subsets; moreover, they can induce tolerogenic CD8⁺ T cells by mutual upregulation of PD-L1 and PD1. On the other hand, the tolerogenic effect of LSECs is also due to constant exposure to endotoxin and gut bacteria-derived antigens¹⁶³⁻¹⁶⁵. It has been shown that LSEC-primed CD8⁺ T cells differentiate into a particular subpopulation of memory T cells or into short-lived effector T cells¹⁶⁶.

Hepatic stellate cells (HSCs) are located in the space of Dissé, where they contribute to the control of the blood flow. If exposed to inflammatory stimuli, they differentiate in myofibroblasts producing collagen and inhibitors of metalloproteases, which lead to liver fibrosis. They express MHC-I and MHC-II, as well as lipid-presenting CD1b and CD1c and costimulatory molecules. HSCs are known to have tolerogenic capability by inhibiting immunogenic T cells and leading to apoptosis of CD8⁺ T cells. Moreover, they contribute to T_{reg} activation via the secretion of retinoic acid and TGF-β^{162,164}.

Hepatocytes are the main producers of acute phase protein, most of the complement components and cytokines. They constitutively express MHC-I and CD1d molecules, and are able to present peptide and lipid antigens to CD8⁺ T cells and NKs by direct contact through LSEC fenestration. Hepatocytes can prime naïve T cells and induce T cell proliferation; however, because of the lack of costimulatory molecules, they fail to sustain T cell survival leading to apoptosis and intrahepatic tolerance by clonal deletion. Furthermore, hepatocytes actively induce T cell apoptosis via Fas and TNF¹⁶²⁻¹⁶⁴. Under certain conditions, crosstalk with NK cells may lead to induction of effector T cell, resulting in immunogenic rather than tolerogenic presentation¹⁶⁶.

Cholangiocytes, or bile epithelial cells (BECs), line the bile ducts and are responsible for the immediate innate immune response against pathogens invading these structures. They express PRRs and produce antimicrobial peptides, cytokines and chemokines. Infection by hepatotropic viruses enhance cholangiocyte MHC-I and MHC-II expression^{163,164}.

B lymphocytes represent less than 10% of human hepatic lymphocytes, and can make up to 50% of intrahepatic lymphocytes in mouse¹⁶⁷. Their contribution to the tolerogenic environment in the liver has not yet been determined¹⁶⁴.

T lymphocytes (CD3⁺ cells) represent the majority of the liver lymphoid cells, with 80% being conventional αβ T cells, and the remainder expressing the γδ TCR. CD8⁺ T cells predominate in the human liver, whereas CD4⁺ T cells are more abundant in the mouse liver. Among the CD4⁺ cells, T_{H1}, T_{H2}, T_{H17} and T_{reg} subsets are present. T_{reg} cells are important elements of the peripheral tolerance by inhibiting T_{H1}, T_{H2}, and T_{H17} responses. In turn, T_{reg} cells can be divided into natural T_{reg} (nT_{reg}) and inducible (iT_{reg}) cells; in a healthy mouse liver nT_{reg} are less abundant than in lymph nodes and their relative amount has been shown to increase in case of HBV and HCV infection. CD8⁺ T_{reg} cells have also been identified but they are poorly defined^{163,164}.

4.3.1 Hepatotropic infections

Although most of the blood-borne pathogens are cleared by phagocytosis by KCs and LSECs, hepatotropic viruses and parasites often exploit the tolerogenic environment of the liver to establish chronic infections [Fig. 18].

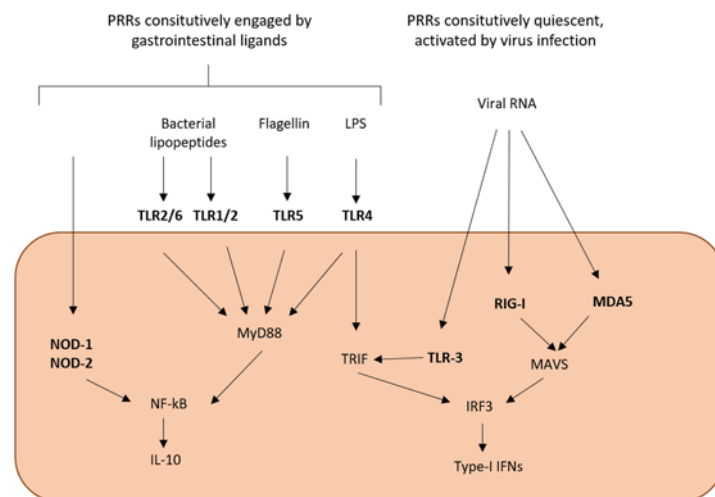


Fig. 18 PRRs involved in immunity and tolerance in the liver. Adapted from 139.

A common mechanism of escape for hepatotropic pathogens is the initial antigen presentation in the liver rather than in the lymphoid organs, which leads to immune tolerance instead of activation¹⁶⁸.

Blood-borne bacteria are taken up by KCs and bacterial antigens are presented on CD1 surface molecules, which recruits NKT cells in a CXCR3-dependent manner. This mechanism intercepts bacteria in the sinusoids, thereby avoiding hepatocyte infection¹⁶⁹. Pathogens that escape the vascular innate immune system of the liver and are able to access the parenchyma, are more difficult to eradicate because of the tolerogenic microenvironment.

Plasmodium spp. parasites go through a hepatic phase; after delivery into the skin by a mosquito bite, sporozoites are able to elude clearance by phagocytic cells and to reach the liver through the blood stream. Once in the sinusoids, they attach and enter KCs. Here they avoid lysosomal fusion and subsequently trans-infect hepatocytes, where they develop into merozoites and are released again into the sinusoids^{170,171}.

Hepatitis viruses can cause acute or chronic infection, and their clearance requires a strong adaptive immune response. They are able to circumvent immunity or innate immune sensing during entry into the liver, or they modulate the adaptive immunity during hepatocyte infection.

Hepatitis A virus (HAV) is a food-borne pathogen of the family *picornavirus* that never causes chronic hepatitis. The HAV genome is single-stranded, positive-sense RNA genome of 7.5 kb. There are two forms of infectious virus: infectious particles exist as non-enveloped virions and quasi-enveloped virions (eHAV) that are secreted non-lytically from infected cells. HAV infection induces a minimal intrahepatic type I-IFN response, partly due to the ability of the precursors of the viral protease 3C^{pro} to cleave

MAVS and TRIF. HAV replication itself is not cytotoxic and liver injury is likely to be mediated by a strong CTL and NKT cell response¹⁷².

Hepatitis C virus (HCV) is a positive ssRNA *flavivirus* causing chronic infection in 50% of the cases. HCV induces a strong type-III, and to a lesser extent also type-I, -IFN response in the liver, which is mediated by TLR and RIG-I sensing of viral RNA. It can either be completely cleared after acute hepatitis, or establish a persistent infection. Chronic HCV can either be an asymptomatic disease or cause immune-mediated liver injury. The viral protease NS3/A4 is able to impair IRF3 signaling by cleaving TRIF and MAVS, thus limiting the antiviral state of the infected cells and its bystanders^{173,174}. HCV is also able to escape from adaptive and humoral responses by accumulating mutations in its antigen-encoding genes, and by the production of secreted antigens that, presented in the absence of adequate co-stimulation, lead to clonal deletion^{174,175}.

HBV is considered a stealth virus, since it is able to replicate in hepatocytes without eliciting a strong innate immune response. Infection persists to chronicity in ~5% of the cases in adults, and resolution of acute hepatitis is mediated by a polyclonal CD8⁺ T cell response against HBcAg and HBeAg, as well as by a non-cytopathic NKT- and NK-dependent response mediated by IFN- γ ¹⁷⁶. Moreover, the activation of CD4⁺ T cells can induce the production of neutralizing antibodies against HBsAg. The adaptive immune response to HBV is necessary to clear the pathogen or destroy infected cells, but in many cases it leads to immunopathology¹⁷⁷. HBV is also able to evade innate immunity by interfering with TLR9 in pDCs via its surface antigen¹⁷⁸, by maintaining its circular covalently closed genome (cccDNA) in the nucleus, and by synthesizing the genomic DNA from a pregenomic RNA molecule (pgRNA) inside the viral capsid⁶⁰.

Patients with CHB develop only a weak or undetectable polyclonal T cell response; NK cells in these patients show an inhibitory phenotype and cause clonal T cell deletion;

moreover, intrahepatic T cells express high levels of PD1 and cytotoxic T lymphocyte antigen 4 (CTLA4), which are both inhibitory molecules. In this context, the innate immune cells - in particular granulocytes and KCs - suppress the cellular adaptive immune response, thereby limiting immunopathology, but also promoting tolerance and virus persistence. The immunomodulatory cytokine IL-10 is abundantly produced during CHB; CTLs also produce IL-10 themselves, thus attenuating the antiviral activity in an autocrine way. In addition, the huge amount of HBsAg secreted by infected cells usually outnumbers the infectious particles and saturates circulating neutralizing antibodies, thereby allowing the virus to overcome humoral immunity^{176,179}.

HDV is commonly considered a non-cytopathic virus, since HDV viremia has no correlation with the extent of liver disease and HDAg expression in transgenic mice does not cause cytotoxicity in hepatocytes. HDV-associated hepatic damage is thus thought to be immune-dependent like in HBV and HCV infection^{95,180}. HDV infection in humanized or hNTCP-transgenic mice causes the activation of intra-hepatic IFN and ISG expression (e.g. 2'-5'-oligoadenylate synthetase - OAS – and MxA), of the IFN-inducible PRR RIG-I, and it triggers the JAK/STAT signaling cascade^{101,181}. However, the interaction between infected hepatocytes and immune cells has not been completely elucidated in animal models.

In comparison to HBV and HCV patients, a high frequency of cytotoxic perforin-positive CD4⁺ T cells have been found in the peripheral blood of HDV patients¹⁸², and some MHC-I and MHC-II epitopes have been identified to date^{183,184}. However, the specific T cell response generated in patients with chronic HDV is weak and insufficient to contain the infection. One study limited to peripheral blood mononuclear cells (PBMCs) of HDV infected patients showed the HDV-specific IL-2 and IFN- γ response

exerted by T cells, as well as the IP-10 response exerted by activated monocytes, both contributing to the inflammatory environment¹⁸⁵. The activation of T_H cells also induces the production of anti-HDV antibodies that do not have any protective function since the recognized HDAGs are situated inside the viral particle. This way HDV evades the humoral immune response.

As in HBV and HCV mono-infection, HBV-HDV coinfected patients show a higher frequency of NK cells, but with a less activated phenotype (low expression of the activating receptors CD244 and CD48). In addition, the proportion of the CD56^{bright} subset (immunoregulatory) is increased over the CD56^{dim} subset (cytolytic). Inhibition of NK activity thus seems to be a common escape mechanism of hepatitis viruses, relying more on the inflammatory environment than on virus-specific factors¹⁸⁶.

OBJECTIVES

The limited availability of adequate small animal models for the study of HDV infection has hampered a complete understanding of the pathology and the development of specific antiviral treatments. In this context, the main aim of this doctoral research was:

1. To develop and characterize a mouse model for HDV infection based on recombinant adeno-associated vectors (rAAV).

The specific objectives of the thesis were:

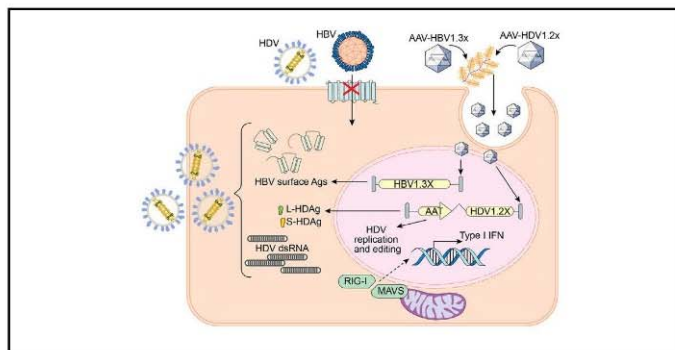
2. To determine whether this model recapitulates the characteristics of human infection.
3. To identify the innate immune pathways involved in HDV recognition and the type-I IFN response.
4. To characterize the immune infiltrate recruited to the liver after rAAV-mediated HDV infection.
5. To determine the role of the immune infiltrate in the observed liver pathology.
6. To determine the cytotoxicity of the virus components (HDAGs, viral genome).

MANUSCRIPTS

Suárez-Amarán L, Usai C, Di Scala M. A new HDV mouse model identifies mitochondrial antiviral signaling protein (MAVS) as a key player in IFN - β induction. *Journal of Hepatology*, 67(4):669-679. <http://dx.doi.org/10.1016/j.jhep.2017.05.010>

A new HDV mouse model identifies mitochondrial antiviral signaling protein (MAVS) as a key player in IFN- β induction

Graphical abstract



Highlights

- Description of a new mouse model of HDV infection mimicking aspects of human disease.
- HDV replication is sustained and induces a robust type-I IFN and anti-HBV response.
- Liver damage is observed.
- MAVS was identified as a key player in HDV detection.
- The innate immune response is amplified by adaptive immunity.

Authors

Lester Suárez-Amarán, Carla Usai, Marianna Di Scala, ..., Francisco Rodríguez-Frias, Rafael Aldabe, Gloria González-Aseguinolaza

Correspondence

ggasegui@unav.es
(G. Gonzalez-Aseguinolaza)

Lay summary

Co-infection with hepatitis B and D virus (HBV and HDV, respectively) often causes a more severe disease condition than HBV alone. Gaining more insight into HDV and developing new treatments is hampered by limited availability of adequate immune competent small animal models and new ones are needed. Here, a mouse model of HDV infection is described, which mimics several important characteristics of the human disease, such as the initiation and maintenance of replication in murine hepatocytes, genome editing and, in the presence of HBV, generation of infectious particles. Lastly, the involvement of an adaptive immunity and the intracellular signaling molecule MAVS in mounting a strong and lasting innate response was shown. Thus, our model serves as a useful tool for the investigation of HDV biology and new treatments.

Erratum to “A new HDV mouse model identifies mitochondrial antiviral signaling protein (MAVS) as a key player in IFN- β induction” [J Hepatol 67 (2017) 669–679]

Lester Suárez-Amarán^{1,2,†,‡}, Carla Usai^{1,2,†}, Marianna Di Scala^{1,2,§}, Cristina Godoy^{3,4,5}, Yi Ni⁶,
Mirja Hommel^{1,2}, Laura Palomo^{1,2}, Víctor Segura^{2,7}, Cristina Olagüe^{1,2}, Africa Vales^{1,2},
Alicia Ruiz-Ripa^{3,4,5}, Maria Buti^{3,4,5}, Eduardo Salido⁸, Jesús Prieto^{1,2,9}, Stephan Urban⁶,
Francisco Rodríguez-Frias^{3,4,5}, Rafael Aldabe^{1,2}, Gloria González-Aseguinolaza^{1,2,*}

¹Gene Therapy and Regulation of Gene Expression Program, Center for Applied Medical Research (CIMA), Pamplona, Spain; ²Instituto de Investigación Sanitaria de Navarra (IdiSNA), Calle Iruñlarrea 3, Pamplona 31008, Spain; ³Centro de Investigación Biomédica en red: Enfermedades Hepáticas y Digestivas (CIBERehd), Instituto de Salud Carlos III, Barcelona, Spain; ⁴Liver Pathology Unit, Departments of Biochemistry and Microbiology, Hospital Vall d'Hebron, Universitat Autònoma de Barcelona, Barcelona, Spain; ⁵Virology Unit, Department of Microbiology, Hospital Vall d'Hebron, Universitat Autònoma de Barcelona, Barcelona, Spain; ⁶Department of Infectious Diseases, Molecular Virology, University Hospital Heidelberg, Heidelberg, Germany; ⁷Bioinformatics Unit, Center for Applied Medical Research (CIMA), University of Navarra, Pamplona, Spain; ⁸Department of Pathology, Centre for Biomedical Research on Rare Diseases (CIBERER), La Laguna, S/C Tenerife, Spain; ⁹Centro de Investigación Biomédica en red: Enfermedades Hepáticas y Digestivas (CIBERehd), Instituto de Salud Carlos III, Pamplona, Spain

It has come to our attention that there were errors in Fig. 1A, Fig. 2A, and Fig. 8D and F in the published version of this manuscript. The corrected figures are provided below, with an explanation of the errors.

In Fig. 1A, the colour of the lines was incorrect and the light blue legend representing the HBV viral genome was missing. In

Fig. 2A the legend within the figure was incorrectly labelled. The light blue circle and the light blue triangle, represented AAV-HBV/HDV and AAV-HBV, respectively. In Fig. 8D, left panel, the axis labels should have been AAV-HDV. In Fig. 8F the light blue legend should have been labelled AAV-HDV. Please see the corrected figures below:

Keywords: Hepatitis B; EASL guidelines; Treatment; Interferon; Entecavir; Tenofovir; TAF; HBsAg; Hepatocellular carcinoma; HBV DNA; HBV reactivation; Mother to child transmission.

[†] DOI of original article: <http://dx.doi.org/10.1016/j.jhep.2017.05.010>.

* Corresponding author.

E-mail address: ggasegui@unav.es (G. González-Aseguinolaza).

[†] These authors contributed equally to this work.

[‡] Current address: Molecular and Cell Biology Laboratory, The Salk Institute for Biological Studies, 10010 North Torrey Pines Road, La Jolla, CA, United States.

[§] Current address: Fundación Centro Nacional de Investigaciones Cardiovasculares, Madrid, Spain.



ELSEVIER

Journal of Hepatology 2018 vol. xxx | xxx–xxx

Please cite this article in press as: Suárez-Amarán L. et al. Erratum to “A new HDV mouse model identifies mitochondrial antiviral signaling protein (MAVS) as a key player in IFN- β induction” [J Hepatol 67 (2017) 669–679], J Hepatol (2018), <https://doi.org/10.1016/j.jhep.2018.04.003>

Erratum

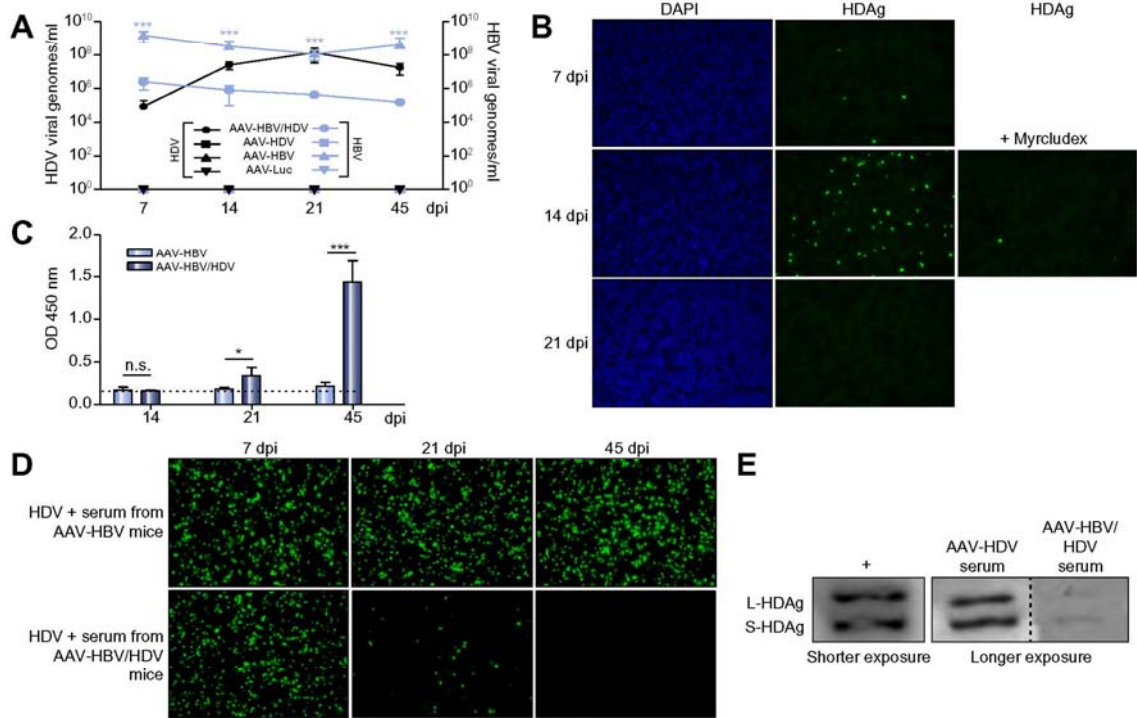


Fig. 1. Infection of C57BL/6 mice with AAV-HBV/HDV gives rise to the production of circulating HDV infectious particles and a detectable humoral immune response against viral antigens, while anti-HBsAg and anti-HDAg humoral response is induced.

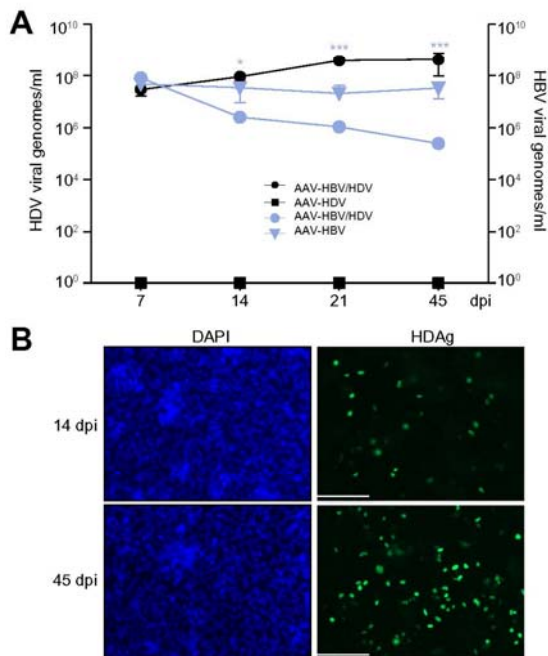


Fig. 2. Infection of RAGB6 mice with AAV-HBV/HDV gives rise to the sustained production of circulating HDV infectious particles and HBV particles.

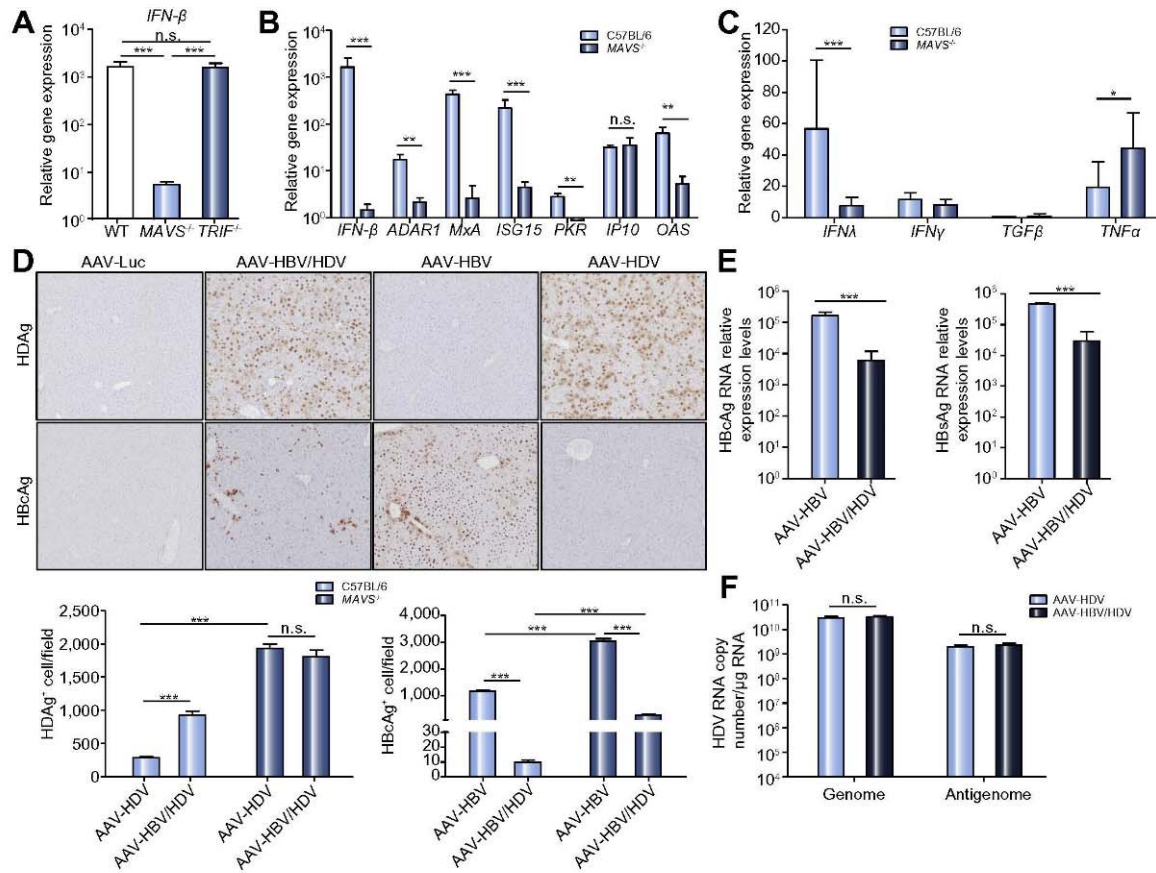


Fig. 8. AAV-HDV infection induces an innate immune response that is partially dependent on MAVS.

Supplementary material

Cell culture

HEK293 cells, Huh7, and HepG2-hNTCP [25] were cultured in Dulbecco's modified Eagle's medium supplemented with 10% fetal bovine serum, 2 mM L-glutamine, 50 U/ml penicillin, and 50 µg/ml streptomycin. Culture medium for HepG2-hNTCP was supplemented with puromycin at a final concentration of 5 µg/ml. Cells were maintained at 37°C with 5% CO₂ and 95% relative humidity.

Serum ALT levels.

Alanine aminotransferase (ALT) serum levels were analyzed with a Hitachi Automatic Analyzer (Boehringer Mannheim, Indianapolis, IN).

RNA isolation, reverse transcription and quantitative PCR (RT-qPCR).

Total RNA from liver samples and cell lines was isolated using TRIzol Reagent (Invitrogen) according to the manufacturer's instructions. Viral nucleic acids were extracted from serum samples using the QIAmpViral RNA Mini Kit (Qiagen). Total RNA was pre-treated with DNase I using the TURBO DNA-free™ Kit (Applied Biosystems) and retro-transcribed into complementary DNA (cDNA) using M-MLV reverse-transcriptase (Invitrogen). Real-time quantitative polymerase chain reaction assays (RT-qPCR) were performed using iQ SYBR Green Supermix (BioRad) in a CFX96 Real-Time Detection System (BioRad) and primers as specified in Supporting Table 1. HDV strand-specificity was analyzed as described elsewhere [1]. HDV viremia was quantified by RT-qPCR reaction using the Power SYBR® Green RNA-to-CT™ 1-Step kit (Applied Biosystems)

after DNase I treatment using the TURBO DNA-free™Kit (Ambion). Known amounts of HDV-containing plasmid were used as standard for quantification.

Patient samples

Samples and data from patients included in the study were provided by the Biobank of the University of Navarra and were processed following standard operating procedures approved by the Ethics and Science Committees. We analyzed several patients for anti-HDAg reactivity and selected the serum from patient CUN-36.

Histology and immunohistochemistry (IHC)

Cells were grown on coverslips, washed three times with PBS, fixed with 4% paraformaldehyde (PFA) and washed again with PBS. HDAg immunostaining was achieved after permeabilization with Triton X-100 (0.1%; 10 minutes, room temperature) using a patient-derived serum, CUN-36. As secondary antibody goat anti-human IgG labeled with AlexaFluor® 488 (Invitrogen, Carlsbad, CA) was used. Slides were covered with mounting medium containing DAPI (VECTASHIELD®, Vector Laboratories, Inc).

Liver sections were fixed with 4% PFA, embedded in paraffin, sectioned (5 µm), and stained with hematoxylin and eosin. Sections were mounted and analyzed by light microscopy. For HDV-Ag IHC analysis, PFA-fixed liver sections were deparaffinized, rehydrated and subjected to heat-mediated antigen retrieval in TE pH9 at 95°C for 30 min. Endogenous peroxidase and biotin were blocked prior to incubating the sample with CUN-36 serum diluted 1:30.000 at 4°C overnight, followed by secondary antibody biotinylated sheep anti-human IgG 30 min, RT, 1:200 (GE Healthcare, UK) and streptavidin-HRP 30 min, RT, 1:200 (Burlingame, CA). Thermo Scientific NeutrAvidin High Sensitivity HRP Conjugate in combination with Thermo Scientific Pierce Metal-

Enhanced DAB was used to detect HDV Ag expression. Cell nuclei were counterstained with hematoxylin. Slides were covered with mounting medium and image acquisition was performed on an Axio Imager M1 microscope with an AxioCam ERC 5s camera using ZEN Pro software (Carl Zeiss Inc., Thornwood, NY). All images were stored in uncompressed 24-bit color TIFF format and image analysis was performed using a plugin developed for Fiji, ImageJ (NIH, Bethesda, MD).

Determination of HDV infectious particles in vitro

To determine HDV infectious particles HepG2-hNTCP cells were seeded in BD Falcon™ Culture Slides (8-well, BD Biosciences, US) and infected overnight. HDV-containing cell supernatant or mouse serum diluted in DMEM-5% FBS containing 4% polyethylene glycol 8000 (Sigma-Aldrich). After washing (PBS), culture medium with DMSO (final conc. 2.5% v/v) was added and the medium was changed every 2–3 days. As positive control HDV particles purified from patient serum [2] (9×10^4 HDV-RNA copies as quantified by qRT-PCR) were used. HDV antigen expression was assessed by immunofluorescence as described above.

Anti-HBsAg ELISA

The specific anti-HBsAg antibody response was measured using a direct ELISA. In short, wells were coated with 1 µg of Ag in 100 µl of PBS (pH 7.4) at 37°C for 3 h. They were blocked with 100 µl of 5% (w/v) solution of nonfat dry milk powder at 37°C for 2 h and washed thoroughly. Aliquots of 100 µl of diluted mouse sera (1:10) were added and incubated overnight at 4°C. After washing, wells were incubated with 100 µl of HRP-labeled secondary antibody at 37°C for 90 min. HRP was detected with o-phenylenediamine at 490 nm. Serum antibodies were tested in duplicates and the mean absorbance values are reported.

Western blotting

Whole-cell or liver samples were lysed in RIPA buffer (20 mM Tris-HCL pH 7.5, 150 mM NaCl, 1% NaDeoxycholate, 1% Triton X-100 and 1% SDS) supplemented with protease inhibitors. Protein concentration was determined by Pierce™ BCA Protein Assay Kit (Thermo Scientific, US) according to the manufacturer's recommendations. Western blot was performed using CUN-36 serum diluted 1:10,000 in PBS/1% powdered milk for HDAg detection and anti-actin polyclonal rabbit serum (Sigma-Aldrich, US) followed by HRP-conjugated rabbit anti-human IgG (Dako) or goat anti-rabbit IgG (Cell Signaling Technology). SuperSignal® West Pico Chemiluminescent Substrate (Thermo Scientific) was used to detect expression.

Microarray hybridization and data analysis

RNA isolated from mouse liver was extracted according to the manufacturer's instructions. As a last step of the extraction procedure, the RNA was purified with the RNeasy Mini-kit (Qiagen, Hilden, Germany). Before cDNA synthesis, RNA integrity from each sample was confirmed on Agilent RNA Nano LabChips (Agilent Technologies).

Sense cDNA was prepared from 300 ng of total RNA using the Ambion® WT Expression Kit. It was then fragmented and biotinylated with the Affymetrix GeneChip® WT Terminal Labeling Kit (PN 900671). Labeled sense cDNA was hybridized with the Affymetrix Mouse Gene 2.0 ST microarray according to the manufacturer's protocols using GeneChip® Hybridization, Wash and Stain Kit. Gene chips were scanned with the Affymetrix GeneChip® Scanner 3000.

Both background correction and normalization were done using RMA (Robust Multi-Array) algorithm [3]. After quality assessment a filtering process was performed to eliminate low expression probe sets. Applying the criterion of an expression value greater than 16 in 2 samples for each experimental condition (AAV-Luc, AAV-HDV, AAV-HBV or AAV-HBV+AAV-HDV), 25603 probe sets were selected for statistical analysis. R and Bioconductor were used for

preprocessing and statistical analysis [4] and LIMMA (Linear Models for Microarray Data) [5] to identify the probe sets that showed significant differential expression between experimental conditions. Genes were selected as significant using a criteria of $B > 3$.

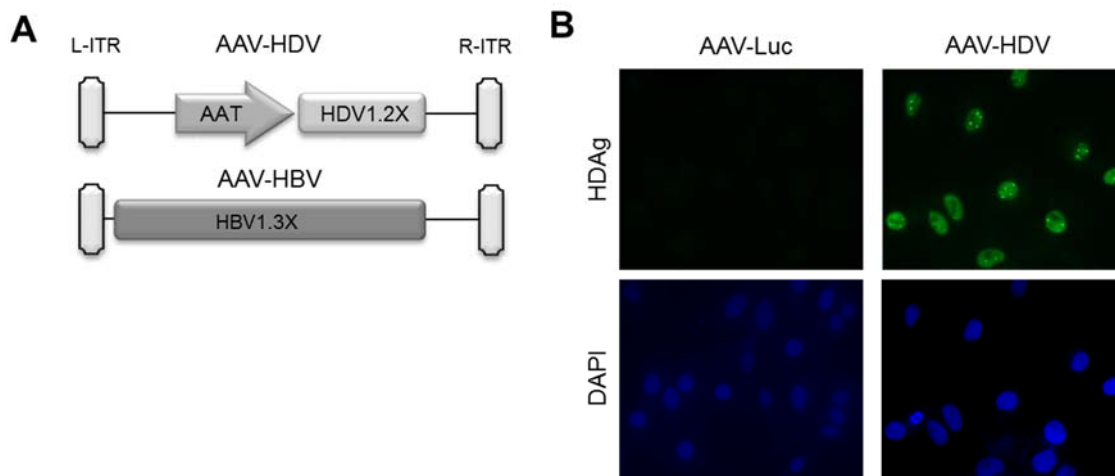
Functional enrichment analysis of gene ontology (GO) categories was carried out using a standard hypergeometric test [5]. Extracted information was complemented with the use of Ingenuity Pathway Analysis (Ingenuity Systems, www.ingenuity.com), a database including manually curated and fully traceable data derived from literature sources [6].

1. Jardi R, Buti M, Cotrina M, Rodriguez F, Allende H, Esteban R, Guardia J. Determination of hepatitis delta virus RNA by polymerase chain reaction in acute and chronic delta infection. *HEPATOLOGY* 1995;21:25-29.
2. Lamas Longarela O, Schmidt TT, Schöneweis K, Romeo R, Wedemeyer H, Urban S, et al. Proteoglycans act as cellular hepatitis delta virus attachment receptors. *PLoS One* 2013;8:e58340.
3. Irizarry RA, Bolstad BM, Collin F, Cope LM, Hobbs B, Speed. Summaries of affymetrix genechip probe level data. *Nucleic Acids Res* 2003;31:e15.
4. Gentleman V, Carey S, Dudoit R, Irizarry R, Huber W. Bioinformatics and computational biology solutions using R and Bioconductor. *Statistics for biology and health*. Springer, New York, NY. 2005.
5. Smyth GK. Linear models and empirical Bayes methods for assessing differential expression in microarray experiments. *Statistical Applications in Genetics and Molecular Biology* 3, No. 1, Article 3. 2004.
6. Draghici, S. *Data analysis tools for DNA microarrays*. Chapman Hall/CRC 2003, London.

Supplementary table

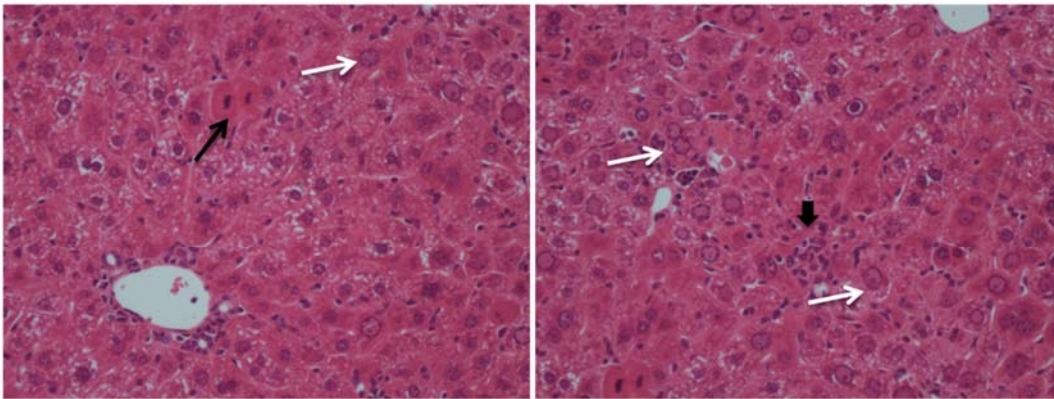
Supplementary Table 1: Primer sequences for RT-qPCR analysis

Target gene	Primer sequences	
	Forward primer (5'-3')	Reverse primer (5'-3')
HDV	5'-GGACCCCTTCAGCGAACA-3'	5'-CCTAGCATCTCCTCCTATCGCTAT-3'
mADAR-1	5'-AGCCTGTGTACCTGAAATCTGTAAC-3'	5'-TTGACAATAAAGGGATAGCGTAGTC-3'
mIP-10	5'-CCAGTGAGAATGAGGGCCATA-3'	5'-CTCAACACGTGGGCAGGAT-3'
mISG-15	5'-GATTGCCCAGAAGATTGGTG-3'	5'-TCTGCGTCAGAAAGACCTCA-3'
mMx1	5'-ATCTGTGCAGGCACTATGAG-3'	5'-CCTTCCTTCTTTACGCTTCC-3'
m2'-5' OAS	5'-ATGAGGGCCTCTAAAGGGGT-3'	5'-CTCTCATGCTGAACCTCGCA-3'
mPKR	5'-TGGGCAGACAATGTATGGTAC-3'	5'-ATGTGACAACGCTAGAGGATG-3'
mIFN- β	5'-ATGAGTGGTGGTTGCAGGC-3'	5'-ACCTTCAAATGCAGTAGATTCA-3'
mGAPDH	5'-TGCACCACCAACTGCTTA-3'	5'-GGATGCAGGGATGATGTTC-3'
mGAPDH	5'-GGTCGGAGTCAACGGATTT-3'	5'-CCAGCATCGCCCACTTGA-3'

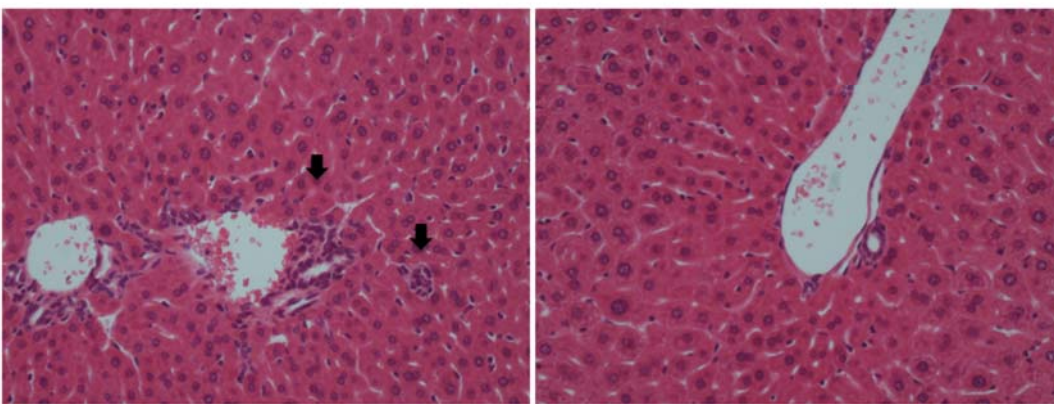


Supplementary Fig. 1. (A) Schematic representation of recombinant AAV-CMV-HDV, AAV-HDV and AAV-HBV. (B) Immunofluorescence analysis of HDAg expression in Huh7 cells 8 days after AAV-CMV-HDV- or AAV-Luc infection.

A AAV-HDV



B AAV-HBV



Supplementary Fig. 2. Mild liver pathology in wt after mono-infection with AAV-HDV and AAV-HBV. (A) Mild lobular inflammation (thick black arrows) of the liver parenchyma without significant structural changes in an HDV-infected wt mouse. Occasional lymphocytes can be observed in portal spaces as well as some mitotic figures (thin black arrows). Also, some areas with "sanded" nuclei are indicated (thin white arrows). (B) Tissue sections from AAV-HBV-injected C57BL/6 mice present very mild changes, with occasional lymphocytes in an otherwise normal hepatic structure.

Manuscript 2

Elucidating the mechanisms of HDV-induced liver damage in a AAV-HBV/HDV mouse model

Authors: Carla Usai^{1,2}, Sheila Maestro^{1,2}, Gracián Camps^{1,2}, Lester Suárez^{1,2}, África Vales^{1,2}, Cristina Olague^{1,2}, Rafael Aldabe^{1,2}, Mirja Hommel^{1,2}, Gloria González-Aseguinolaza^{1,2}

Affiliations: ¹ Gene Therapy and Regulation of Gene Expression Program, Center for Applied Medical Research (CIMA), Pamplona, Spain; ² Instituto de Investigación Sanitaria de Navarra (IdiSNA), Calle Irunlarrea 3, Pamplona 31008, Spain

Keywords: HDV, inflammation, immune infiltrate, immune response, liver damage, hepatitis, intrahepatic leukocytes, HDVg

Abstract: Hepatitis delta virus (HDV) is a defective RNA virus that depends on hepatitis B virus (HBV) for the formation of new virions. HDV induces the most severe form of human viral hepatitis with the worst prognosis. However, the specific reasons for the severity of the disease remain unknown. Recently, we have developed a HDV replication mouse model in which, for the first time, liver damage associated with HDV is detected. In these mice, a strong activation of MAVS-mediated innate immune response as well as a significant liver inflammatory infiltrate were observed. Activated T lymphocytes, natural killer cells, dendritic cells and pro-inflammatory macrophages account for the majority of the inflammatory infiltrate and play a major role in the hepatic expression of TGF- β , ISG15, ADAR-1, IP10, PKR, and USP18. However, neither T cells, natural killer cells nor macrophages are necessary for the induction of the observed liver damage; on the contrary, our data indicate that macrophages have a protective role early after infection. The role of type I- and type II IFN was also discarded. Moreover, we found that the hepatic expression of the HDV antigens in the absence of active HDV replication is sufficient to induce a dose-dependent liver toxicity.

Introduction

Hepatitis delta virus (HDV), the only member of the genus Deltavirus, is a defective RNA virus that requires the surface antigens of hepatitis B virus (HBV) (HBsAg) for viral assembly and transmission¹. Specific interaction between HBsAg and the human Na⁺/taurocholate cotransporting polypeptide (hNTCP) determines the hepatotropism and species-specificity of both viruses^{2,3}. Even though HDV genome replication and ribonucleoprotein (RNP) formation are HBV-independent, HDV can productively complete its infective cycle only in HBV-infected hepatocytes, being *de facto* an obligated HBV satellite virus. HDV can either infect naïve patients simultaneously with HBV (coinfection), or chronically infected HBV carriers (superinfection)⁴. Approximately 5% of HBV carriers have been exposed to HDV, with a total of 15-20 million patients worldwide. HDV causes the most severe form of viral hepatitis with a twofold higher risk of developing cirrhosis, a threefold higher risk of developing hepatocellular carcinoma (HCC), and a twofold increased mortality in comparison with HBV monoinfection⁴⁻⁶.

HDV infection in different mouse models causes the MAVS-mediated activation of intra-hepatic expression of type-I IFN and IFN-stimulated genes (ISG) (e.g. 2'-5'-oligoadenylate synthetase - OAS - and myxovirus resistance gene A - MxA - among others), of the IFN-inducible pattern recognition receptor (PRR) RIG-I, and it also triggers the JAK/STAT signaling cascade⁷⁻⁹. Moreover, a recent *in vitro* study in cells of human origin has shown that MDA5 is the PRR responsible for HDV RNA detection¹⁰.

HDV is commonly considered a noncytotoxic virus, since HDV viremia has no correlation with the extent of liver disease, and hepatitis delta antigen (HDAg) expression in transgenic mice does not cause cytotoxicity in hepatocytes^{11,12}. HDV-associated hepatic damage is thus thought to be immune-dependent like in HBV and HCV infection^{13,14}. It is known that HDV patients have a higher frequency of CD4⁺ T and natural killer cells (NK) in peripheral blood than HBV and HCV patients, and that circulating NKs have an immunoregulatory rather than cytolytic phenotype^{15,16}. However, the interaction between the infected hepatocytes and the immune cells, as well as the

immunologic environment of the liver during HDV infection have not been elucidated, since the models available so far - developed in immunodeficient humanized mice^{7,17}, or mice not permissive to HBV coinfection¹⁸ - do not completely reproduce the characteristics of the infection as it occurs in humans.

Recently, we developed a mouse model of HDV replication that mimics most of the features of HDV infection in humans, including the induction of liver inflammation and liver injury, associated with the expression of genes involved in the development of HCC, cirrhosis, fibrosis, cell death, and proliferation⁹.

Aims of this work were to characterize the immune infiltrate in the liver of AAV-HBV/HDV coinfecting mice and to determine the underlying mechanisms of liver damage in this model.

Materials and methods

Animals and treatment

C57BL/6 mice were purchased from Harlan Laboratories (Barcelona, Spain). RAG1- (RAGB6), MAVS-, IFN α / β R- and IFN γ R- deficient mice, all of them on a C57BL/6 background, were bred and maintained at the animal facility of the University of Navarra. Six- to eight-week-old male mice were used in all experiments. Mice were kept under controlled temperature, light, and pathogen-free conditions. Mice were injected intravenously (i.v.) with the AAV vectors (5×10^{10} viral genomes (vg)/mouse in the case of AAV-HDV and AAV-HBV, or 10^{10} , 3×10^{10} or 10^{11} vg/mouse in the case of AAV-S-HDAg and AAV-L-HDAg) in a volume of 150 μ l. For all procedures, animals were anesthetized by intraperitoneal (i.p.) injection of a mixture of xylazine (Rompun 2%, Bayer) and ketamine (Imalgene 50, Merial) 1:9 v/v. Blood collection was performed by submandibular bleeding, and serum samples were obtained after centrifugation of total blood. Animals were euthanized by cervical dislocation after being anesthetized at the indicated time points. Liver samples were collected for histological analysis and for nucleic acid and protein extraction. The

experimental design was approved by the Ethics Committee for Animal Testing of the University of Navarra.

Viral constructs, vector production, and purification

AAV vectors were constructed based on the pAAV-MCS vector (Agilent Technologies). AAV-HDV was constructed by the insertion of 1.2x copies of the HDV genome (genotype 1) obtained from pDL456 plasmid (kindly provided by Professor John Taylor) under the transcriptional control of the liver-specific chimeric promoter composed of the albumin enhancer sequence and the α -1-antitrypsin promoter (Enh/AAT)¹⁹. AAV-HBV vector was constructed by insertion of 1.3x copies of the HBV genome (genotype D, serotype ayw) obtained from the pSP65 plasmid (kindly provided by Dr. Francis Chisari) into pAAV-MCS. The AAV genomes were packaged in AAV serotype 8 capsids (AAV8).

The coding sequences for HDAGs (genotype I) were amplified using the primers described in **Table 1**. Directed mutagenesis was performed to edit the STOP codon in position 1012 to a tryptophane codon and generate the L-HDAG coding sequence. Amplification products were digested with BamHI and BglII and inserted in the vector under the chimeric Enh/AAT promoter in order to generate the AAV-S-HDAG and AAV-L-HDAG vectors.

Recombinant AAV were produced by polyethyleneimine (PEI)-mediated co-transfection of 80% confluent HEK-293T cells with the packaging plasmid pDP8.ape (PF478, Plasmid Factory) and the plasmid carrying the HDV1.2x, HBV1.3x or HDAG expressing constructs. Cells were harvested 72 h post transfection and the virus was released from the cells by three rounds of freeze-thawing in lysis buffer (50 mM TRIS, 2 mM Cl₂Mg, 150 mM NaCl, 0,1% Triton X-100), and centrifugation. The resulting supernatant was then incubated with DNaseI and RNaseA (Roche) and added to an iodixanol gradient in an ultracentrifuge tube. After ultracentrifugation at 16° C and 69000 rpm for 2:30 hours (Beckman Coulter Type 70Ti rotor, Optima L-90 K Ultracentrifuge), the virus-containing layer was collected and concentrated in a PBS-sucrose 5 % solution.

Name	Sequence	Supplier
5pHDAg-BamHI	TTTTTGGATCCACCATGAGCCGGTCCGAGTCGAGGAAGAACC	Sigma-Aldrich
3pSHDAg-BGIII	AAAAAAGATCTCTATGGAAATCCCTGGTTACCCCTG	Sigma-Aldrich
3pLHDAg-BGIII	TTTTTAGATCTTCACTGGGGTCGACAACTCTGGGGAGAAAAGGGCGG ATCGGCAGGAAAGAGTATATCCCATGGAAATCCC	Sigma-Aldrich

Table 1 Primers used for amplification and cloning of HDAg coding sequences.

Statistical analysis

Statistical analysis was performed using GraphPad Prism 5.0 software. The data are presented as mean values \pm standard deviation. Differences in alanine aminotransferase (ALT) levels, in gene expression, and in % of stained tissue area among groups were analyzed with one-way ANOVA followed by Bonferroni multiple-comparison test or by non-parametric one-way ANOVA (Kruskal-Wallis test) followed by Dunns' multiple comparison test. A p-value ≤ 0.05 was considered significant.

Serum ALT levels.

ALT serum levels were analyzed with a Hitachi Automatic Analyzer (Boehringer Mannheim, Indianapolis, IN).

RNA isolation, reverse transcription and quantitative PCR (RT-qPCR).

Total RNA from liver samples and cell lines was isolated using TRIzol Reagent (Invitrogen) according to the manufacturer's instructions. Viral nucleic acids were extracted from serum samples using the QIAmpViral RNA Mini Kit (Qiagen). Total RNA was pre-treated with DNase I using the TURBO DNasefree™ Kit (Applied Biosystems) and retro-transcribed into complementary DNA (cDNA) using M-MLV reverse-transcriptase (Invitrogen). Real-time quantitative polymerase chain reaction assays (RT-qPCR) were performed using iQ SYBR Green Supermix (BioRad) in a CFX96 Real-Time Detection System (BioRad) and primers specified in **Table 2**. HDV strand-specificity was

analyzed as described elsewhere²⁰. Known amounts of HDV- or HBcAg sequence-containing plasmid were used as a standard curve for quantification.

Name	Sequence	Supplier
HDV Forward Primer	GGACCCCTTCAGCGAACA	Sigma-Aldrich
HDV Reverse Primer	CCTAGCATCTCCTCTATCGCTAT	Sigma-Aldrich
HBsAg Forward Primer	GGTTCTTCTGGACTATCAAGGTATGT	Sigma-Aldrich
HBsAg Reverse Primer	ATSGAGGTTCTTGAGCAGTAGTCAT	Sigma-Aldrich
HBcAg Forward Primer	TTCGCACTCCTCCAGCTTAT	Sigma-Aldrich
HBcAg Reverse Primer	GGCGAGGGAGTTCTTCTTCTA	Sigma-Aldrich
GAPDH Forward Primer	TGAACCACCAACTGCTTA	Sigma-Aldrich
GAPDH Reverse Primer	GGATGCAGGGATGATGTTC	Sigma-Aldrich
IFN α 1 Forward Primer	TCTCTCCTGCCTGA	Sigma-Aldrich
IFN α 1 Reverse Primer	CACAGGGGCTGTGTTTCTTC	Sigma-Aldrich
IFN β 1 Forward Primer	ATGAGTGGTGGTTGCAGGC	Sigma-Aldrich
IFN β 1 Reverse Primer	ACCTTTCAAATGCAGTAGATTCA	Sigma-Aldrich
IFN γ 1 Forward Primer	TCAAGTGGCATAGATGTGGAAGAA	Sigma-Aldrich
IFN γ 1 Reverse Primer	TGGCTCTGCAGGATTTTCATG	Sigma-Aldrich
IFN λ Forward Primer	AGCTGCAGGCCTTCAAAAAG	Sigma-Aldrich
IFN λ Forward Primer	TGGGAGTGAATGTGGCTCAG	Sigma-Aldrich
ADAR1 Forward Primer	AGCCTGTGTACCTGAAATCTGTAAC	Sigma-Aldrich
ADAR1 Reverse Primer	TTGACAATAAAGGGATAGCGTAGTC	Sigma-Aldrich
MxA Forward Primer	ATCTGTGCAGGCACTATGAG	Sigma-Aldrich
MxA Reverse Primer	CCTTCCTTCTTAGCCTTCC	Sigma-Aldrich
ISG15 Forward Primer	GATTGCCAGAAGATTGGTG	Sigma-Aldrich

Name	Sequence	Supplier
ISG15 Reverse Primer	TCTGCGTCAGAAAGACCTCA	Sigma-Aldrich
PKR Forward Primer	TGGGCAGACAATGTATGGTACA	Sigma-Aldrich
PKR Reverse Primer	TGTGACAACGCTAGAGGATG	Sigma-Aldrich
IP10 Forward Primer	CCAGTGAGAATGAGGGCCATA	Sigma-Aldrich
IP10 Reverse Primer	CTCAACACGTGGGCAGGAT	Sigma-Aldrich
2'-5'OAS Forward Primer	ACTGTCTGAAGCAGATTGCG	Sigma-Aldrich
2'-5'OAS Reverse Primer	TGGAACTGTTGGAAGCAGTC	Sigma-Aldrich
TGF β Forward Primer	TGGAGCAACATGTGGAACTC	Sigma-Aldrich
TGF β Reverse Primer	CAGCAGCCGTTACCAAG	Sigma-Aldrich
TNF α Forward Primer	ACGTGGAAGTGGCAGAAGAG	Sigma-Aldrich
TNF α Reverse Primer	CTCCTCCACTTGGTGGTTTG	Sigma-Aldrich
NK1.1 Forward Primer	TCATCCTCCTTGTCTGACC	Sigma-Aldrich
NK1.1 Reverse Primer	TTGAATGAGCAGCAAAGTGG	Sigma-Aldrich
CD4 Forward Primer	GAGAGTCAGCGGAGTTCTC	Sigma-Aldrich
CD4 Reverse Primer	CTCACAGGTCAAAGTATTGTT	Sigma-Aldrich
CD8 Forward Primer	CCAGAGACCAGAAGATTGTCG	Sigma-Aldrich
CD8 Reverse Primer	AGAAGGGCCACGCAGATT	Sigma-Aldrich

Table 2 Primers used for quantitative real-time PCR.

Patient sera

Samples and data from patients included in the study were provided by the Biobank of the University of Navarra and were processed following standard operating procedures approved by the

Ethical and Scientific Committees. We analyzed several patients for anti-HDAg reactivity and selected the serum from patient CUN-36.

Histology and immunohistochemistry (IHC).

Liver sections were fixed with 4% paraformaldehyde (PFA), embedded in paraffin, sectioned (3 μ m), and stained with hematoxylin and eosin. Sections were mounted and evaluated histologically by light microscopy.

For HDAg IHC analysis, PFA-fixed liver sections were deparaffinized, rehydrated and subjected to heat-mediated antigen retrieval in 0,01 M Tris-1 mM EDTA pH9 at 95°C for 30 min in a Pascal pressure chamber (Dako, S2800). Endogenous peroxidase and biotin were blocked with 3% H₂O₂ in deionized water for 10 min or with the avidin-biotin blocking system (Dako, X0590) respectively, prior to incubating the sample with serum CUN-36 diluted 1:30.000 at 4°C overnight. Incubation was followed by secondary antibody (biotinylated sheep anti-human IgG, (GE Healthcare, UK; 1:200) for 30 min at RT) and streptavidin-HRP, diluted (Burlingame, CA; 1:200) for 30 min, at RT. NeutrAvidin High Sensitivity HRP conjugate (Thermo Scientific) in combination with Metal-Enhanced DAB (Thermo Scientific Pierce) was used to detect HDAg. Cell nuclei were counterstained with hematoxylin.

Commercial antibodies were used for the other IHC: HBcAg (Dako B0586; 1:8.000), CD4 (Abcam ab183685; 1:1.000), CD8a (Cell Signaling 98941; 1:400), CD45 (BioLegend 103102; 1:2.000), Ly-6G and Ly-6C (Abcam ab2557; 1:10.000), F4/80 (BioLegend 123102; 1:400). All reactions required antigen retrieval by heating for 30 min at 95 °C in 0,01 M Tris-1 mM EDTA pH 9, except for Ly-6G/Ly-6C staining that required a pretreatment with proteinase K 20 μ g/ml for 30 min at 37°C, and HBcAg reaction that required none. Incubations with primary antibodies at their optimal dilutions were performed overnight at 4°C. After rinsing in TBS-T, the sections were incubated with the corresponding secondary antibodies for 30 min at RT as described in **Table 3**. Peroxidase activity was revealed using DAB⁺ and sections were lightly counterstained with Harris

hematoxylin. Finally, slides were dehydrated in graded series of ethanol, cleared in xylene and mounted with Eukitt (Labolan, 28500).

Antibody	Manufacturer and reference	Origin	Antigen retrieval	Dilution	Detection system
<i>HDV</i>		Human	TE, pH = 9, 95°C, 30 min	1:30.000	Sheep-anti-human biotinylated ¹ Streptavidin-HRP ²
<i>HBcAg</i>	Dako, B0586	Rabbit (polyclonal)	None	1:8.000	EnVision anti-rabbit ³
<i>CD4</i>	Abcam, ab183685	Rabbit (clone EPR19514)	TE, pH = 9 95°C, 30 min	1:1.000	EnVision anti-rabbit ³
<i>CD8a</i>	Cell Signaling, 98941	Rabbit (clone D4W2Z)	TE, pH = 9, 95°C, 30 min	1:400	EnVision anti-rabbit ³
<i>CD45</i>	BioLegend, 103102	Rat (clone 30-F11)	TE, pH = 9, 95°C, 30 min	1:2.000	Rabbit-anti-rat ⁴ EnVision anti-rabbit ³
<i>Ly-6G/6C</i>	Abcam, ab2557	Rat (clone NIMP-R14)	PK 20 µg/ml; 37°C, 30 min	1:10.000	Rabbit-anti-rat ⁴ EnVision anti-rabbit ³
<i>F4/80</i>	BioLegend, 123102	Rat (clone BM8)	PK 20 µg/ml; 37°C, 30 min	1:400	Rabbit-anti-rat ⁴ EnVision anti-rabbit ³

Table 3 *Antibodies used for immunohistochemistry and corresponding detection system.* ¹Sheep-anti-human biotinylated, GE Healthcare, RPN1003V (1:200); ²Streptavidin-HRP, Vector Labs SA5004 (1:200); ³EnVision anti-rabbit, Dako, K401; ⁴Rabbit anti-rat, Dako, E0468 (1:200); PK: proteinase K; TE: 10mM Tris, 1 mM EDTA.

Image acquisition was performed on an Aperio CS2 slide scanner using ScanScope Software (Leica Biosystems). All images were stored in uncompressed 24-bit color TIFF format and image analysis was performed using a plugin developed for Fiji, ImageJ (NIH, Bethesda, MD).

Isolation of intrahepatic leukocytes

Mice were perfused via the portal vein with 10 ml of Ca²⁺- and Mg²⁺-free phosphate buffer solution preheated to 37°C. After perfusion, the vena cava was cut and the liver extracted. After incubation in 10 ml of phosphate-buffered saline (PBS) containing 1,000U of type II collagenase (Gibco) for

20 min, the liver homogenate was passed through a 70- μ m nylon cell strainer, and the cell suspension was centrifuged at 1,200 rpm for 10 min. The cell pellet was resuspended in 40% Percoll and was centrifuged at 1,800 rpm for 10 min. Red blood cells were removed using erythrocyte lysis buffer (NH_4Cl 0.15M, KHCO_3 10 mM, EDTA_2Na 0.1 mM); the remaining cells were washed and were resuspended in RPMI 1640 medium.

Antibodies and Cytometry

Cells were labeled with the following antibodies according to the manufacturer's recommendations: anti-CD4-FITC (clone H1.2F3, BD), anti-CD44-PE (BD), anti-CD25-PE and -APC (both ImmunoTools), anti-CD8-FITC (ImmunoTools), anti-CD44-PE (ImmunoTools), anti-NK1.1-PE (clone PK136, BD), anti-CD3-PerCP (clone 17A2, Biolegend), anti-CD11c-APC (clone HL3, BD), anti-CD11b-FITC (ImmunoTools), anti-F4/80-PE (clone BM8, Biolegend), anti-CD19-APC (ImmunoTools), anti-CD25-PE (ImmunoTools), anti-FoxP3-Alexa647 (clone 150DTE439, eBioscience), anti-Sca-1-APC (clone D-7, Biolegend), anti-CD16/32-APC (ImmunoTools), anti-CD80-BV421 (clone 16-10A1, Biolegend).

Data were acquired with an 8-color BD FACSCanto II system equipped with three lasers (488 nm, 633 nm, and 405 nm) or with a 4-color FACSCalibur system equipped with two lasers (argon [488 nm] and diode [635 nm]). Data were analyzed with FlowJo (FloJo LLC).

NK cells and macrophage depletion

Mice were NK-depleted by IP administration of 500 mg of the anti-mouse NK1.1 antibody (PK136, BioXcell) 2 days before virus injection and subsequently every 48 hours until day 6 post-infection. Depletion levels of circulating NK cells were determined to be ~98% by flow cytometry on whole blood. Irrelevant mouse immunoglobulin isotypes were used as controls (BE0085 clone C1.18.4, BioXcell).

Macrophage depletion was achieved by i.v administration of 100 μ l clodronate liposomes (Clodlip BV) 2 days before virus injection and then every 4 days until day 6 post-infection.

Results

The liver inflammatory infiltrate of AAV-HDV-treated mice is composed of activated CD4⁺ and CD8⁺ T cells, dendritic cells, inflammatory macrophages and natural killer cells.

We have recently developed a mouse model of HBV-HDV infection based on AAV-mediated delivery of replication competent genomes that reproduces important characteristics of human HDV infection. In this mouse model, we detected the presence of an important inflammation in the liver of AAV-HBV/HDV coinfecting mice at 45 days after vector injection⁹. For a better characterization of the hepatic inflammation observed in mice, C57BL/6 were injected with AAV-HBV, AAV-HDV and AAV-HBV/HDV or saline (control). Mice were sacrificed 21 and 45 days after injection, and liver sections were analyzed by immunostaining for the common leukocyte marker CD45 to confirm and quantify hepatic liver infiltration. At day 45, the extent of the immune infiltrate was significantly higher in mice that had received AAV-HDV alone or in combination with AAV-HBV than in AAV-HBV or untreated animals [Figure 1].

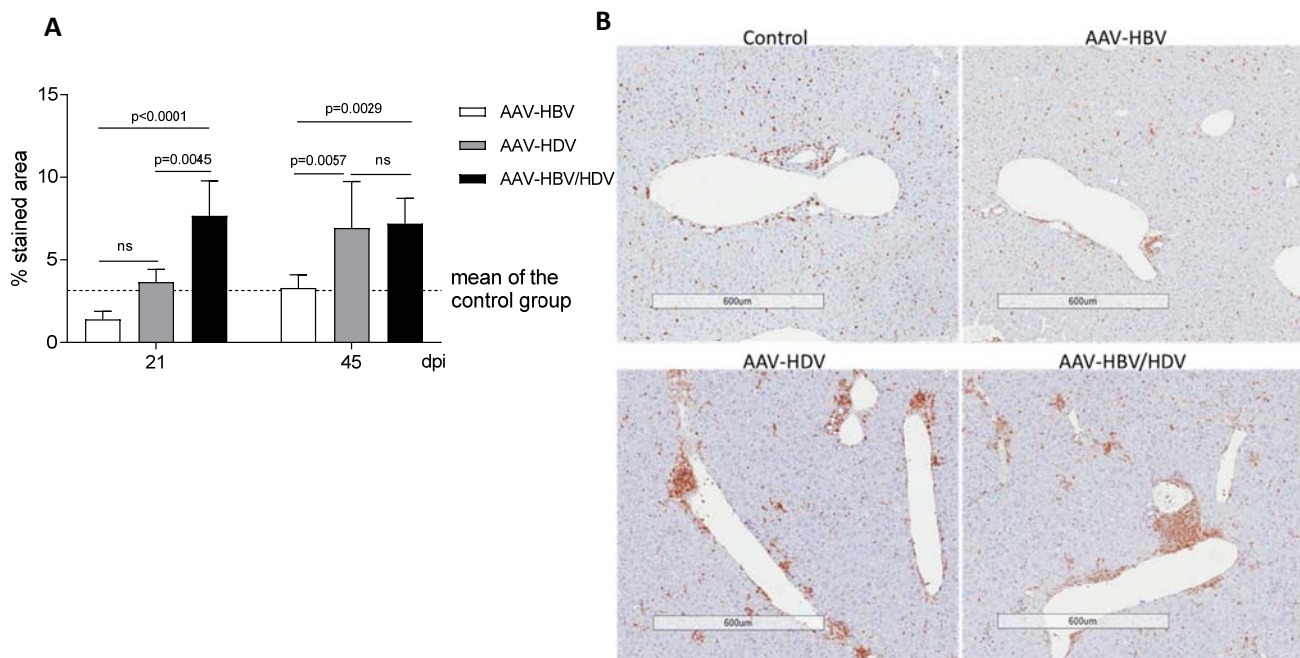


Figure 1 The presence of HDV induces liver inflammation. 21 and 45 dpi mice were sacrificed, and livers were submitted to immunohistochemistry for the pan-leukocyte marker CD45. A) Data are given as mean values \pm standard deviation (n=4) and significance was determined by two-way ANOVA followed by Bonferroni multiple-comparison test. B) One representative picture of non-infected, AAV-HBV, AAV-HDV and AAV-HBV/HDV infected mice (4X). dpi = days post infection.

In order to characterize the infiltrate, intrahepatic leukocytes isolated 21 dpi from the four experimental groups were analyzed by flow cytometry. The percentage of CD4⁺ and CD8⁺ did not change between groups; nevertheless, there is an enrichment in activated (CD25⁺) CD4⁺ and CD8⁺ subpopulations in the animals receiving AAV-HDV [Figure 2 A, B]. In those animals we also observed an increase in DCs (CD11c⁺) and NK1.1⁺ cells, while NKT cells and B lymphocytes (CD19⁺) proportions were decreased in comparison to AAV-HBV or control animals [Figure 2 C].

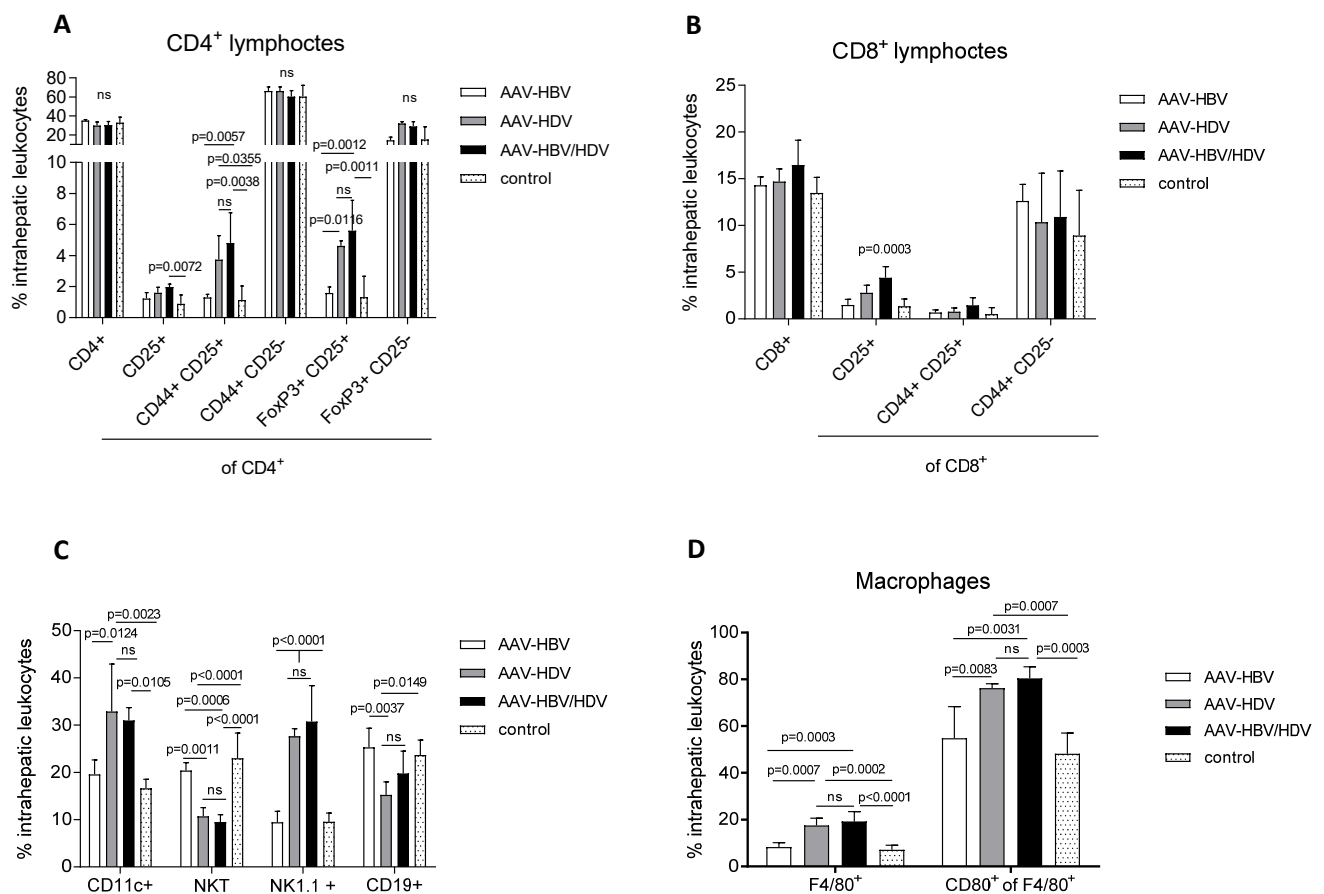


Figure 2 Activated T lymphocytes, NK cells, DCs and pro-inflammatory macrophages account for the majority of the immune cells infiltrating the HDV-infected liver. Intrahepatic leukocytes isolated from wild-type mice 21 dpi were analyzed by flow cytometry. Graphs show (A, B) the percentage of T lymphocytes, (C) DC, NKs, NKTs and B lymphocytes and (D) macrophages. Data are given as mean values \pm standard deviation (n=5) and significance were determined by two-way ANOVA followed by Bonferroni multiple-comparison test.

Furthermore, the percentage of liver macrophages, in particular the pro-inflammatory CD80⁺ subpopulation, increased significantly in AAV-HDV mice in comparison to the other two groups

[Figure 2 D]. In summary, activated T lymphocytes, NK cells, DCs and pro-inflammatory macrophages account for the majority of the immune cells infiltrating the HDV-infected liver.

Flow cytometry results were corroborated by immunohistochemistry. A significant increase in CD4⁺ lymphocytes was observed in AAV-HBV/HDV coinfecting mice 21 and 43 dpi, and in AAV-HDV infected mice at day 43 [Figure 3 A]. On the other hand, the percentage of CD8⁺ area was higher in the presence of HDV from day 21 post infection [Figure 3 B]. Similarly, the increase of intrahepatic macrophages observed by cytometry 21 dpi is confirmed by IHC and persists 43 dpi [Figure 3 C]. Immunostaining allowed the detection of a significant increase in the proportion of neutrophils (Ly-6G/6C⁺ cells) in AAV-HDV monoinfected mice in comparison to the control and AAV-HBV monoinfection groups [Figure 3 D].

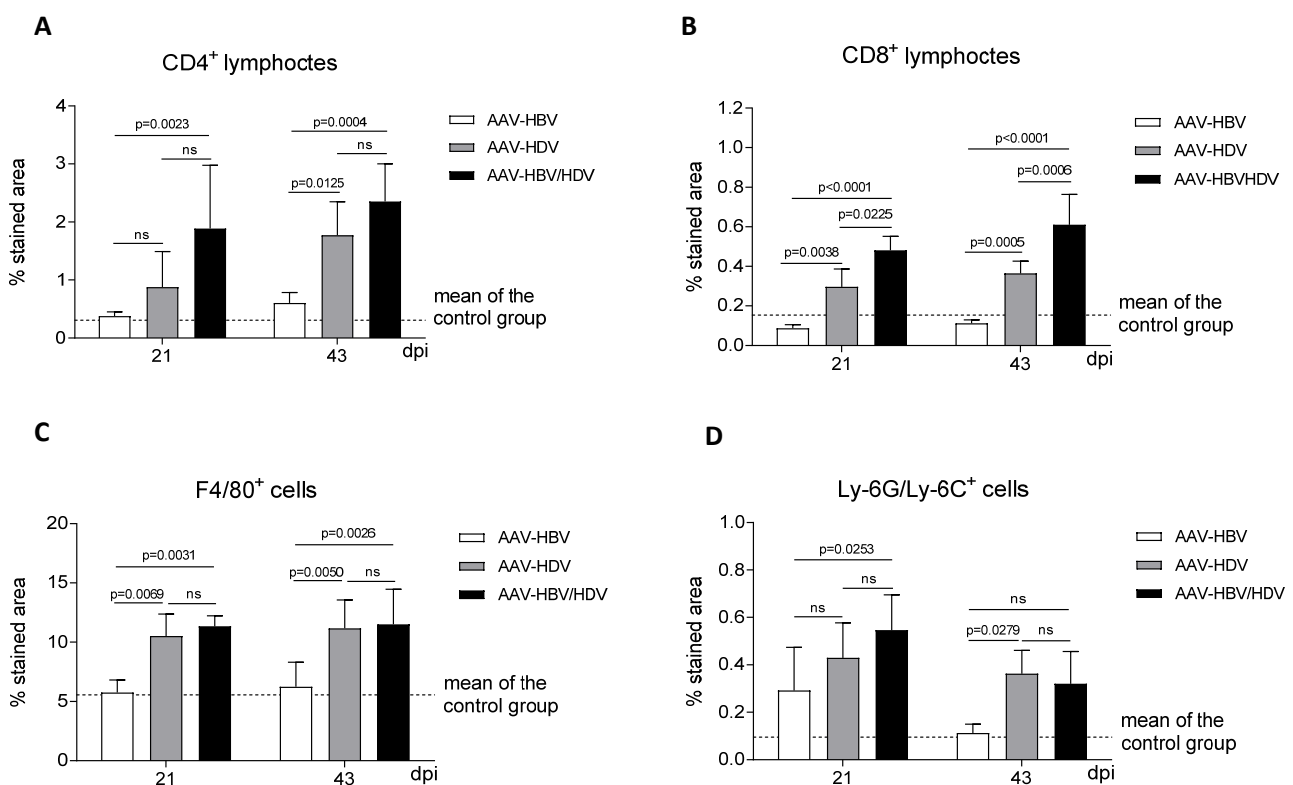


Figure 3 The proportion of macrophages and CD4⁺, as well as CD8⁺ lymphocytes, increases with time in AAV-HDV and AAV-HDV/HDV infected mice with time. Liver sections of wild-type mice of the four experimental groups sacrificed 21 and 43 dpi, were analyzed by IHC. Graphs show the percentage of positive immunohistochemically stained area for (A, B) CD4⁺ and CD8⁺ lymphocytes, (C) macrophage- and (D) neutrophil-specific markers. Data are given as mean values \pm standard deviation (n=4) and differences between groups were analysed by two-way ANOVA followed by Bonferroni multiple-comparison test.

Taken together these data suggest that cells from both the innate and the adaptive arms or the immune system are activated in hepatitis delta infection and may have a role in HDV-induced pathogenesis.

Intrahepatic leukocytes contribute to the type-I IFN response induced by HDV.

Next, we wanted to determine whether the strong and sustained type-I IFN response associated with AAV-HDV infection that we previously observed⁹ was ascribable to the leukocyte infiltrate. Eight-week-old male C57BL/6 mice were divided into four different groups (n=5) and received 5×10^{10} genome copies of AAV-HDV, of AAV-HBV, of both AAV-HDV and AAV-HBV (AAV-HBV/HDV), or were left untreated (uninfected control group); intrahepatic leukocytes (IHL) were isolated 21 days after vector injection. The expression levels of IFN- β , IFN- γ , IFN- λ , TNF- α , TGF- β and different ISGs were analyzed in RNA extracted from total liver and from IHLs. The study of gene expression revealed that IHLs contribute to the overall liver expression of TGF- β and ISG15, ADAR-1, IP10, PKR and USP18 among the analyzed ISGs, while the expression of IFN- β , IFN- γ , IFN- λ , TNF- α , and MxA is largely independent of the immune cells [Figure 4]. There is no difference in the mRNA levels of the analyzed genes between AAV-HBV-infected mice and the control group (data not shown).

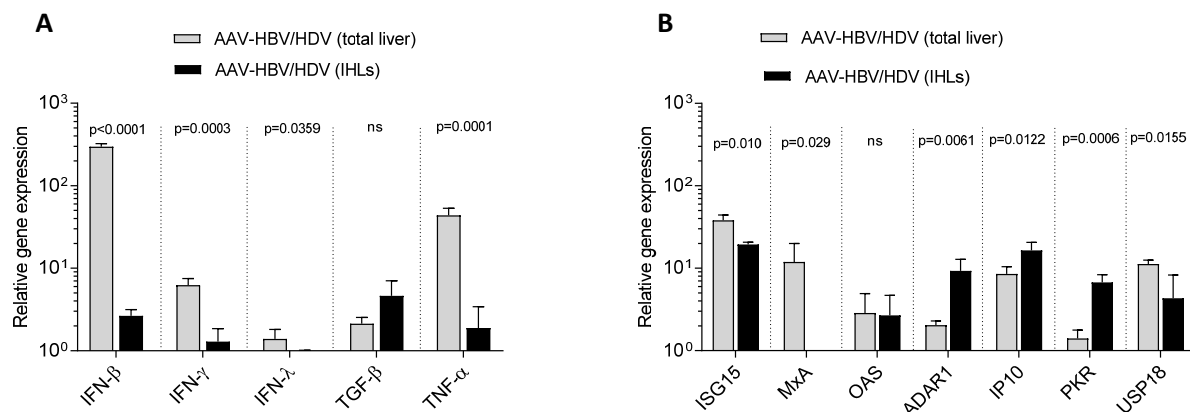


Figure 4 HDV induces a strong type-I IFN response, put into effects by both parenchymal cells and intrahepatic leukocytes. 21 days after vector injection mice were sacrificed and intrahepatic leukocytes were isolated. Total RNA from total liver and intrahepatic leukocytes was extracted to determine the contribution of resident and recruited immune cells to the expression of cytokines (A) and ISGs (B). The relative gene expression was calculated with the $2^{-\Delta\Delta Ct}$ method²⁹, using the uninfected group as control group and GAPDH as housekeeping gene. All data are given as mean values \pm standard deviation (n=5) and significant differences between total liver and IHL for each gene are determined by t test.

Liver damage is observed in AAV-HBV/HDV coinfecting wild-type as well as in IFN α / β R KO, IFN γ R KO and MAVS KO mice

One of the most remarkable features of this HDV animal model in comparison to the previously developed ones is the development of liver damage associated with HDV replication and/or antigen expression. In order to determine the relevance of the innate immune response, in particular of type-I and type-II IFNs, in the HDV-induced liver damage, C57BL/6 wild-type, IFN α / β R KO, IFN γ R KO, and MAVS KO (in which IFN- β was not detected after AAV-HDV administration⁹) were administered with AAVHBV/HDV and 7, 14 and 21 dpi ALT levels were analyzed. As early as day 7 post-infection, ALT levels increase above the normal range in all the groups of animals. At day 14 levels were higher than at day 7, and they were significantly higher in IFN α / β R KO in comparison to the rest of the groups. The levels further increased by day 21 with no significant differences among the groups [Figure 5].

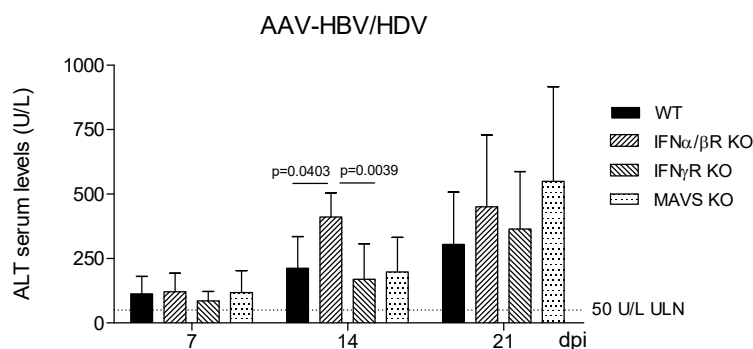


Figure 5 Levels of alanine aminotransferase increase beyond the physiological range in AAV-HBV/HDV coinfecting mice, for all the lineages analyzed. Eight-week-old mice of each lineage received 5×10^5 genome copies of AAV-HDV and AAV-HBV. Peripheral blood was collected every seven days after vector injection and alanine aminotransferase (ALT) concentration in serum was measured. Data are given as mean values \pm standard deviation ($n = 10$) and significance levels between groups at each time point are determined by nonparametric one-way ANOVA (Kruskal-Wallis test) followed by Dunns multiple-comparison test. The dotted line represents the ALT upper limit of normal (ULN, 50U/L).

Moreover, 21 dpi with AAV-HBV/HDV, the typical pattern of liver damage, characterized by sanded nuclei and “ground-glass” hepatocytes, ballooning degeneration, mitotic figures and Councilman bodies was present. All lineages shared the same pattern [Figure 6]. These data indicate that IFN- α and IFN- γ are not required for the observed hepatic damage, and that MAVS does not play a role in the HDV-induced liver damage independently of IFN- α and IFN- γ as has been described for HAV²¹. It is noteworthy to point out that similar levels of HDV RNA and HDAg expression were detected in all groups [Figure S1].

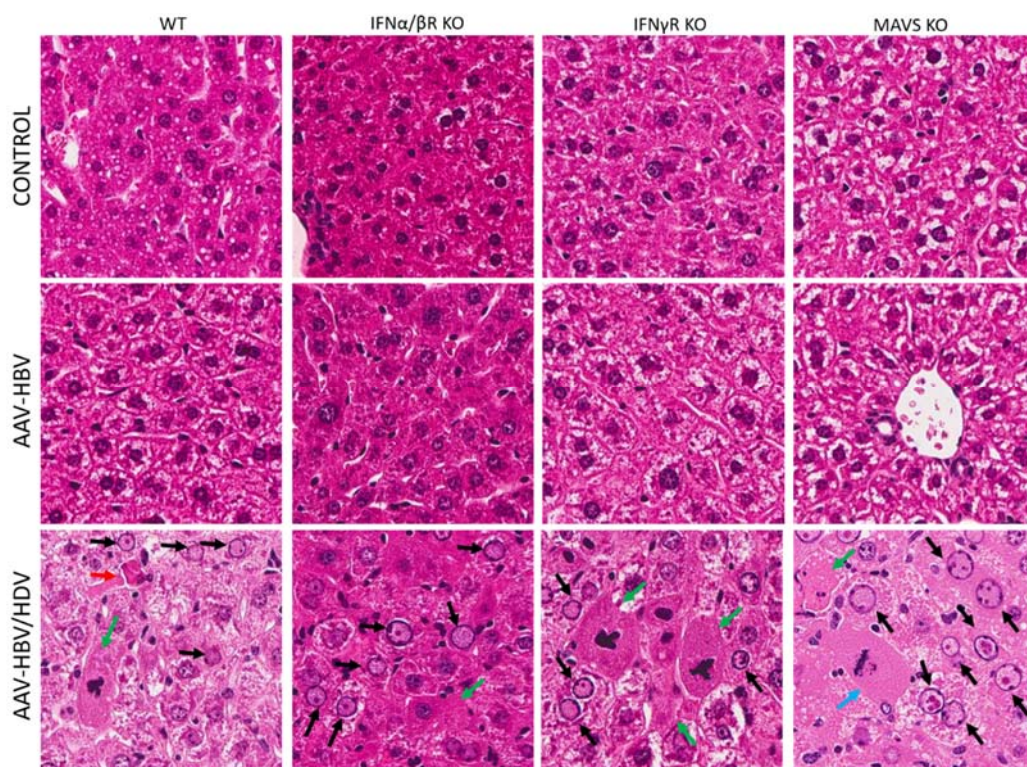


Figure 6 Coinfection with AAV-HBV and AAV-HDV induced liver damage in all mouse strains. Liver sections of wild-type and KO mice sacrificed 21 days post-infection, were stained with hematoxylin and eosin. Histological evaluation revealed the presence of ground-glass hepatocytes (black arrow), ballooning degeneration (green arrow), mitotic figures (light blue arrow) and Councilman bodies (red arrow). One representative picture of non-infected, AAV-HBV and AAV-HBV/HDV infected mice is shown for each of the analyzed lineages (20x).

Neither T cells, macrophages, or natural killer cells are a pre-requisite for liver damage.

In order to determine the role of the different cell subtypes infiltrating the liver on HDV-induced liver damage, *Rag1*^{-/-} mice lacking T and B cells were injected with AAV-HBV/HDV, and transaminase levels were measured 7, 14 and 21 days after injection. As shown in **Figure 7** transaminase levels increase as previously observed in WT mice. Therefore, we excluded a main role for cytotoxic T lymphocytes in the induction of liver damage.

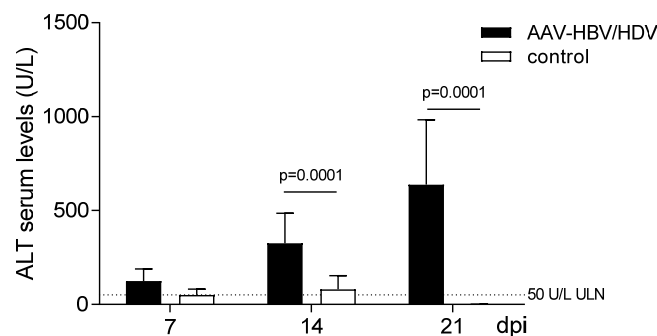


Figure 7 Levels of alanine aminotransferase increase beyond the physiologic range in AAV-HBV/HDV coinfecting C57BL/6 *Rag1*^{-/-} mice. Eight-week old mice received 5×10^{10} genome copies of AAV-HDV and AAV-HBV or were left untreated. Peripheral blood was collected 7, 14, and 21 days after vector injection to determine serum alanine aminotransferase (ALT) levels. Data are given as mean values \pm standard deviation (AAV-HBV/HDV n = 10, control n=5) and differences were analysed by two-way ANOVA followed by Bonferroni multiple-comparison test. The dotted line represents the ALT upper limit of normal (ULN, 50U/L).

To determine the role of NK cells and macrophages in the liver pathology, we performed depletion experiments in C7BL/6 WT mice. NK cells were depleted by intraperitoneal administration of 500 μ g of anti-NK1.1 antibody two days before virus injection and every 48 hours until day 6 post-infection; macrophage depletion was achieved by i.v. administration of 100 μ l of liposome containing clodronate two days before virus injection and every 4 days until day 6 post-infection. In both cases, we did not observe any difference between the depleted and the undepleted group 15 dpi in terms of ALT levels [**Figure 8**], virological parameters, and cytokine expression [**Figure S2**]. Interestingly, macrophages seem to have a protective role during the first week of infection, since transaminitis was observed at this time point only in mice treated with clodronate liposomes (CL).

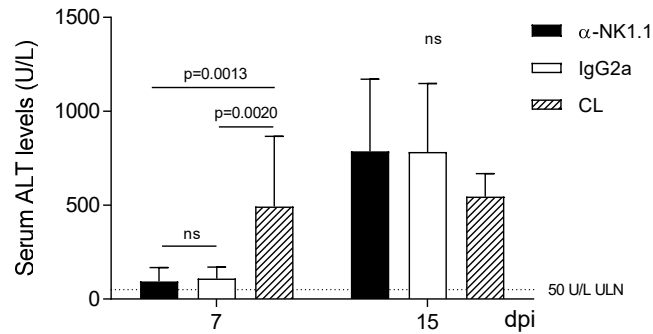


Figure 8 Macrophage depletion in C57BL/6 WT mice causes early transaminitis 7 dpi, while depletion of neither NK nor macrophage does not have any effect 15 dpi. C57BL/6 WT mice underwent macrophage or NK depletion with clodronate liposomes or α -NK1.1 antibody, respectively. Peripheral blood was collected 7 and 15 dpi to analyze serum ALT levels. Data are given as mean values \pm standard deviation (n=9 for 7 dpi and n=5 for 15 dpi). Differences between treatments for each time point were determined by one-way ANOVA followed by Bonferroni multiple comparison test. CL= clodronate liposomes. The dotted line represents the ALT upper limit of normal (ULN, 50U/L).

Injection of L-HDAg or S-HDAg alone causes dose-dependent cytotoxicity and liver damage without inflammatory infiltrate or ISG induction.

Taken together all the data obtained so far indicate that the activation of the innate and adaptive immune response are not responsible for the liver damage observed in AAV-HBV/HDV-injected mice, leaving HDAGs as the main candidates involved in hepatic injury. To determine the role of HDAG in liver damage, we produced AAV vectors expressing short or long HDAG under the control of a liver specific promoter (AAV-S-HDAg or AAV-L-HDAg). Next, eight-week-old C57 BL/6 male mice were divided into seven groups and received 1×10^{10} , 3×10^{10} or 1×10^{11} genome copies of AAV-S-HDAg or AAV-L-HDAg, or were left untreated. Both antigens caused liver damage as detected by means of high ALT serum levels and histological alterations of the liver. It stands out that the liver damage induced by L- or S-HDAg follow different kinetics [Figure 9]. L-HDAg-infected mice present a peak in ALT serum levels around 7 dpi, while in the case of S-HDAg-infected mice the peak is one week delayed. The dose-dependent effect is evident for L-HDAg expressing vectors, while in the case of ALT elevation caused by S-HDAg, the pattern observed looks like a reverse dose dependence 3 and 7 dpi, while this relation is lost at later time points. All the mice infected with the high dose of AAV-L-HDAg lose weight between the first and

the second week post-infection, concomitant to serum ALT elevation, and recovered by day 21 post-infection (data not shown).

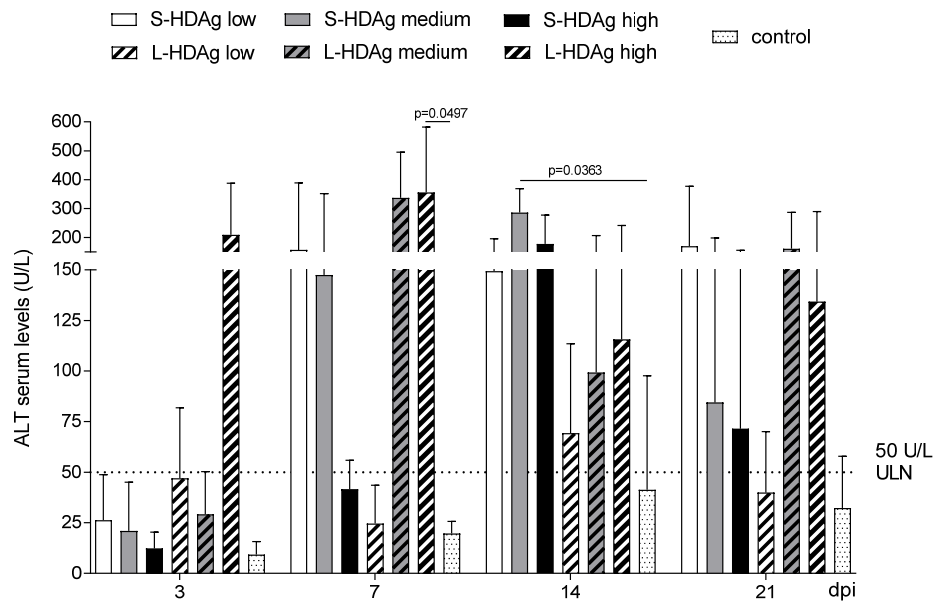


Figure 9 Levels of alanine aminotransferase in serum increase beyond the physiologic range in AAV-S-HDAg and AAV-L-HDAg infected mice. Data are given as mean values \pm standard deviation (n=4) and significant differences between different doses of the injected vectors and the control group at each time point are determined by one-way ANOVA followed by Dunnett's multiple-comparison test. The dotted line represents the ALT upper limit of normal (ULN, 50U/L).

Interestingly, 21 dpi, the percentage of liver staining positive for HDAg in AAV-S-HDAg infected mice detected by IHC, correlates inversely with the dose of the injected vector [Figure 10 A], suggesting that the higher dose induces a faster elimination of the transduced hepatocytes. This hypothesis is supported by the histological analysis, which shows a less altered tissue with no mitotic or apoptotic bodies and smaller hepatocytes derived from liver regeneration [Figure 10 C]. All the other groups present with cytoplasmic swelling, Councilman bodies, mitotic figures and a disorganized architecture of the liver parenchyma. In general, the three groups infected with AAV-L-HDAg show a very low percentage of HDAg⁺ area in the liver (<2%) 21 dpi. One mouse infected with the higher dose of S-HDAg died 14 dpi. IHC revealed that virtually all the hepatocytes were expressing the viral antigen (some showing cytoplasmic staining and others both nuclear and cytoplasmic staining) [Figure 10 B].

IHC for CD45 demonstrates the presence of immune infiltrate 21 dpi [Figure 11 C]. Gene expression analysis of the cytokines previously detected 21 dpi with AAV-HDV shows that IFN- β expression is not induced by either S- or L-HDAg alone; a slight induction of IFN- γ , TNF- α and TGF- β is observed, but the interpretation of these data is made difficult by the high variability [Figure 11 B]. Our data suggest a major role of HDAgs in HDV-induced liver pathology.

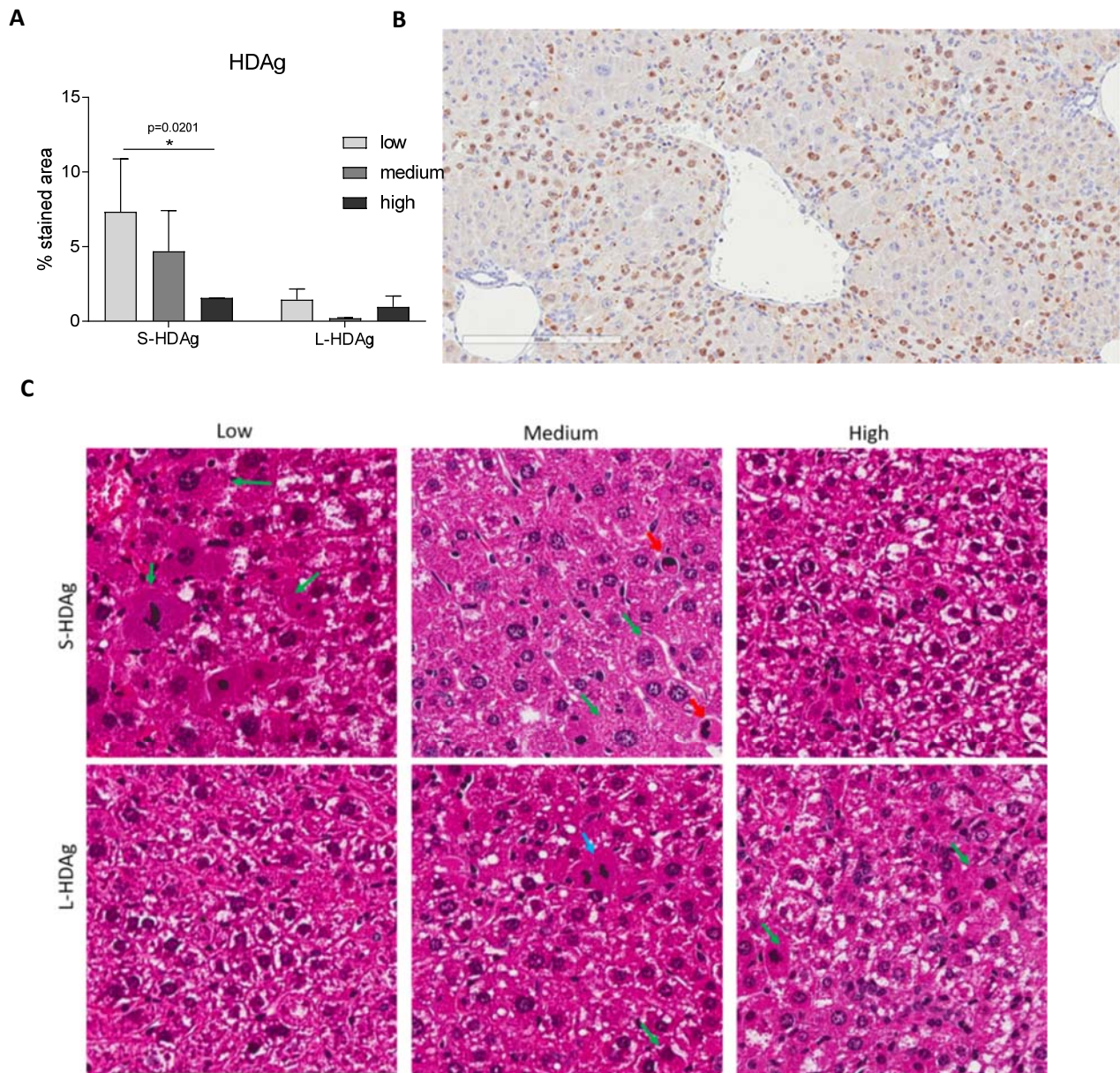


Figure 10 The percentage of HDAG⁺ area is very small in L-HDAg infected mice and inversely correlated with S-HDAg dose. Liver sections of mice sacrificed 21 days post-infection, were analyzed by IHC and stained with hematoxylin and eosin. (A) The graph shows the percentage of area positively stained for HDAG. Data are given as mean values \pm standard deviation (n=4) and differences were analyzed by two-way ANOVA followed by Bonferroni multiple-comparison test. (B) IHC staining for HDAG in a liver section of an AAV-S-HDAg mouse dead by 14 dpi (20x). (C) Histological evaluation revealed the presence of ballooning degeneration (green arrow), mitotic figures (light blue arrow), and Councilman bodies (red arrow). One representative picture of each dose of AAV-S-HDAg and AAV-L-HDAg is shown (20x).

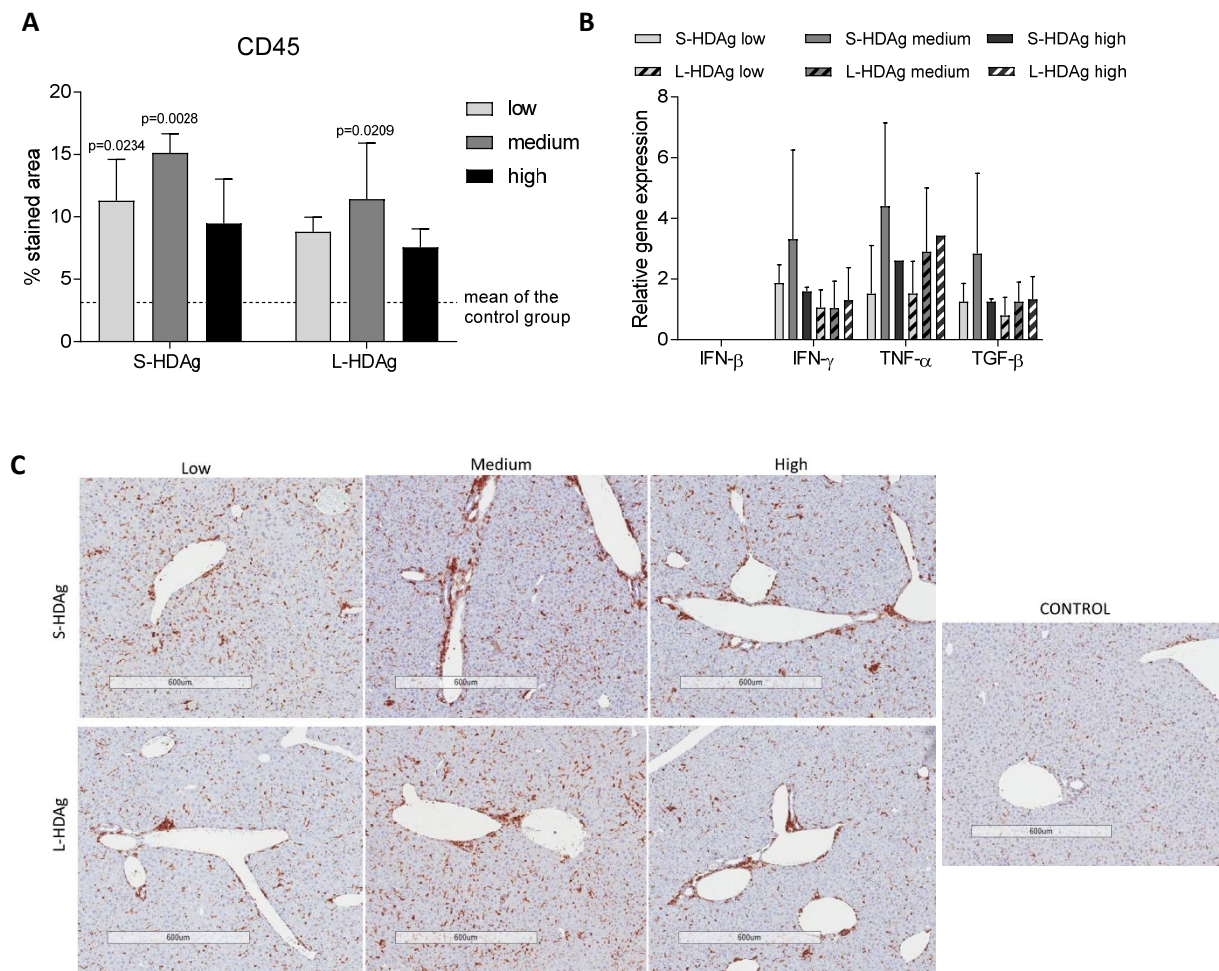


Figure 11 *AAV-S-HDAg or AAV-L-HDAg infection recruits immune cells into the liver and does not induce IFN- β expression.* Liver sections of mice sacrificed 21 dpi were analysed by IHC; (A) the graph shows the percentage of positive immunohistochemically stained area for CD45. Total RNA from liver was extracted 21 dpi; (B) cytokine relative gene expression was calculated with the $2^{-\Delta\Delta Ct}$ method, using the uninfected group as a control group and GAPDH as housekeeping gene. Data are given as mean values \pm standard deviation ($n=4/5$). Significant differences between treatments and the control group are determined by one-way ANOVA followed by Turkey's multiple comparison test. C) Immunostaining for CD45; one representative picture of each experimental group is shown (4x).

Supplementary

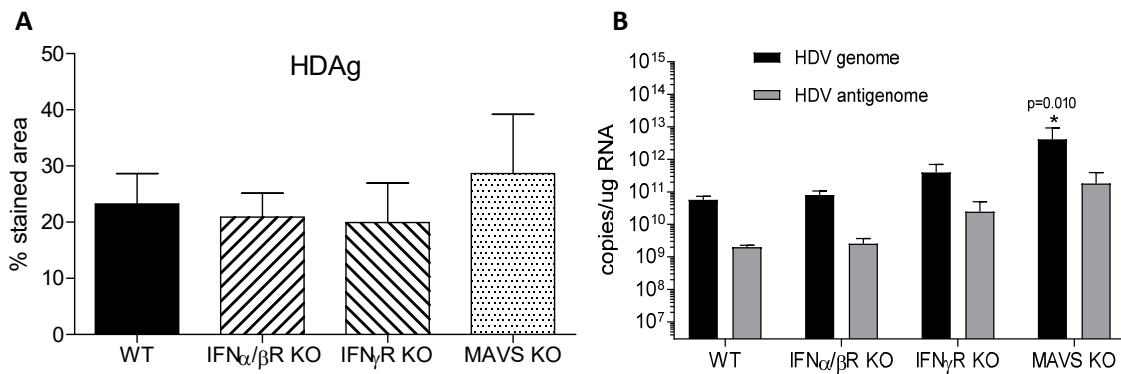


Figure S1 Similar levels of HDV Ag expression (A) and of genomic and antigenomic HDV RNA (B) were detected in WT and KO mice. HDV RNA copy numbers were calculated using a plasmid carrying HDV genome as a standard. All data are given as mean values \pm standard deviation (n = 5). Significant differences between treatments for each time point were determined by one-way ANOVA followed by Bonferroni multiple comparison test.

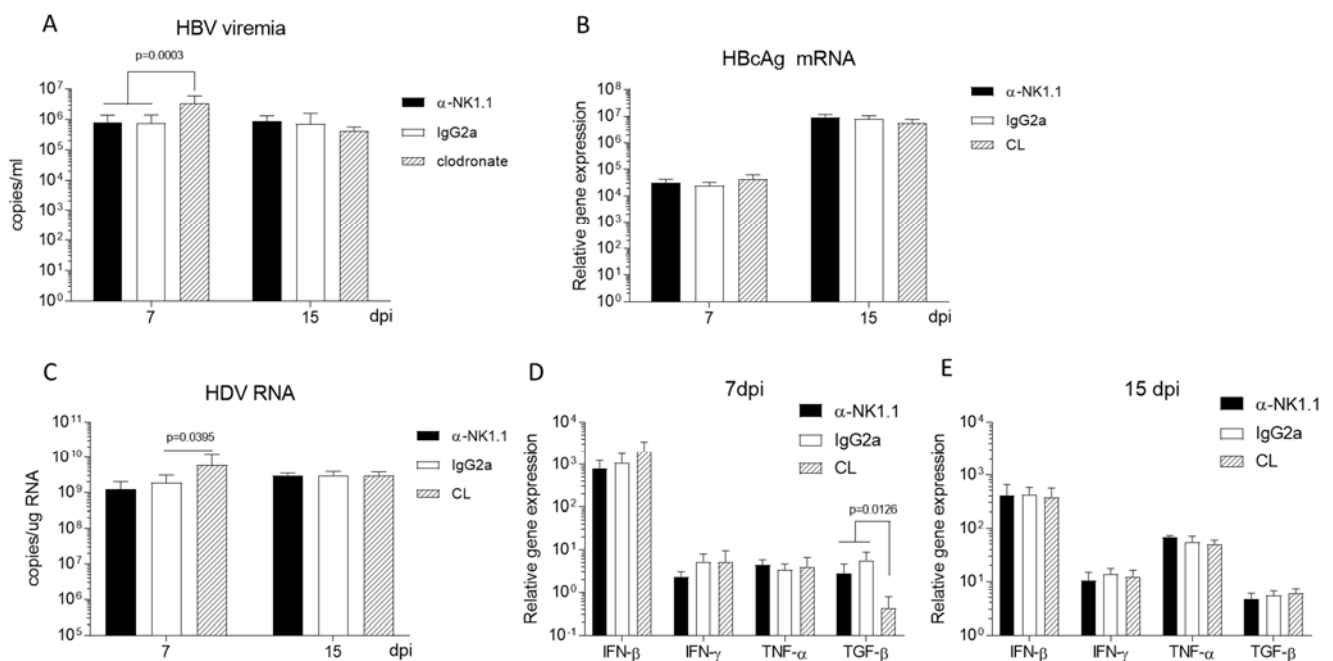


Figure S2 Depletion of macrophages or NKs depletion has no effect on virological parameters and cytokine expression 15 days post infection in C57BL/6 WT mice. Seven days post vector administration, higher HBV viremia (A) and higher levels of total HDV RNA (C) were detected in the liver of mice treated with clodronate liposomes. The drop in TGF- β expression levels in the same group 7 dpi (D) confirms macrophage depletion; this difference disappeared 15 dpi (E) when depletion had recovered. HBcAg (B) and cytokine relative gene expression (D,E) was calculated with the $2^{-\Delta\Delta C_t}$ method, using the uninfected group as a control group and GAPDH as housekeeping gene; HBV DNA (A) HDV RNA copy number (C) were calculated using a plasmid carrying HBcAg sequence and HDV genome as a standard, respectively. All data are given as mean values \pm standard deviation (n = 5). Differences between treatments for each time point are determined by one-way ANOVA followed by Bonferroni multiple comparison test. CL= clodronate liposomes.

Discussion

HDV infection causes the most severe form of viral hepatitis. The mechanisms involved in the pathogenesis of the disease remain unknown mainly because of the absence of simple animal models. We have recently demonstrated that coinfection with two AAV vectors carrying replication-competent genomes of HBV and HDV resulted in HDV hepatic replication and formation of HDV infectious particles in mice⁹. In this mouse model, HDV replication was associated with a MAVS-dependent activation of the innate immune system, a significant hepatic inflammatory response and liver injury. Here we show that the liver of AAV-HBV/HDV coinfecting animals present with the features commonly observed in patient biopsies -ground-glass hepatocytes with sanded nuclei, ballooning degeneration, mitotic figures and Councilman bodies^{22,23} - confirming the soundness of this mouse model as a tool to investigate the pathogenesis of hepatitis delta infection.

It is known that in some individuals, a strong innate immune response against a viral infection can lead to tissue damage and chronic disease rather than to viral clearance, as in the case of HCV¹³. For HDV infection, the interaction between the infected cells and the host immune system has not been characterized so far, and the same holds true for the viral factors responsible for the disease.

In our model, the strong induction of the type-I and type-II IFN response does not inhibit HDV replication, as was also reported in a recent *in vitro* study¹⁰, and it is in line with the low efficacy of PEG-IFN α , the only licensed therapy for chronic HDV infection²⁴.

The phenotypic characterization of the liver immune infiltrate in AAV-HBV/HDV coinfecting C57BL/6 mice showed activated CD4⁺ and CD8⁺ T cells, pro-inflammatory macrophages, DCs and NKs. We found that cells of the inflammatory infiltrate express high TGF- β levels as well as a number of ISGs, like ISG15, ADAR-1, IP10, PKR, and USP18. However, the expression of IFN- β , IFN- γ , IFN- λ , TNF- α , and MxA was significantly higher when mRNA extracted from the whole liver was analyzed²⁵, indicating that these molecules are mainly produced by the infected hepatocytes, pointing out the relevance of the intracellular innate immunity.

To determine the role of such a cell-intrinsic antiviral response in the liver pathology observed in AAV-HBV/HDV-infected mice, liver injury was analyzed in IFN α / β R KO and IFN γ R KO; our study revealed no differences compared to wild-type mice, indicating that the activation of the innate immune response plays no role in HDV-induced liver damage.

Despite the presence of populations with cytolytic potential in the infiltrate, such as T cells and NKs, our experiments with Rag1^{-/-} mice, lacking mature B, T, and NKT cells, suggest that these cell types are not responsible for the observed liver damage. Indeed, Rag1^{-/-} mice show the same pattern of hepatic disease and serum transaminase elevation. Moreover, the depletion of NK did not have any effect on HDV-induced liver damage, further excluding a role for this population in the disease. Interestingly though, the depletion of macrophages caused an exacerbation of the hepatic damage during the first week after infection, suggesting a protective role, as previously reported for Kupffer cells in HBV-transgenic mice, in which macrophages contain the pathology - possibly by removing dying infected hepatocytes - rather than worsen it²⁵.

These results led us to believe that innate and adaptive immune response are not the cause of tissue injury, pointing to the viral antigens as the triggers of liver damage. In fact, the administration of rAAVs carrying the coding sequence for L- or S-HDAg under the control of a liver specific promoter, caused a severe pathology, with high serum transaminase levels and histologic alterations (mitotic figures, cytoplasmic swelling, Councilman bodies, altered architecture of the parenchyma). However, analysis of the mRNA extracted from the liver of these animals revealed no IFN- β expression and a very low induction of other cytokines. This is in agreement with similar observations in HepG2-hNTCP cells¹⁰. This result suggests that the observed pathology is not entirely immune-mediated, but a direct cytotoxic effect of the HDAGs. Here we show that AAV-HDV/HDV-induced liver damage was resolved once the expression of HDV antigens had disappeared. Nevertheless, the presence of the inflammatory infiltrate 21 dpi does not correlate with the levels of antigen expression.

Our findings are in contrast to what previously published about an HDAg-transgenic mouse model, in which no histopathologic changes were observed at monthly or bimonthly intervals during 18 months¹². One possible explication for such a difference may be that in HDAg-tg mice, the synthesis of the transgenes could be regulated by the hepatocyte in order to not go above safe levels, or that, during the production of the transgenic lineage, mice more resistant to the detrimental effects of the antigens were selected. Interestingly, in our study, vector genomes completely disappeared by 21 dpi. More experiments are required, including the analysis of shorter time points, to determine the exact mechanisms involved in the disappearance of the HDAg expressing hepatocytes, and to determine how the antigens exert their cytotoxicity.

In preliminary experiments, we have observed that five months after AAV-HBV/HDV coinfection, the expression of the HDAGs is undetectable, in spite of genomic and anti-genomic HDV RNA still being present. Transaminases levels in serum and histology were normal. These observations support the hypothesis that the presence of HDV RNA itself or its replication are not sufficient to determine the liver pathology observed, and prompted us to investigate further the mechanisms underlying this phenomenon.

Taken together our results strongly discard the hypothesis that liver damage is mediated by a cellular immune response, and suggest the possibility of an attempt for a non-cytolytic mechanism for viral clearance, as already described in acute HBV-infected chimpanzees²⁶. Moreover, we did not detect significant caspase 3 activation by IHC in wild-type mice, therefore other kinds of programmed cell death, e.g pyroptosis, described in HIV infection²⁷, or necroptosis, correlated with high TNF- α expression levels²⁸, are to be considered.

In conclusion, our AAV-based mouse model has turned out to be a suitable tool for the study of hepatitis delta-associated disease, allowing us to characterize the hepatic immune infiltrate in the established infection and its role in the previously observed innate immune response. The results led us to discard a main role for the innate and adaptive immune responses in the liver injury, and we have highlighted the relevance of HDAG in the HDV-induced hepatic damage.

Bibliography

1. Rizzetto, M. The adventure of delta. *Liver Int.* **36**, 135–140 (2016).
2. Yan, H. *et al.* Sodium taurocholate cotransporting polypeptide is a functional receptor for human hepatitis B and D virus. *Elife* **1**, e00049 (2012).
3. Ni, Y. *et al.* Hepatitis B and D viruses exploit sodium taurocholate co-transporting polypeptide for species-specific entry into hepatocytes. *Gastroenterology* **146**, 1070–1083.e6 (2014).
4. Negro, F. Hepatitis D virus coinfection and superinfection. *Cold Spring Harb. Perspect. Med.* **4**, a021550 (2014).
5. Fattovich, G., Bortolotti, F. & Donato, F. Natural history of chronic hepatitis B: special emphasis on disease progression and prognostic factors. *J. Hepatol.* **48**, 335–52 (2008).
6. Fattovich, G. *et al.* Influence of hepatitis delta virus infection on morbidity and mortality in compensated cirrhosis type B. *Gut* **46**, 420–426 (2000).
7. Giersch, K. *et al.* Hepatitis Delta co-infection in humanized mice leads to pronounced induction of innate immune responses in comparison to HBV mono-infection. *J. Hepatol.* **63**, 346–353 (2015).
8. He, W. *et al.* Hepatitis D Virus Infection of Mice Expressing Human Sodium Taurocholate Co-transporting Polypeptide. *PLOS Pathog.* **11**, e1004840 (2015).
9. Suárez-Amarán, L. *et al.* A new HDV mouse model identifies mitochondrial antiviral signaling protein (MAVS) as a key player in IFN- β induction. *J. Hepatol.* **67**, 669–679 (2017).
10. Zhang, Z. *et al.* Hepatitis D Virus replication is sensed by MDA5 and induces IFN- β/λ

responses in hepatocytes. *J. Hepatol.* (2018). doi:10.1016/j.jhep.2018.02.021

11. Zachou, K. *et al.* Quantitative HBsAg and HDV-RNA levels in chronic delta hepatitis. *Liver Int.* **30**, 430–437 (2010).
12. Guilhot, S. *et al.* Expression of the Hepatitis Delta Virus Large and Small Antigens in Transgenic Mice. *J Virol* **68**, 1052–1058 (1994).
13. Bang, B. R., Elmasry, S. & Saito, T. Organ system view of the hepatic innate immunity in HCV infection. *Journal of Medical Virology* **88**, 2025–2037 (2016).
14. Bocher, W. O. *et al.* Regulation of the neutralizing anti-hepatitis B surface (HBs) antibody response in vitro in HBs vaccine recipients and patients with acute or chronic hepatitis B virus (HBV) infection. *Clin. Exp. Immunol.* **105**, 52–58 (1996).
15. Aslan, N. *et al.* Cytotoxic CD4⁺ T cells in viral hepatitis. *J. Viral Hepat.* **13**, 505–514 (2006).
16. Lunemann, S. *et al.* Compromised function of natural killer cells in acute and chronic viral hepatitis. *J. Infect. Dis.* **209**, 1362–73 (2014).
17. Lütgehetmann, M. *et al.* Humanized chimeric uPA mouse model for the study of hepatitis B and D virus interactions and preclinical drug evaluation. *Hepatology* **55**, 685–694 (2012).
18. He, W. *et al.* Modification of Three Amino Acids in Sodium Taurocholate Cotransporting Polypeptide Renders Mice Susceptible to Infection with Hepatitis D Virus In Vivo. *JOURNAL. Virol.* **90**, 8866–8874 (2016).
19. Kramer, M. G. *et al.* In vitro and in vivo comparative study of chimeric liver-specific promoters. *Mol. Ther.* **7**, 375–85 (2003).
20. Jardi, R. *et al.* Determination of hepatitis delta virus RNA by polymerase chain reaction in

- acute and chronic delta infection. *Hepatology* **21**, 25–29 (1995).
21. Hirai-Yuki, A. *et al.* MAVS-dependent host species range and pathogenicity of human hepatitis A virus. *Science* (80-.). **353**, (2016).
 22. Mani, H. & Kleiner, D. E. Liver biopsy findings in chronic hepatitis B. *Hepatology* **49**, S61–S71 (2009).
 23. Verme, G. *et al.* A histological study of Hepatitis Delta Virus Liver Disease. *Hepatology* **6**, 1303–1307 (1986).
 24. Heidrich, B. *et al.* Late HDV RNA relapse after peginterferon alpha-based therapy of chronic hepatitis delta. *Hepatology* **60**, 87–97 (2014).
 25. Sitia, G. *et al.* Kupffer cells hasten resolution of liver immunopathology in mouse models of viral hepatitis. *PLoS Pathog.* **7**, (2011).
 26. Guidotti, L. G. Viral Clearance Without Destruction of Infected Cells During Acute HBV Infection. *Science* (80-.). **284**, 825–829 (1999).
 27. Pasparakis, M. & Vandenabeele, P. Necroptosis and its role in inflammation. *Nature* **517**, 311–320 (2015).
 28. Doitsh, G. & Greene, W. C. Dissecting How CD4 T Cells Are Lost during HIV Infection. *Cell Host Microbe* **19**, 280–291 (2016).
 29. Livak, K. J. & Schmittgen, T. D. Analysis of Relative Gene Expression Data Using Real-Time Quantitative PCR and the $2^{-\Delta\Delta CT}$ Method. *Methods* **25**, 402–408 (2001).

GENERAL DISCUSSION

HDV causes the most severe form of viral hepatitis with a twofold higher risk of developing cirrhosis, a threefold higher risk of developing hepatocellular carcinoma (HCC), and a twofold increased mortality in comparison with HBV monoinfection. However, the mechanism of HDV-associated pathogenesis remains unclear and, more importantly, there is no specific treatment for this devastating disease. One of the main reasons for this situation is the absence of adequate animal models.

Animal models like hepadnavirus-infected chimpanzees or woodchucks have been useful for unraveling some of the characteristics of HDV infection, but they have important limitations associated with ethical considerations and limited the lack of experimental reagents¹². Additionally, none of the HDV mouse models developed so far recapitulates the main characteristics of human infection appropriately, especially the development of severe liver pathology. In mice with humanized liver, the interaction between host immune system and HDV cannot be evaluated^{99,181}, and infection of hNTCP-transgenic animals is transient and can only be achieved in mice less than 17 days of age when the immune system is still immature¹⁰¹. An immunocompetent mouse model in which the three NTCP residues implicated in HBsAg binding were humanized, and therefore should allow HBV and HDV infection, is permissive to HDV expression and RNA replication up to six days after HDV inoculation, but does not support HBV infection, thus prohibiting coinfection studies¹⁰².

Our model takes advantage of an AAV vector as a vehicle to initiate HDV replication in hepatocytes of fully immunocompetent adult mice, leading to stable HDV expression, viral replication, and genome editing. Our data show that HDV replication and HDV expression are HBV-independent and that HBV is required only for the formation and release of infectious particles. Interestingly, the presence of HBV appeared to augment HDV replication since HDV genome and anti-genome levels were higher in HBV/HDV-infected mice in comparison to HDV-infected mice, suggesting that an interaction of both vectors benefits HDV replication.

As has been demonstrated in patients, in our model, animals receiving AAV-HBV/HDV showed a strong suppression of HBV virological markers, including viremia and intrahepatic antigen expression in comparison with AAV-HBV-infected mice. Only AAV-HBV/HDV coinfecting animals developed a strong humoral response against HBsAg, which was able to neutralize HDV infection *in vitro*. On the other hand, animals receiving AAV-HBV/HDV or AAV-HDV developed anti-HDAg antibodies (with higher levels in the monoinfected group). High and sustained levels of anti-HDAg antibodies are also found in chronic hepatitis delta patients¹⁸⁷. There are no reports in the literature about the effect of HDV infection on the immune response against HBsAg, and we hypothesize that the strong type I IFN response induced by HDV may act as an adjuvant for the induction of an adaptive response¹⁸⁸.

With no doubt, one of the most interesting and surprising findings was the significant reduction of the AAV vector genomes in the HDV harboring livers, indicating that HDV replication and antigen expression is independent of the shuttle vector and that HDV induces a not yet characterized process that eliminates episomal DNA. AAV vectors are considered the most promising vector for gene therapy^{189,190}, allowing long-term transgene expression thanks to the episomal maintenance of AAV concatameric genomes in the nucleus of the cell¹⁹⁰. Our findings indicate that certain viral infections (e.g. HDV but not HBV) can result in the elimination of the therapeutic vector genome; the identification of the responsible mechanisms is part of ongoing research.

As previously indicated, HDV-HBV coinfection is associated with a more severe form of viral hepatitis than HBV monoinfection^{45,47,191}. Davies et al. demonstrated that HDV requires HBV coinfection to cause liver damage¹⁹²; in agreement, here we found that, although HDV alone can induce a moderate and transient transaminase elevation, liver damage is stronger and sustained in coinfecting mice. Transcriptomic analysis revealed that AAV-HDV mono- and particularly AAV-HBV/HDV coinfection induced the upregulation of genes implicated in hepatocyte death, damage, inflammation and cirrhosis, and the downregulation of genes with protective activity. Furthermore, we have shown that the liver of coinfecting animals shows the features commonly observed in

patient biopsies - ground-glass hepatocytes with sanded nuclei, ballooning degeneration, mitotic figures and Councilman bodies^{50,51} – thus confirming the soundness of this mouse model to investigate the pathogenesis of hepatitis delta infection.

In line with published work^{101,181} we observed the production of IFN- β and the upregulation of a number of ISGs upon HDV infection - an induction that was almost completely abolished in MAVS KO mice. In fact, MAVS is an adaptor protein acting downstream of the PRRs RIG-I and MDA5, which could recognize the double stranded-like secondary structure of HDV RNA and induce the activation of the type-I IFN pathway¹⁹³. This strong dependence on MAVS, never described before, together with the significant upregulation of both MDA5 and RIG-I, are consistent with a recent *in vitro* study that has identified MDA5 as the PRR responsible for HDV detection¹⁹⁴. Interestingly, the strong induction of type-I and type-II IFN response does not inhibit HDV replication in our model, as was also reported¹⁹⁴, and which is in line with the low efficacy of PEG-IFN α , the only licensed therapy for chronic HDV infection⁶⁷.

In our study in MAVS-deficient mice, in the absence of IFN- β induction, HDV replication had a profound antiviral effect against HBV. The fact that IFN- γ induction was maintained and TNF- α significantly increased in these mice, suggests that these cytokines might be responsible for the observed anti-HBV effect. Additional studies need to be performed to clarify their role. Interestingly, in IFN α / β R / IFN γ R-deficient mice, HAV induces a significant liver pathology only when MAVS is present, indicating that MAVS is an important factor in HAV-induced liver damage, independently of type-I IFN production¹⁹⁵. On the contrary, our study showed no differences in liver injury between MAVS KO and wild-type mice, revealing that MAVS is not necessary for HDV-induced pathology. Moreover, the analysis of liver injury in IFN α / β R KO and IFN γ R KO aimed at determining the role of the cell-intrinsic antiviral response in AAV-HBV/HDV coinfection, revealed no differences with wild-type mice, indicating that the activation of the innate immune response plays no role in HDV-induced liver damage.

We found that cells of the inflammatory infiltrate, mainly composed of activated CD4⁺ and CD8⁺ T cells, pro-inflammatory macrophages, DCs and NK, express high cytokine levels as well as a number of ISGs, like ISG15, ADAR-1, IP10, PKR, and USP18. However, the expression of IFN- β , IFN- γ , TNF- α , and MxA was significantly higher when mRNA extracted from the whole liver was analyzed, indicating that these molecules are mainly produced non-immune cells, most likely the infected hepatocytes. Furthermore, our results exclude a role for T- and NK cells in liver injury, since Rag1^{-/-} mice -lacking mature B-, T-, and NKT cells and wild-type mice depleted of NK cells, still have the same pattern of hepatic disease and serum transaminase elevation. On the contrary, the depletion of macrophages caused an exacerbation of the hepatic damage during the first week after infection, suggesting a protective role as was previously reported for Kupffer cells in HBV-transgenic mice, in which macrophages contain the pathology - possibly by removing dying infected hepatocytes - rather than worsen it¹⁹⁶.

These results led us to believe that innate and adaptive immune responses are not the cause of tissue injury, but rather that viral antigens as the triggers of liver damage. In fact, the administration of AAV-L-HDAg or AAV-S-HDAg caused a severe pathology in animals, which was associated with a very low induction of cytokines in the liver and that was not accompanied by IFN- β expression. This result suggests that the observed pathology is not entirely immune-mediated, indicating a direct cytotoxic effect of the HDAGs; indeed, AAV-HDV/HDV induced liver damage was resolved once the expression of HDV antigens had disappeared.

Our findings are in contrast to what was previously published about an HDAG-transgenic mouse model, in which no histopathological changes were observed at monthly or bimonthly intervals during 18 months⁹⁵. One possible explication for such a difference may be that in HDAG-tg mice, the synthesis of the transgenes could be regulated by the hepatocyte in order not to go above safe levels, or that, during the generation of the transgenic lineage, mice more resistant to the detrimental effects of the antigens were selected. Interestingly, in our study, the genomes of the vectors completely disappeared by 21 days post-infection. More experiments are required to determine the

exact mechanisms involved in the disappearance of the HDAg expressing hepatocytes, and to determine how the antigens exert their cytotoxicity, including the analysis of shorter time points.

In preliminary experiments, we have observed that five months after AAV-HBV/HDV coinfection, the expression of the HDAGs is undetectable, in spite of genomic and anti-genomic HDV RNA still being present. Transaminase levels in serum and histology were normal. These observations support the hypothesis that the presence of HDV RNA itself or its replication are not sufficient to determine the liver pathology observed, and prompted us to investigate further the mechanisms underlying this phenomenon.

Taken together our results strongly opposed the hypothesis that liver damage is mediated by a cellular immune response, and they suggest the possibility of an attempt for a non-cytolytic mechanism for viral clearance, as already described in acute HBV-infected chimpanzees¹⁹⁷. Moreover, we did not detect significant caspase 3 activation by IHC in wild-type mice, therefore other kinds of programmed cell death, e.g pyroptosis, described in HIV infection¹⁹⁸, or necroptosis, correlated with high TNF- α expression levels¹⁹⁹, are to be considered.

In conclusion, our AAV-based mouse model has turned out to be a suitable tool for the study of hepatitis delta-associated disease, allowing us to characterize the hepatic immune infiltrate in an established infection and its role in the previously observed innate immune response. The results led us to discard a main role for the innate and adaptive immune responses in the observed liver injury, and we have highlighted the relevance of HDAG in HDV-induced hepatic damage. Additionally, the model permits genetic alteration of viral genomes to study phenotypic changes *in vivo* and to identify key elements important for the interaction between HBV and HDV⁵⁹. Furthermore, it is a promising tool for testing new antiviral strategies.

CONCLUSIONS

1. A recombinant vector carrying 1.2x copies of HDV genome under the transcriptional control of a liver-specific promoter (AAV-HDV) is able to initiate HDV replication in hepatocytes of fully immunocompetent adult mice, and this replication is independent of the shuttle AAV vector.
2. The model recapitulates the characteristics of human infection including the synthesis of genomic and anti-genomic RNA, antigenome editing, HDAG translation, and infective particle production when AAV-HBV is coinfecting or in HBV-tg mice. As a result, transaminase elevation in serum and liver damage are induced, as observed in patients.
3. The adaptor protein MAVS plays a central role in the type-I IFN response induced by HDV infection, strongly pointing towards RIG-I or MDA5 as the PRR responsible for sensing HDV RNA in infected cells.
4. The immune infiltrate in the liver of AAV-HDV infected mice is mainly composed of activated CD4⁺ and CD8⁺ T cells, DCs, proinflammatory macrophages, and NK cells.
5. The observed liver damage is not due to the presence of the immune infiltrate, and liver macrophages seem to have a protective role during the initial phases of infection.
6. The observed liver damage is neither due to the activation of a -type I-or type II IFN response nor to activation of a cell intrinsic immune mechanism.
7. AAV-dependent S-HDAG or L-HDAG expression in the hepatocytes of fully immunocompetent adult mice causes liver damage in a dose-dependent manner.

GENERAL BIBLIOGRAPHY

1. Chen, P.-J. *et al.* Structure and replication of the genome of the hepatitis delta virus. *Proc. Natl. Acad. Sci. USA* **83**, 8774–8778 (1986).
2. Bonino, F., Heermann, K. H., Rizzetto, M. & Gerlich, W. H. Hepatitis Delta Virus: Protein Composition of Delta Antigen and Its Hepatitis B Virus-Derived Envelope. *J. Virol.* **58**, 945–950 (1986).
3. Rizzetto, M. *et al.* Immunofluorescence detection of new antigen-antibody system (delta/anti-delta) associated to hepatitis B virus in liver and in serum of HBsAg carriers. *Gut* **18**, 997–1003 (1977).
4. Rizzetto, M. *et al.* delta Agent: association of delta antigen with hepatitis B surface antigen and RNA in serum of delta-infected chimpanzees. *Proc. Natl. Acad. Sci.* **77**, 6124–6128 (1980).
5. Bonino, F. *et al.* Delta Hepatitis Agent: Structural and Antigenic Properties of the Delta-Associated Particle. *Infect. Immun.* **43**, 1000–1005 (1984).
6. Wang, K. S. *et al.* Structure, sequence and expression of the hepatitis delta (delta) viral genome. *Nature* **323**, 508–14 (1986).
7. Weiner, A. J. *et al.* A single antigenomic open reading frame of the hepatitis delta virus encodes the epitope(s) of both hepatitis delta antigen polypeptides p24 delta and p27 delta. *J. Virol.* **62**, 594–599 (1988).
8. Radjef, N. *et al.* Molecular Phylogenetic Analyses Indicate a Wide and Ancient Radiation of African Hepatitis Delta Virus, Suggesting a Deltavirus Genus of at Least Seven Major Clades. *J. Virol.* **78**, 2537–2544 (2004).
9. Le Gal, F. *et al.* Eighth major clade for hepatitis delta virus. *Emerg. Infect. Dis.* **12**, 1447–1450 (2006).
10. Gudima, S., Chang, J., Moraleda, G., Azvolinsky, A. & Taylor, J. Parameters of Human Hepatitis Delta Virus Genome Replication: the Quantity, Quality, and Intracellular Distribution of Viral Proteins and RNA. *J. Virol.* **76**, 3709–3719 (2002).
11. Taylor J, Mason W, Summers J, Goldberg J, Aldrich C, Coates L, Gerin J, G. E. Replication of human hepatitis delta virus in primary cultures of woodchuck

- hepatocytes. *J Virol* **61**, 2891–2895 (1987).
12. Aldabe, R., Suárez-Amarán, L., Usai, C. & González-Aseguinolaza, G. Animal Models of Chronic Hepatitis Delta Virus Infection Host-Virus Immunologic Interactions. *Pathogens* **4**, 46–65 (2015).
 13. Greco-Stewart, V. S., Miron, P., Abraham, A. & Pelchat, M. The human RNA polymerase II interacts with the terminal stem–loop regions of the hepatitis delta virus RNA genome. *Virology* **357**, 68–78 (2007).
 14. Greco-Stewart, V. S., Schissel, E. & Pelchat, M. The hepatitis delta virus RNA genome interacts with the human RNA polymerases I and III. *Virology* **386**, 12–15 (2009).
 15. Sharmeen, L., Kuo, M. Y. P., Dinter-Gottlieb, G. & Taylor, J. Antigenomic RNA of Human Hepatitis Delta Virus Can Undergo Self-Cleavage. *J. Virol.* **62**, 2674–2679 (1988).
 16. Kuo, M. Y.-P., Sharmeen, L., Dinter-Gottlieb, G. & Taylor, J. Characterization of Self-Cleaving RNA Sequences on the Genome and Antigenome of Human Hepatitis Delta Virus. *J. Virol.* **62**, 4439–4444 (1988).
 17. Wu, H. N. *et al.* Human hepatitis delta virus RNA subfragments contain an autocleavage activity. *Proc. Natl. Acad. Sci. U. S. A.* **86**, 1831–5 (1989).
 18. Macnaughton, T. B., Wang, Y. J. & Lai, M. M. Replication of hepatitis delta virus RNA: effect of mutations of the autocatalytic cleavage sites. *J. Virol.* **67**, 2228–34 (1993).
 19. Luo, G. X. *et al.* A specific base transition occurs on replicating hepatitis delta virus RNA. *J. Virol.* **64**, 1021–7 (1990).
 20. Casey, J. L. & Gerin, J. L. Hepatitis D Virus RNA Editing: Specific Modification of Adenosine in the Antigenomic RNA. *J. Virol.* **69**, 7593–7600 (1995).
 21. Wong, S. K. & Lazinski, D. W. Replicating hepatitis delta virus RNA is edited in the nucleus by the small form of ADAR1. *Proc. Natl. Acad. Sci. U. S. A.* **99**, 15118–15123 (2002).

22. Heermann, K. H. *et al.* Large surface proteins of hepatitis B virus containing the pre-s sequence. *J. Virol.* **52**, 396–402 (1984).
23. Yan, H. *et al.* Sodium taurocholate cotransporting polypeptide is a functional receptor for human hepatitis B and D virus. *Elife* **1**, e00049 (2012).
24. Stieger, B. *et al.* In Situ Localization of the Hepatocytic Na⁺/Taurocholate Cotransporting Polypeptide in Rat Liver. *Gastroenterology* **107**, 91–1787 (1994).
25. Geyer, J., Wilke, T. & Petzinger, E. The solute carrier family SLC10: More than a family of bile acid transporters regarding function and phylogenetic relationships. *Naunyn. Schmiedebergs. Arch. Pharmacol.* **372**, 413–431 (2006).
26. Schulze, A., Gripon, P. & Urban, S. Hepatitis B virus infection initiates with a large surface protein-dependent binding to heparan sulfate proteoglycans. *Hepatology* **46**, 1759–1768 (2007).
27. Leistner, C. M., Gruen-Bernhard, S. & Glebe, D. Role of glycosaminoglycans for binding and infection of hepatitis B virus. *Cell. Microbiol.* **10**, 122–133 (2008).
28. Lamas Longarela, O. *et al.* Proteoglycans Act as Cellular Hepatitis Delta Virus Attachment Receptors. *PLoS One* **8**, e58340 (2013).
29. Abou-Jaoudé, G. & Sureau, C. Entry of Hepatitis Delta Virus Requires the Conserved Cysteine Residues of the Hepatitis B Virus Envelope Protein Antigenic Loop and Is Blocked by Inhibitors of Thiol-Disulfide Exchange. *J. Virol.* **81**, 13057–13066 (2007).
30. Verrier, E. R. *et al.* A targeted functional RNA interference screen uncovers glypican 5 as an entry factor for hepatitis B and D viruses. *Hepatology* **63**, 35–48 (2016).
31. Sureau, C. & Negro, F. The hepatitis delta virus: Replication and pathogenesis. *J. Hepatol.* **64**, S102–S116 (2016).
32. Chao, M., Hsieh, S. Y. & Taylor, J. Role of two forms of hepatitis delta virus antigen: evidence for a mechanism of self-limiting genome replication. *J. Virol.* **64**, 5066–9 (1990).

33. Lee, C. H., Chang, S. C., Wu, C. H. H. & Chang, M. F. A Novel Chromosome Region Maintenance 1-independent Nuclear Export Signal of the Large Form of Hepatitis Delta Antigen That Is Required for the Viral Assembly. *J. Biol. Chem.* **276**, 8142–8148 (2001).
34. Alves, C., Freitas, N. & Cunha, C. Characterization of the nuclear localization signal of the hepatitis delta virus antigen. *Virology* **370**, 12–21 (2008).
35. Lee, C. *et al.* RNA-Binding Activity of Hepatitis Delta Antigen Involves Two Arginine-Rich Motifs and Is Required for Hepatitis Delta Virus RNA Replication Hepatitis delta antigen (HIAg) is an RNA-binding protein with binding specificity for hepatitis delta virus. *J. Virol.* **67**, 2221–2227 (1993).
36. Mu, J.-J. *et al.* Characterization of the Phosphorylated Forms and the Phosphorylated Residues of Hepatitis Delta Virus Delta Antigens. *J. Virol.* **73**, 10540–10545 (1999).
37. O'Malley, B. & Lazinski, D. W. Roles of Carboxyl-Terminal and Farnesylated Residues in the Functions of the Large Hepatitis Delta Antigen. *J. Virol.* **79**, 1142–1153 (2005).
38. Glenn, J. S., Watson, J. A., Havel, C. M. & White, J. M. Identification of a prenylation site in delta virus large antigen. *Science (80-.)*. **256**, 1331–1333 (1992).
39. Hwang, S. B. & Lai, M. M. C. Isoprenylation Mediates Direct Protein-Protein Interactions between Hepatitis Large Delta Antigen and Hepatitis B Virus Surface Antigen. *J. Virol.* **67**, 7659–7662 (1993).
40. Hwang, S. B. & Lap, M. M. C. Isoprenylation Masks a Conformational Epitope and Enhances trans-Dominant Inhibitory Function of the Large Hepatitis Delta Antigen. *J. Virol.* **68**, 2958–2964 (1994).
41. Alves, C., Cheng, H., Roder, H. & Taylor, J. Intrinsic disorder and oligomerization of the hepatitis delta virus antigen. *Virology* **407**, 333–40 (2010).
42. Lin, B. C., Defenbaugh, D. A. & Casey, J. L. Multimerization of hepatitis delta antigen is a critical determinant of RNA binding specificity. *J. Virol.* **84**, 1406–

- 13 (2010).
43. Zuccola, H. J., Rozzelle, J. E., Lemon, S. M., Erickson, B. W. & Hogle, J. M. Structural basis of the oligomerization of hepatitis delta antigen. *Structure* **6**, 821–30 (1998).
 44. Komla-Soukha, I. & Sureau, C. A Tryptophan-Rich Motif in the Carboxyl Terminus of the Small Envelope Protein of Hepatitis B Virus Is Central to the Assembly of Hepatitis Delta Virus Particles. *J. Virol.* **80**, 4648–4655 (2006).
 45. Negro, F. Hepatitis D virus coinfection and superinfection. *Cold Spring Harb. Perspect. Med.* **4**, a021550 (2014).
 46. Fattovich, G., Bortolotti, F. & Donato, F. Natural history of chronic hepatitis B: special emphasis on disease progression and prognostic factors. *J. Hepatol.* **48**, 335–52 (2008).
 47. Fattovich, G. *et al.* Influence of hepatitis delta virus infection on morbidity and mortality in compensated cirrhosis type B. *Gut* **46**, 420–426 (2000).
 48. Hughes, S. A., Wedemeyer, H. & Harrison, P. M. Hepatitis delta virus. *Lancet* **378**, 73–85 (2011).
 49. Ishak, K. G. Pathologic features of chronic hepatitis. A review and update. *Am. J. Clin. Pathol.* **113**, 40–55 (2000).
 50. Mani, H. & Kleiner, D. E. Liver biopsy findings in chronic hepatitis B. *Hepatology* **49**, S61–S71 (2009).
 51. Verme, G. *et al.* A histological study of Hepatitis Delta Virus Liver Disease. *Hepatology* **6**, 1303–1307 (1986).
 52. Suárez-Amarán, L. *et al.* A new HDV mouse model identifies mitochondrial antiviral signaling protein (MAVS) as a key player in IFN- β induction. *J. Hepatol.* **67**, 669–679 (2017).
 53. Pollicino, T. *et al.* Replicative and Transcriptional Activities of Hepatitis B Virus in Patients Coinfected with Hepatitis B and Hepatitis Delta Viruses. *J. Virol.* **85**, 432–439 (2011).

54. Colombo, P. *et al.* Smouldering hepatitis B virus replication in patients with chronic liver disease and hepatitis delta virus superinfection. *J. Hepatol.* **12**, 64–69 (1991).
55. Schaper, M. *et al.* Quantitative longitudinal evaluations of hepatitis delta virus RNA and hepatitis B virus DNA shows a dynamic, complex replicative profile in chronic hepatitis B and D. *J. Hepatol.* **52**, 658–664 (2010).
56. Wu, J.-C. *et al.* Production of hepatitis delta virus and suppression of helper hepatitis B virus in a human hepatoma cell line. *J. Virol.* **65**, 1099–1104 (1991).
57. Williams, V. *et al.* Hepatitis delta virus proteins repress hepatitis B virus enhancers and activate the alpha/beta interferon-inducible MxA gene. *J. Gen. Virol.* **90**, 2759–2767 (2009).
58. Alfaiate, D. *et al.* HDV RNA replication is associated with HBV repression and interferon-stimulated genes induction in super-infected hepatocytes. *Antiviral Res.* **136**, 19–31 (2016).
59. Giersch, K. & Dandri, M. Hepatitis B and Delta Virus: Advances on Studies about Interactions between the Two Viruses and the Infected Hepatocyte. *J. Clin. Transl. Hepatol.* **3**, 220–229 (2015).
60. Gish, R. G. *et al.* Chronic hepatitis B: virology, natural history, current management and a glimpse at future opportunities. *Antiviral Res.* **121**, 47–58 (2015).
61. Goto, T. *et al.* Synergistic activation of the serum response element-dependent pathway by hepatitis B virus X protein and large-isoform hepatitis delta antigen. *J. Infect. Dis.* **187**, 820–828 (2003).
62. Rosmorduc, O. *et al.* Inhibition of interferon-inducible MxA protein expression by hepatitis B virus capsid protein. *J. Gen. Virol.* **80**, 1253–1262 (1999).
63. Fernández, M., Quiroga, J. A. & Carreño, V. Hepatitis B virus downregulates the human interferon-inducible MxA promoter through direct interaction of precore/core proteins. *J. Gen. Virol.* **84**, 2073–2082 (2003).
64. Yen, L. Identification of inhibitors of ribozyme self-cleavage in mammalian cells

- via high-throughput screening of chemical libraries. *RNA* **12**, 797–806 (2006).
65. Chang, J. & Taylor, J. M. Susceptibility of Human Hepatitis Delta Virus RNAs to Small Interfering RNA Action. *J. Virol.* **77**, 9728–9731 (2003).
 66. Wedemeyer, H. *et al.* Peginterferon plus Adefovir versus Either Drug Alone for Hepatitis Delta. *N. Engl. J. Med.* **364**, 322–331 (2011).
 67. Heidrich, B. *et al.* Late HDV RNA relapse after peginterferon alpha-based therapy of chronic hepatitis delta. *Hepatology* **60**, 87–97 (2014).
 68. Gripon, P., Cannie, I. & Urban, S. Efficient Inhibition of Hepatitis B Virus Infection by Acylated Peptides Derived from the Large Viral Surface Protein. *J. Virol.* **79**, 1613–1622 (2005).
 69. Petersen, J. *et al.* Prevention of hepatitis B virus infection in vivo by entry inhibitors derived from the large envelope protein. *Nat. Biotechnol.* **26**, 335–341 (2008).
 70. Volz, T. *et al.* The entry inhibitor Myrcludex-B efficiently blocks intrahepatic virus spreading in humanized mice previously infected with hepatitis B virus. *J. Hepatol.* **58**, 861–7 (2013).
 71. Bogomolov, P. *et al.* Treatment of chronic hepatitis D with the entry inhibitor myrcludex B: First results of a phase Ib/IIa study. *J. Hepatol.* **65**, 490–498 (2016).
 72. Donkers, J. M. *et al.* Reduced hepatitis B and D viral entry using clinically applied drugs as novel inhibitors of the bile acid transporter NTCP. *Sci. Rep.* **7**, (2017).
 73. Shimura, S. *et al.* Cyclosporin derivatives inhibit hepatitis B virus entry without interfering with NTCP transporter activity. *J. Hepatol.* **66**, 685–692 (2017).
 74. Tsukuda, S. *et al.* A new class of hepatitis B and D virus entry inhibitors, proanthocyanidin and its analogs, that directly act on the viral large surface proteins. *Hepatology* **65**, 1104–1116 (2017).
 75. Glenn, J. S., Marsters, J. C. & Greenberg, H. B. Use of a Prenylation Inhibitor as

- a Novel Antiviral Agent. *J. Virol.* **72**, 9303–9306 (1998).
76. Koh, C. *et al.* Oral prenylation inhibition with lonafarnib in chronic hepatitis D infection: A proof-of-concept randomised, double-blind, placebo-controlled phase 2A trial. *Lancet Infect. Dis.* **15**, 1167–1174 (2015).
77. Ghosal, A. *et al.* Identification of human liver cytochrome P450 enzymes responsible for the metabolism of lonafarnib (Sarasar). *Drug Metab. Dispos.* **34**, 628–635 (2006).
78. Yurdaydin, C. *et al.* Optimizing lonafarnib treatment for the management of chronic delta hepatitis: The LOWR HDV-1 study. *Hepatology* (2018).
doi:10.1002/hep.29658
79. Beilstein, F., Blanchet, M., Vaillant, A. & Sureau, C. Nucleic acid polymers are active against Hepatitis Delta Virus infection in vitro. *J. Virol.* **92**, e01416-17 (2018).
80. Noordeen, F., Vaillant, A. & Jilbert, A. R. Nucleic acid polymers prevent the establishment of duck hepatitis B virus infection in vivo. *Antimicrob. Agents Chemother.* **57**, 5299–5306 (2013).
81. Noordeen, F., Vaillant, A. & Jilbert, A. R. Nucleic acid polymers inhibit duck hepatitis B virus infection in vitro. *Antimicrob. Agents Chemother.* **57**, 5291–5298 (2013).
82. Al-Mahtab, M., Bazinet, M. & Vaillant, A. Safety and Efficacy of Nucleic Acid Polymers in Monotherapy and Combined with Immunotherapy in Treatment-Naive Bangladeshi Patients with HBeAg+ Chronic Hepatitis B Infection. *PLoS One* **11**, e0156667 (2016).
83. Guillot, C., Hantz, O., Vaillant, A. & Chemin, I. P0556 : Antiviral effects of nucleic acid polymers on hepatitis B virus infection. *J. Hepatol.* **62**, S523 (2015).
84. Bazinet, M. *et al.* Update on the Safety and Efficacy of REP 2139 Monotherapy and Subsequent Combination Therapy with Pegylated Interferon Alpha-2A in Caucasian Patients with Chronic HBV/HDV Co-Infection. *J. Hepatol.* **64**, S584–S585 (2016).

85. Gerin, J. L. Animal models of hepatitis delta virus infection and disease. *ILAR J.* **42**, 103–106 (2001).
86. Gripon, P. *et al.* Hepatitis B Virus Infection of Adult Human Hepatocytes Cultured in the Presence of Dimethyl Sulfoxide. *J. Virol.* **62**, 4136–4143 (1988).
87. Gripon, P. *et al.* Infection of a human hepatoma cell line by hepatitis B virus. *Proc. Natl. Acad. Sci. U. S. A.* **99**, 15655–60 (2002).
88. Verrier, E. R., Colpitts, C. C., Schuster, C., Zeisel, M. B. & Baumert, T. F. Cell culture models for the investigation of Hepatitis B and D Virus infection. *Viruses* **8**, 261 (2016).
89. Iwamoto, M. *et al.* Evaluation and identification of hepatitis B virus entry inhibitors using HepG2 cells overexpressing a membrane transporter NTCP. *Biochem. Biophys. Res. Commun.* **443**, 808–813 (2014).
90. Negro, F. *et al.* Chronic hepatitis D virus (HDV) infection in hepatitis B virus carrier Chimpanzees experimentally superinfected with HDV. *J. Infect. Dis.* **158**, 151–159 (1988).
91. Barrera, A., Guerra, B., Lee, H. & Lanford, R. E. Analysis of Host Range Phenotypes of Primate Hepadnaviruses by In Vitro Infections of Hepatitis D Virus Pseudotypes. *J. Virol.* **78**, 5233–5243 (2004).
92. Negro, F. *et al.* Hepatitis Delta Virus (HDV) and Woodchuck Hepatitis Virus (WHV) Nucleic Acids in Tissues of HDV-Infected Chronic WHV Carrier Woodchucks. *J. Virol.* 1612–1618 (1989). at <http://jvi.asm.org/content/63/4/1612.full.pdf>
93. Casey, J. L. & Gerin, J. L. The woodchuck model of HDV infection. *Curr. Top. Microbiol. Immunol.* **307**, 211–25 (2006).
94. Li, Q., Ding, M. & Wang, H. The infection of hepatitis D virus in adult tupaia. *Zhonghua Yi Xue Za Zhi* **75**, 611–3, 639–40 (1995).
95. Guilhot, S. *et al.* Expression of the Hepatitis Delta Virus Large and Small Antigens in Transgenic Mice. *J Virol* **68**, 1052–1058 (1994).

96. Polo, J. M. *et al.* Transgenic mice support replication of hepatitis delta virus RNA in multiple tissues, particularly in skeletal muscle. *J. Virol.* **69**, 4880–7 (1995).
97. Grompe, M. & Strom, S. Mice with human livers. *Gastroenterology* **145**, 1209–1214 (2013).
98. Dandri, M. *et al.* Repopulation of mouse liver with human hepatocytes and in vivo infection with hepatitis B virus. *Hepatology* **33**, 981–988 (2001).
99. Lütgehetmann, M. *et al.* Humanized chimeric uPA mouse model for the study of hepatitis B and D virus interactions and preclinical drug evaluation. *Hepatology* **55**, 685–694 (2012).
100. Giersch, K. *et al.* Persistent hepatitis D virus mono-infection in humanized mice is efficiently converted by hepatitis B virus to a productive co-infection. *J. Hepatol.* **60**, 538–544 (2014).
101. He, W. *et al.* Hepatitis D Virus Infection of Mice Expressing Human Sodium Taurocholate Co-transporting Polypeptide. *PLOS Pathog.* **11**, e1004840 (2015).
102. He, W. *et al.* Modification of Three Amino Acids in Sodium Taurocholate Cotransporting Polypeptide Renders Mice Susceptible to Infection with Hepatitis D Virus In Vivo. *JOURNAL. Virol.* **90**, 8866–8874 (2016).
103. Gonçalves, M. A. Adeno-associated virus: from defective virus to effective vector. *Virol. J.* **2**, 43 (2005).
104. Atchison, R. W., Casto, B. C. & Hammon, W. M. Adeno-associated defective virus particles. *Science (80-.)*. **149**, 754–6 (1965).
105. Berns, K. I. Parvovirus replication. *Microbiol. Mol. Biol. Rev.* **54**, 316 (1990).
106. Chejanovsky 'and, N. & Carter, B. J. Mutagenesis of an AUG Codon in the Adeno-Associated Virus rep Gene: Effects on Viral DNA Replication. *Virology* **173**, 120–128 (1989).
107. Pereira, D. J., Mccarty, D. M. & Muzyczka, N. The Adeno-Associated Virus (AAV) Rep Protein Acts as both a Repressor and an Activator To Regulate AAV

- Transcription during a Productive Infection. *J. Virol.* **71**, 1079–1088 (1997).
108. Sonntag, F., Schmidt, K. & Kleinschmidt, J. A. A viral assembly factor promotes AAV2 capsid formation in the nucleolus. *Proc. Natl. Acad. Sci.* **107**, 10220–10225 (2010).
 109. Chen, H. Adeno-associated virus vectors for human gene therapy. *World J. Med. Genet.* **5**, 28 (2015).
 110. Geoffroy, M.-C. & Salvetti, A. Helper functions required for wild type and recombinant adeno-associated virus growth. *Curr. Gene Ther.* **5**, 265–71 (2005).
 111. Kotin, R. M. *et al.* Site-specific integration by adeno-associated virus. *Proc. Natl. Acad. Sci. U. S. A.* **87**, 2211–5 (1990).
 112. Yakobson, B., Koch, T. & Winocour, E. Replication of adeno-associated virus in synchronized cells without the addition of a helper virus. *J. Virol.* **61**, 972–81 (1987).
 113. Nicolas, A. *et al.* Factors influencing helper-independent adeno-associated virus replication. *Virology* **432**, 1–9 (2012).
 114. Salganik, M., Hirsch, M. L. & Samulski. Adeno-associated virus as a mammalian DNA vector. *Microbiol. Spectr.* **3**, (2015).
 115. Vannucci, L., Lai, M., Chiappesi, F., Ceccherini-Nelli, L. & Pistello, M. Viral vectors: a look back and ahead on gene transfer technology. *New Microbiol.* **36**, 1–22 (2013).
 116. Kotterman, M. A. & Schaffer, D. V. Engineering adeno-associated viruses for clinical gene therapy. *Nat. Rev. Genet.* **15**, 445–451 (2014).
 117. Skubis-Zegadło, J., Stachurska, A. & Małecki, M. Vectrology of adeno-associated viruses (AAV). *Med. Wieku Rozwoj.* **17**, 202–6 (2013).
 118. Smith, R. H. Adeno-associated virus integration: Virus versus vector. *Gene Therapy* **15**, 817–822 (2008).
 119. Zinn, E. *et al.* In silico reconstruction of the viral evolutionary lineage yields a potent gene therapy vector. *Cell Rep.* **12**, 1056–1068 (2015).

120. Smith, J. K. & Agbandje-McKenna, M. Creating an arsenal of Adeno-associated virus (AAV) gene delivery stealth vehicles. *PLOS Pathog.* **14**, e1006929 (2018).
121. Dunbar, C. E. *et al.* Gene therapy comes of age. *Science (80-.)*. **359**, eaan4672 (2018).
122. Huang, Y. H. *et al.* A murine model of hepatitis B-associated hepatocellular carcinoma generated by adeno-associated virus-mediated gene delivery. *Int. J. Oncol.* **39**, 1511–1519 (2011).
123. Dion, S., Bourguine, M., Godon, O., Levillayer, F. & Michel, M.-L. Adeno-Associated Virus-Mediated Gene Transfer Leads to Persistent Hepatitis B Virus Replication in Mice Expressing HLA-A2 and HLA-DR1 Molecules. *J. Virol.* **87**, 5554–5563 (2013).
124. Lucifora, J. *et al.* Detection of the hepatitis B virus (HBV) covalently-closed-circular DNA (cccDNA) in mice transduced with a recombinant AAV-HBV vector. *Antiviral Res.* **145**, 14–19 (2017).
125. Delves, P. J. & Roitt, I. M. The Immune System - First of two parts. *N. Engl. J. Med.* **343**, 37–49 (2000).
126. Akira, S., Uematsu, S. & Takeuchi, O. Pathogen recognition and innate immunity. *Cell* **124**, 783–801 (2006).
127. Turvey, S. E. & Broide, D. H. Innate immunity. *J. Allergy Clin. Immunol.* **125**, S24–S32 (2010).
128. Borden, E. C. *et al.* Interferons at age 50: past, current and future impact on biomedicine. *Nat. Rev. Drug Discov.* **6**, 975–990 (2007).
129. Ivashkiv, L. B. & Donlin, L. T. Regulation of type I interferon responses. *Nat. Rev. Immunol.* **14**, 36–49 (2014).
130. Cheon, H. *et al.* IFN β -dependent increases in STAT1, STAT2, and IRF9 mediate resistance to viruses and DNA damage. *EMBO J.* **32**, 2751–2763 (2013).
131. Lemaitre, B., Nicolas, E., Michaut, L., Reichhart, J. M. & Hoffmann, J. A. The dorsoventral regulatory gene cassette spatzle/Toll/Cactus controls the potent

- antifungal response in *Drosophila* adults. *Cell* **86**, 973–983 (1996).
132. Kawai, T. & Akira, S. The roles of TLRs, RLRs and NLRs in pathogen recognition. *Int. Immunol.* **21**, 317–337 (2009).
 133. Kawai, T. & Akira, S. TLR signaling. *Semin. Immunol.* **19**, 24–32 (2007).
 134. Bowie, A. & O’Neill, L. A. The interleukin-1 receptor/Toll-like receptor superfamily: signal generators for pro-inflammatory interleukins and microbial products. *J. Leukoc. Biol.* **67**, 508–14 (2000).
 135. Alexopoulou, L., Czopik Holt, A., Medzhitov, R. & Flavell, R. A. Recognition of double-stranded RNA and activation of NF-kappa B by Toll-like receptor 3. *Nature* **413**, 732–738 (2001).
 136. Diebold, S. S., Kaisho, T., Hemmi, H., Akira, S. & Reis e Sousa, C. Innate antiviral responses by means of TLR7-mediated recognition of single-stranded RNA.pdf. *Science (80-.)*. **303**, 1529–1531 (2004).
 137. Heil, F. *et al.* Species-specific recognition of single-stranded RNA via toll-like receptor 7 and 8. *Science (80-.)*. **303**, 1526–1529 (2004).
 138. Haas, T. *et al.* The DNA Sugar Backbone 2’ Deoxyribose Determines Toll-like Receptor 9 Activation. *Immunity* **28**, 315–323 (2008).
 139. Hayashi, F. *et al.* The innate immune response to bacterial flagellin is mediated by Toll-like receptor 5. *Nature* **410**, 1099–103. (2001).
 140. Hoshino, K. *et al.* Cutting edge: Toll-like receptor 4 (TLR4)-deficient mice are hyporesponsive to lipopolysaccharide: evidence for TLR4 as the Lps gene product. *J. Immunol.* **162**, 3749–52 (1999).
 141. Miyake, K. Innate immune sensing of pathogens and danger signals by cell surface Toll-like receptors. *Semin. Immunol.* **19**, 3–10 (2007).
 142. Latz, E. *et al.* TLR9 signals after translocating from the ER to CpG DNA in the lysosome. *Nat. Immunol.* **5**, 190–198 (2004).
 143. Nishiya, T., Kajita, E., Miwa, S. & DeFranco, A. L. TLR3 and TLR7 are targeted to the same intracellular compartments by distinct regulatory elements. *J. Biol.*

- Chem.* **280**, 37107–37117 (2005).
144. Tabeta, K. *et al.* The Unc93b1 mutation 3d disrupts exogenous antigen presentation and signaling via Toll-like receptors 3, 7 and 9. *Nat. Immunol.* **7**, 156–164 (2006).
 145. Kingeter, L. M. & Lin, X. C-type lectin receptor-induced NF- κ B activation in innate immune and inflammatory responses. *Cellular and Molecular Immunology* **9**, 105–112 (2012).
 146. Yoneyama, M., Onomoto, K., Jogi, M., Akaboshi, T. & Fujita, T. Viral RNA detection by RIG-I-like receptors. *Curr. Opin. Immunol.* **32**, 48–53 (2015).
 147. Schlee, M. *et al.* Recognition of 5' Triphosphate by RIG-I Helicase Requires Short Blunt Double-Stranded RNA as Contained in Panhandle of Negative-Strand Virus. *Immunity* **31**, 25–34 (2009).
 148. Habjan, M. & Pichlmair, A. Cytoplasmic sensing of viral nucleic acids. *Curr. Opin. Virol.* **11**, 31–37 (2015).
 149. Xu, L. *et al.* RIG-I is a key antiviral interferon-stimulated gene against hepatitis E virus regardless of interferon production. *Hepatology* **65**, 1823–1839 (2017).
 150. Goulet, M.-L. *et al.* Systems Analysis of a RIG-I Agonist Inducing Broad Spectrum Inhibition of Virus Infectivity. *PLoS Pathog.* **9**, e1003298 (2013).
 151. Satoh, T. *et al.* LGP2 is a positive regulator of RIG-I- and MDA5-mediated antiviral responses. *Proc. Natl. Acad. Sci.* **107**, 1512–1517 (2010).
 152. Seth, R. B., Sun, L., Ea, C. K. & Chen, Z. J. Identification and characterization of MAVS, a mitochondrial antiviral signaling protein that activates NF- κ B and IRF3. *Cell* **122**, 669–682 (2005).
 153. Motta, V., Soares, F., Sun, T. & Philpott, D. J. NOD-Like Receptors: Versatile Cytosolic Sentinels. *Physiol. Rev.* **95**, 149–178 (2015).
 154. Kim, Y. K., Shin, J. S. & Nahm, M. H. NOD-like receptors in infection, immunity, and diseases. *Yonsei Med. J.* **57**, 5–14 (2016).
 155. Sabbah, A. *et al.* Activation of innate immune antiviral responses by Nod2. *Nat.*

- Immunol.* **10**, 1073–1080 (2009).
156. Lugrin, J. & Martinon, F. The AIM2 inflammasome: Sensor of pathogens and cellular perturbations. *Immunological Reviews* **281**, 99–114 (2018).
 157. Murphy, K. & Weaver, C. *Janeway's immunobiology*. (Garland Science, Taylor & Francis Group, LLC, 2017).
 158. Kumar, A. *et al.* Natural Killer T Cells: An Ecological Evolutionary Developmental Biology Perspective. *Front. Immunol.* **8**, 1858 (2017).
 159. Delves, P. J. & Roitt, I. M. The Immune System - Second of two parts. *N. Engl. J. Med.* **343**, 108–117 (2000).
 160. Schietinger, A. & Greenberg, P. D. Tolerance and exhaustion: Defining mechanisms of T cell dysfunction. *Trends in Immunology* **35**, 51–60 (2014).
 161. Gururajan, M., Sindhava, V. & Bondada, S. B Cells and Immunological Tolerance. *Antibodies* **3**, 116–129 (2014).
 162. Heymann, F. & Tacke, F. Immunology in the liver — from homeostasis to disease. *Nat. Rev. Gastroenterol. Hepatol.* **13**, 88–110 (2016).
 163. Bogdanos, D. P., Gao, B. & Gershwin, M. E. in *Comprehensive Physiology* **3**, 567–598 (2013).
 164. Nemeth, E., Baird, A. W. & O'Farrelly, C. Microanatomy of the liver immune system. *Seminars in Immunopathology* **31**, 333–343 (2009).
 165. Thomson, A. W. & Knolle, P. A. Antigen-presenting cell function in the tolerogenic liver environment. *Nat. Rev. Immunol.* **10**, 753–766 (2010).
 166. Knolle, P. A., Böttcher, J. & Huang, L. R. The role of hepatic immune regulation in systemic immunity to viral infection. *Medical Microbiology and Immunology* **204**, 21–27 (2015).
 167. Novobrantseva, T. I. *et al.* Attenuated liver fibrosis in the absence of B cells. *J. Clin. Invest.* **115**, 3072–3082 (2005).
 168. Bowen, D. G. *et al.* The site of primary T cell activation is a determinant of the

- balance between intrahepatic tolerance and immunity. *J. Clin. Invest.* **114**, 701–712 (2004).
169. Lee, W.-Y. *et al.* An intravascular immune response to *Borrelia burgdorferi* involves Kupffer cells and iNKT cells. *Nat. Immunol.* **11**, (2010).
170. Pradel, G. & Frevert, U. Malaria sporozoites actively enter and pass through rat Kupffer cells prior to hepatocyte invasion. *Hepatology* **33**, 1154–1165 (2001).
171. Sturm, A. *et al.* Manipulation of Host Hepatocytes by the Malaria Parasite for Delivery into Liver Sinusoids. *Science* **302**, 1560–3 (2003).
172. Lemon, S. M., Ott, J. J., Van Damme, P. & Shouval, D. Type A viral hepatitis: A summary and update on the molecular virology, epidemiology, pathogenesis and prevention. *J. Hepatol.* **68**, 167–184 (2017).
173. Gale, M. & Foy, E. M. Evasion of intracellular host defence by hepatitis C virus. *Nature* **436**, 939–945 (2005).
174. Bang, B. R., Elmasry, S. & Saito, T. Organ system view of the hepatic innate immunity in HCV infection. *Journal of Medical Virology* **88**, 2025–2037 (2016).
175. von Hahn, T. *et al.* Hepatitis C Virus Continuously Escapes From Neutralizing Antibody and T-Cell Responses During Chronic Infection In Vivo. *Gastroenterology* **132**, 667–678 (2007).
176. Tseng, T.-C. & Huang, L.-R. Immunopathogenesis of Hepatitis B Virus. *J. Infect. Dis.* **216**, S765–S770 (2017).
177. Bocher, W. O. *et al.* Regulation of the neutralizing anti-hepatitis B surface (HBs) antibody response in vitro in HBs vaccine recipients and patients with acute or chronic hepatitis B virus (HBV) infection. *Clin. Exp. Immunol.* **105**, 52–58 (1996).
178. Xu, Y. *et al.* HBsAg inhibits TLR9-mediated activation and IFN- α production in plasmacytoid dendritic cells. *Mol. Immunol.* **46**, 2640–2646 (2009).
179. Protzer, U., Maini, M. K. & Knolle, P. A. Living in the liver: hepatic infections. *Nat. Rev. Immunol.* **12**, 201–213 (2012).

180. Zachou, K. *et al.* Quantitative HBsAg and HDV-RNA levels in chronic delta hepatitis. *Liver Int.* **30**, 430–437 (2010).
181. Giersch, K. *et al.* Hepatitis Delta co-infection in humanized mice leads to pronounced induction of innate immune responses in comparison to HBV mono-infection. *J. Hepatol.* **63**, 346–353 (2015).
182. Aslan, N. *et al.* Cytotoxic CD4⁺ T cells in viral hepatitis. *J. Viral Hepat.* **13**, 505–514 (2006).
183. Nisini, R. *et al.* Human CD4⁺ T-cell response to hepatitis delta virus: identification of multiple epitopes and characterization of T-helper cytokine profiles. *J Virol* **71**, 2241–2251 (1997).
184. Huang, Y.-H. Identification of novel HLA-A*0201-restricted CD8⁺ T-cell epitopes on hepatitis delta virus. *J. Gen. Virol.* **85**, 3089–3098 (2004).
185. Grabowski, J. *et al.* Hepatitis D virus-specific cytokine responses in patients with chronic hepatitis delta before and during interferon alfa-treatment. *Liver Int.* **31**, 1395–405 (2011).
186. Lunemann, S. *et al.* Compromised function of natural killer cells in acute and chronic viral hepatitis. *J. Infect. Dis.* **209**, 1362–73 (2014).
187. Abbasi, A., Bhutto, A. R., Butt, N. & Mahmood, K. HDV seroprevalence in HBsAg positive patients. *J. Coll. Physicians Surg. Pakistan* **24**, 624–627 (2014).
188. Bracci, L., La Sorsa, V., Belardelli, F. & Proietti, E. Type I interferons as vaccine adjuvants against infectious diseases and cancer. *Expert Rev. Vaccines* **7**, 373–381 (2008).
189. Murillo, O. *et al.* Long-term metabolic correction of Wilson’s disease in a murine model by gene therapy. *J. Hepatol.* **64**, 419–426 (2016).
190. High, K. A. & Anguela, X. M. Adeno-associated viral vectors for the treatment of hemophilia. *Human molecular genetics* **25**, R36–R41 (2016).
191. Taylor, J. M. Structure and replication of hepatitis delta virus RNA. *Curr. Top. Microbiol. Immunol.* **307**, 1–23 (2006).

192. Davies, S. E. *et al.* Evidence that hepatitis D virus needs hepatitis B virus to cause hepatocellular damage. *Am. J. Clin. Pathol.* **98**, 554–558 (1992).
193. Oshiumi, H., Kouwaki, T. & Seya, T. Accessory Factors of Cytoplasmic Viral RNA Sensors Required for Antiviral Innate Immune Response. *Front. Immunol.* **7**, 200 (2016).
194. Zhang, Z. *et al.* Hepatitis D Virus replication is sensed by MDA5 and induces IFN- β/λ responses in hepatocytes. *J. Hepatol.* (2018).
doi:10.1016/j.jhep.2018.02.021
195. Hirai-Yuki, A. *et al.* MAVS-dependent host species range and pathogenicity of human hepatitis A virus. *Science* (80-.). **353**, (2016).
196. Sitia, G. *et al.* Kupffer cells hasten resolution of liver immunopathology in mouse models of viral hepatitis. *PLoS Pathog.* **7**, (2011).
197. Guidotti, L. G. Viral Clearance Without Destruction of Infected Cells During Acute HBV Infection. *Science* (80-.). **284**, 825–829 (1999).
198. Doitsh, G. & Greene, W. C. Dissecting How CD4 T Cells Are Lost during HIV Infection. *Cell Host Microbe* **19**, 280–291 (2016).
199. Pasparakis, M. & Vandenabeele, P. Necroptosis and its role in inflammation. *Nature* **517**, 311–320 (2015).
200. Srivastava, A. In vivo tissue-tropism of adeno-associated viral vectors. *Curr. Opin. Virol.* **21**, 75–80 (2016).
201. O’Neill, L. A. J., Golenbock, D. & Bowie, A. G. The history of Toll-like receptors-redefining innate immunity. *Nat. Rev. Immunol.* **13**, 453–460 (2013).
202. Pandey, S., Kawai, T. & Akira, S. Microbial Sensing by Toll-Like Receptors and Intracellular Nucleic Acid Sensors. *Cold Spring Harb Perspect Biol* **7**, a016246 (2014).

Annex 1

Pathogens **2015**, *4*, 46–65; doi:10.3390/pathogens4010046

OPEN ACCESS

pathogens

ISSN 2076-0817

www.mdpi.com/journal/pathogens

Review

Animal Models of Chronic Hepatitis Delta Virus Infection Host–Virus Immunologic Interactions

Rafael Aldabe, Lester Suárez-Amarán, Carla Usai, and Gloria González-Aseguinolaza *

Gene Therapy and Regulation of Gene Expression Program, Centro de Investigación Médica Aplicada (CIMA), Universidad de Navarra (UNAV), Pamplona 31008, Spain; E-Mails: raldabe@unav.es

(R.A.); lsuarez.4@alumni.unav.es (L.S.-A.); cusai@alumni.unav.es (C.U.)

* Author to whom correspondence should be addressed; E-Mail: ggasegui@unav.es;
Tel.: +34-948-194-700 (ext. 3005); Fax: +34-948-194-717.

Academic Editor: Moriya Tsuji

Received: 12 November 2014 / Accepted: 5 February 2015 / Published: 12 February 2015

Abstract: Hepatitis delta virus (HDV) is a defective RNA virus that has an absolute requirement for a virus belonging to the hepadnaviridae family like hepatitis B virus (HBV) for its replication and formation of new virions. HDV infection is usually associated with a worsening of HBV-induced liver pathogenesis, which leads to more frequent cirrhosis, increased risk of hepatocellular carcinoma (HCC), and fulminant hepatitis. Importantly, no selective therapies are available for HDV infection. The mainstay of treatment for HDV infection is pegylated interferon alpha; however, response rates to this therapy are poor. A better knowledge of HDV–host cell interaction will help with the identification of novel therapeutic targets, which are urgently needed. Animal models like hepadnavirus-infected chimpanzees or the eastern woodchuck have been of great value for the characterization of HDV chronic infection. Recently, more practical animal models in which to perform a deeper study of host virus interactions and to evaluate new therapeutic strategies have been developed. Therefore, the main focus of this review is to discuss the current knowledge about HDV host interactions obtained from cell culture and animal models.

Keywords: hepatitis delta virus; HDV animal models; liver damage; antiviral treatment; vaccines

1. Introduction

1.1 *The Disease, Chronic HDV infection*

Worldwide there are approximately 350 million individuals chronically infected with the hepatitis B virus (HBV); among them 15 to 20 million are coinfecting with hepatitis delta virus (HDV) [1]. HDV was first described in 1977 when a novel antigen was detected in the nucleus of hepatocytes from patients chronically infected with HBV who developed serious episodes of severe liver disease [2]. In 1980 the same research group discovered that this nuclear antigen was derived from a new virus that they named hepatitis delta virus [3]. Thus, HDV was established as the causative infectious agent responsible for exacerbation of liver disease in HBV-infected patients [4,5]. HBV/HDV coinfection is associated with more severe acute hepatitis, higher risk of cirrhosis and decompensated liver disease, and higher mortality than HBV monoinfection. From 1990, after the initiation of the universal HBV vaccination campaigns, the incidence of HBV and concomitantly of HDV declined in the developed world. However, during the last 10 years, epidemiological studies revealed a stabilization, and in some cases an increase, in the incidence of HDV in several countries [6–11]. Furthermore, the epidemiology of HDV has not changed in developing countries where the HBV vaccine is not being administered to the population. Thus, HDV chronic infection represents a major health problem worldwide. Unfortunately, the treatment options for chronic HDV are limited. The only drug in use is pegylated interferon- α (PEG-IFN- α), which is associated with a low rate of cure and a significant number of patients in whom the virus relapses after cessation of treatment [12–14]. In addition, PEG-IFN- α is associated with a variety of adverse events, including flu-like symptoms, neuropsychiatric events, anemia, and thrombocytopenia. Thus, more effective treatment options are needed. The particular characteristics of HDV make the development of new therapeutic approaches very difficult. HDV depends on the activity of cellular enzymes to complete its life cycle and does not code for viral enzymes, which in the case of other viruses represent the main targets for the development of specific antivirals.

New treatments based on the use of interference RNA molecules [15,16] or—peptides to inhibit HDV-HBsAg interaction to block viral entry into cells—are being explored [17–21]. Moreover, inhibition of enzymatic processes that are required by the virus to complete its life cycle, e.g. the prenylation of viral antigens, represents a very interesting target [22,23]. Currently the antiviral activity of two prenylation inhibitors is being tested by Eiger BioPharmaceuticals in phase 2 clinical trials; these drugs are expected to become the first “specific” treatment for HDV.

1.2 *Main Characteristics of HDV*

HDV is the only member of the genus Deltavirus. HDV is a defective RNA virus that requires the HBV surface antigens (HBsAg) for viral assembly and transmission [14,24]. HDV virion is a small and spherical hybrid particle with a diameter of about 36–46 nm [24]. It is composed of the HDV RNA genome and about 200 molecules of hepatitis delta antigen (HDAg) enclosed by the hepatitis B surface antigen (HBsAg) and host lipids membrane (Figure 1). The HBsAg envelope protects the viral genome from the extracellular environment and dictates the hepatocyte tropism of HDV.

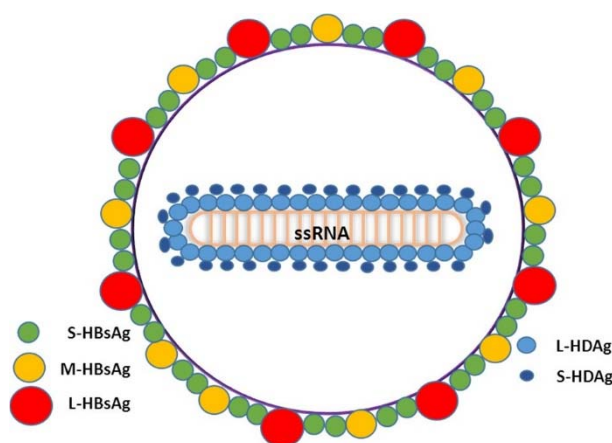


Figure 1. Schematic representation of HDV virions describing all the components of the viral particle. L-HDAg: HDV Large antigen; S-HDAg: HDV short antigen; S-HBsAg: Small HBV surface antigen; M-HBsAg: Medium HBV surface antigen; L-HBsAg: Large HBV surface antigen; ssRNA: single-stranded RNA.

The HDV genome is a circular negative sense RNA molecule of approximately 1700 nucleotides with the ability to fold on itself, appearing as a double-stranded rod-like structure with approximately 70% intramolecular base-pairing [25–27]. Its structure and function is very similar to the genome of plant viroids. In fact, replication of the HDV genome involves a rolling circle mechanism, requiring autocatalytic cleavage of the RNA by an internal ribozyme analogous to that proposed for plant viroids [28–30]. HDV genome replication involves only RNA species; in addition to the genome, infected cells contain, in smaller amounts, an exact complementary RNA species, called the antigenome, and much smaller amounts of a messenger RNA with a 5'-cap and a 3'-poly(A) tail. HDV isolates have been divided in eight clades based on nucleotide sequence and geographic distribution. The different isolates can differ in more than 30% of their nucleotide sequence [31].

1.3 Virus Life Cycle

To complete a cycle of HDV infection the hepatocyte must be infected by both HDV and HBV, since the formation of new viral particles requires HBV surface antigens. HDV infectivity is dependent upon a receptor-binding motif in the N-terminal region of the pre-S1 domain of the HBsAg [18,32]. Very recently, the receptor for both HBV and HDV infection has been identified as the human sodium-taurocholate cotransporting polypeptide (hNTCP) [32–34]. The NTCP is a transmembrane transporter present on the basolateral membrane of hepatocytes and is responsible for the uptake of conjugate bile acids from enterohepatic circulation [35]. After entering the hepatocytes, the virus is uncoated and a signal in the HDAg amino acid sequence mediates the translocation of the nucleocapsid into the nucleus [36]. To replicate its genome, the virus uses the host RNA polymerase/s [37]. Once inside the nucleus, cellular RNA polymerases synthesize the antigenomic RNA in the nucleolus and genomic RNA in the nucleoplasm (Figure 2) [26,37–40]. There is some controversy about which types of cellular RNA polymerases are involved in HDV RNA replication. Host RNA polymerases I, II, and III have been shown to interact with the HDV genome [41]. However, while RNA polymerase II was consistently found to interact with HDV components; the interaction with RNA polymerases I and III was not that clear [42].

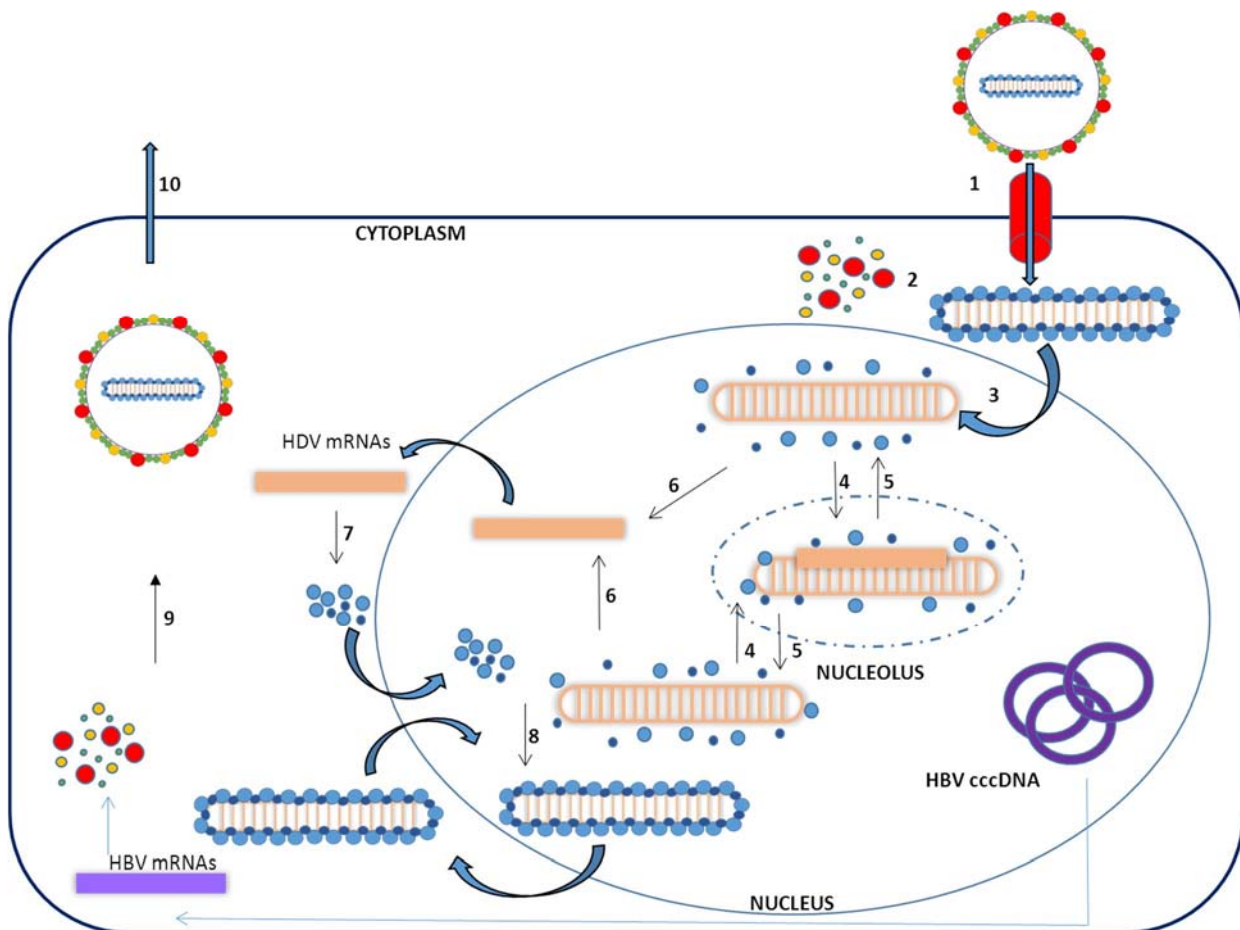


Figure 2. Schematic representation of the HDV viral cycle: (1) Binding to NTCP on human hepatocyte; (2) Uncoating; (3) Translocation of the ribonucleoprotein particle into the nucleus; (4) Transcription of the antigenome in the nucleolus.; (5) Production of genomic RNA in the nucleoplasm; (6) Transcription of the mRNA; (7) Translation of HDAG; (8) Ribonucleoparticle assembly; (9) Asotiation of HBsAg Virion production in the cytoplasm; (10) Virion release. HBV cccDNA: HBV covalently closed circular DNA. HBV mRNAs: HBV messenger RNAs.

Studies performed by different groups, particularly by Taylor and colleagues, indicated that the replication of the RNA genome, antigenome, and messenger RNA of HDV involves RNA polymerase II [43,44]. This is mainly substantiated by the sensitivity of HDV RNA replication to the RNA polymerase inhibitor α amanitin. However, the role of RNA polymerases I and III is still under consideration. RNA polymerase inhibition studies demonstrated *de novo* synthesis of HDV antigenome RNA molecules in the presence of a RNA polymerase II inhibitor, while its synthesis is decreased in the presence of RNA polymerase I inhibitor, suggesting that RNA polymerase I might be involved in this process [45]. More studies need to be performed to clarify these issues; however, what is clear is that the enzyme mainly involved in this HDV replication is RNA polymerase II.

HDV RNA is synthesized first as linear concatameric RNA that contains many copies of the genome. [28,30]. Then, the 85-nt site-specific viral ribozyme, found on each RNA strand, acts to process the RNA transcripts to unit lengths, monomers. These monomers are then ligated to form circular RNA. It is unclear if ligation is carried out by the ribozyme or a host RNA ligase [46]. During HDV replication, it is possible to detect three forms of HDV RNA: circular genomic RNA, circular complementary antigenomic RNA, and a linear polyadenylated

antigenomic RNA, which is the mRNA template containing the open reading frame for the translation of the hepatitis delta antigen (HDAg) [47]. There are two isoforms of the HDAg: the 24 kDa small form (S-HDAg), with 195 amino acid residues, and the 27 kDa large form (L-HDAg) with 214 amino acids [47]. The amino acid sequence of both isoforms is identical in the N-terminus, but L-HDAg is 19 amino acids longer at the C-terminus than S-HDAg.

S-HDAg is encoded by the viral genome and L-HDAg is the result of an RNA editing event mediated by host enzyme adenosine deaminase-1 (ADAR-1). ADAR-1 replaces the stop codon UAG at position 196 with a tryptophan codon UGG, extending the open reading frame and leading to the production of the large antigen [48–51]. The 19 extra amino acids added at the carboxyl terminal end of L-HDAg confer its functional properties that are different from S-HDAg. S-HDAg is required for the initiation of the viral genome replication; it is essential for the transcription and accumulation of newly processed HDV RNAs, whereas L-HDAg, which is synthesized in the late stage of viral replication, serves as a principal inhibitor of replication and is essential in the assembly of HDV virions. L-HDAg, by inhibiting viral replication, also regulates its own synthesis since it prevents the editing of the amber/W site necessary for the expression of L-HDAg. Furthermore, the HDV genome and antigenome associate with multiple copies of the S-HDAg and L-HDAg, forming ribonucleoprotein complexes (RNPs). Only the RNPs containing the HDV genomic molecule interact with HBV surface molecules and form new viral particles [52].

Both antigens suffer posttranslational modifications, which are very important to modulate their functions. S-HDAg is acetylated, phosphorylated, and sumoylated and L-HDAg is acetylated, phosphorylated, and isoprenylated. S-HDAg phosphorylation is crucial for its interaction with cellular RNA polymerase II and RNA binding. Sumoylation of S-HDAg results in an increase in HDV genomic RNA and mRNA synthesis. Acetylation of both antigens modulates HDV replication. Acetylation and phosphorylation of L-HDAgs are essential for the correct trafficking of this antigen inside the nucleus (nucleolus-nuclear speckles) and secretion. Isoprenylation of the L-HDAg is essential for the interaction of L-HDAg with HBsAg and the formation of new virions. The exact location where L-HDAg and HBsAg antigens interact is not well known; isoprenylated L-HDAg is mainly located in the nucleus and HBsAg is in the cytoplasm, thus L-HDAg forming part of HDV RNPs needs to be exported from the nucleus to the cytoplasm. The elucidation of the mechanism involved in this step requires more studies.

HDV viral particle generation depends on HBV surface antigen production; however, it is still not clear if HDV infection can persist in the absence of HBV replication. Contradictory data about this issue are available in the literature. It has been reported that HDV RNA, when introduced in human cells in the absence of HBV, can replicate efficiently, produce HDAgs, and form RNPs that are not able to exit the cell. Furthermore, if another alternative source of HBV envelope proteins is available, like integrated HBV DNA, HDV can replicate itself independently of hepadnavirus replication [53]. In fact, HCC cells that apparently no longer support HBV replication but can still produce the envelope proteins from HBV integrants can generate HDV infectious particles [54]. Recent studies performed in mice with humanized livers showed that HDV mono-infection can persist on human hepatocytes for at least 6 weeks and can be rescued by HBV superinfection [55]. In addition, data in a very small number of patients showed that HDV can survive and synthesize HDAg in the absence of detectable HBV [56]. However, on the other hand, it has been demonstrated that inhibition of hepadnavirus infection in patients

and animal models by the use of antiviral medication led to reduction or loss of HDV replication [57,58]. Thus, nowadays the consensus is that HDV can persist without HBV but only for a brief period of time.

2. *In vitro* HDV-Host Cell Interaction

Although a wide range of cultured cell lines can support HDV replication (HEK-293, HeLa, Huh7) after the transfection of a plasmid containing the HDV genome, the virus fails to infect any cultured cell lines except primary cultures of hepatocytes and Hepa RG cells with a very low efficiency [59]. However, very recently this situation has dramatically changed with the discovery of the HBV/HDV receptor. Human as well as other species cell lines that stably express the sodium taurocholate receptor have been generated; these cells are infected by and are able to sustain HDV replication [32–34].

In order to elucidate the mechanism responsible for the increase in liver pathology observed in patients infected with HDV, several authors have analyzed the interaction of viral components with cell components *in vitro* or in cell culture. The first experiments performed to identify host factors interacting with HDAg were performed using a yeast two-hybrid system [60,61]. From these studies a single protein was identified and named as delta antigen interacting protein A or DIPA. DIPA is a cellular protein with high homology to HDAg. DIPA overexpression inhibits HDV replication; however, confirmatory studies and a deeper analysis about the mechanism are lacking. Later on, different proteomic approaches have been performed in a variety of cell lines, identifying several factors that interact with delta antigen such as subunits of RNA polymerase II complex, hnRNP proteins, RNA helicases, the histone H1, PML, nucleolin, B23, Pol I specific factor SL1, the negative transcription elongation factor DSIF, and PKR [42]—all of these factors have been suggested to affect HDV replication, but only in some cases experimentally proven.

Furthermore, it has been shown that the HDV RNAs interact with the polypyrimidine tract-binding protein-associated splicing factor (PSF), PKR, GAPDH, and ADAR-1 [62–65]. In fact, as previously indicated, ADAR-1 has been shown to be responsible for HDV antigenome editing [51].

Regarding the potential mechanism of HDV-mediated cytotoxicity, it has been reported that cells expressing HDV proteins present multiple cellular signaling pathways modified like enhanced ROS production, leading to oxidative stress and activation of several transcription factors such as STAT-3 or NF- κ B [66] or potentiated TGF- β signal activation [67]. These HDV-mediated cellular modifications can promote several disease phenotypes associated with HDV infection like liver fibrosis or cellular damage. Moreover, HDV can interfere with the JAK-STAT signal transduction pathway in response to IFN- α , impairing the phosphorylation of both STAT1 and STAT2 and leading to inefficient IFN- α stimulated gene expression [68], which might explain the relatively low antiviral efficacy of PEG-IFN- α .

There is also evidence suggesting that both HDAGs are transcriptional inducers, as both are capable of regulating cellular gene expression presenting L-HDAg broader transcriptional activity [69–71]. One mechanism mediating such effects can be histone acetylation, as an upregulation of this modification associated with expression of both HDAGs and HDV replication has been observed [72].

Proteomic analysis of cells producing whole HDV RNPs shows a set of changes in host protein synthesis that in some cases seems to correlate with previous pathologic findings observed in both chronic and acute HDV patients, like changes in enzymes involved in lipid metabolism [63]. Furthermore, this study indicates an overall

deregulation of DNA replication and cell cycle control in liver cells, like downregulation of PCNA and the Fen 1 endonuclease, proteins involved in DNA replication. This observation is in accordance with the subtle growth disadvantage associated with HDV replication in dividing cells and deregulation of cell cycle control [73,74]. Regarding innate immune responses, there are no data in the literature describing molecules implicated in the detection of the virus or pattern recognition receptors that detect HDV. However, it has been shown that elements of the virus are able to transactivate the IFN- α -inducible MxA gene [66] and to activate PKR [75].

3. Chronic HDV Infection Animal Models

3.1. "Natural" Animal Models

In a natural setting, only humans are known to acquire HDV infection [24]; however, it is quite possible that chimpanzees or other large primates can be infected with HDV in the wild. As previously described, the HDV virus requires help from a virus of the family hepadnaviridae for formation of new virions, thus the host range of HDV is limited to those species that support the replication of HBV, like chimpanzees, or a hepadnavirus capable of supplying helper functions [76–80]. Among members of the Hepadnaviridae family, the closest to HBV are the woolly monkey hepatitis B virus (WMHBV) and the woodchuck hepatitis virus (WHV), which can assist in HDV propagation because both encode viral envelope proteins that are competent for HDV ribonucleoprotein (RNP) envelopment [81]. In contrast, the envelope protein of duck hepatitis B virus (DHBV), the most distantly related hepadnavirus, is unable to assist in HDV propagation due to the inability of the envelope protein to package HDV RNP [82]. Recently, bats have been described as a new animal model that could support HDV replication based on the presence of a HBV antigenically related pathogenic hepadnavirus that can generate HDV pseudotyped particles able to infect human and bat primary hepatocytes [83]. Based on its close phylogenetic relation to primates, the tree shrew species *Tupaia belangeri* has been used for infection studies both with HBV and WMHBV [21,84,85], and is also a host for HDV infection [86].

Among these models, the most frequently used for experimental studies is the woodchuck chronically infected with WHV and superinfected with HDV, obtaining interesting and relevant data. Experimental transmission of HDV has been accomplished in the chimpanzee and the eastern woodchuck, hosts of HBV and WHV, respectively [76,87]. In both models upon HDV infection, there is a major suppression of HBV and WHV replication at the peak of HDV replication, as has been observed in humans [88]. Eighty to one hundred percent of HDV superinfections in WHV carrier woodchucks resulted in chronic HDV infection, while coinfection resulted in an acute self-limited infection.

It has been shown that woodchucks treated with cyclosporine A, as an inhibitor of the immune response, showed an increase in HDV viremia and at the same time a reduction of WHV viral load. These results indicate that the host immune response exerts a negative control over HDV replication and that HDV influences HBV replication independently of the host immune response [89]. Furthermore, this model was used during the last years to test vaccination strategies designed to protect HBV carriers from HDV superinfection [90–94].

These natural animal models have provided very useful data and they have allowed for determining the main characteristics of the HDV infective cycle and some immunological responses as they recapitulate several of the biological phenomena observed in humans. However, there are several limitations for performing experiments in these animal models that have delayed the HDV research field, ranging from the relatively large size and genetic

variability of these animals to availability and ethical considerations. Furthermore, several issues limit the number of animals that can be used, affecting the statistical significance of any potential results. On top of that, the experimental tools available to work with most of these animal species are very limited, highlighting the need for the development of more practical animal models.

3.2. *Mouse Models of HDV Replication*

3.2.1. Injection of Mice with HDV Infectious Particles

The mouse represents the premier mammalian model system for disease research. Scientists from a wide range of biomedical fields have gravitated to the mouse because of its close genetic and physiological similarities to humans, as well as the ease with which its genome can be manipulated and analyzed. Additionally, scientists have developed a broad range of technological tools and approaches to dissect molecular and physiological processes in one organism that is easy to maintain. Therefore, there have been several attempts by scientists aimed at developing mice as an HDV experimental system.

The first proof of concept study of HDV infection in mice was performed in 1993, by the group of Dr. Taylor at the Fox Chase Cancer Center in Philadelphia; they showed that human hepatitis delta virus (HDV) obtained from the serum of an experimentally infected woodchuck and injected into either the peritoneal cavity or the tail vein of mice was able to infect the murine liver. In this model, genomic HDV increased in the liver during the first 5 to 10 days postinoculation; antigenomic RNA was also detected, and delta antigen was present in the nuclei of the hepatocytes [44]. The infection was liver-specific but involved no more than 0.6% of the mouse hepatocytes. Once HDV entered mouse hepatocytes, the levels of HDV genome replication were comparable to those obtained in a natural infection of woodchuck hepatocytes; however, the infection was short lived, with a half-life of clearance of about 3 days. Moreover, no obvious cytopathic effects were detected.

The reason for the disappearance of the viral genome from the liver was not determined, but the role of T- and B-cell-dependent immune response can be excluded, since the rate of this decrease was the same in both normal mice and those with a severe combined immunodeficiency. Unfortunately, there are no more reports suggesting HDV infectivity in mice, probably as a consequence of the unproductive HBsAg binding to mNTCP receptor, as has been recently described.

3.2.2. HDV Transgenic Mice

As previously described, HDV infection clearly increases the severity of liver pathology in patients with HBV chronic infection, but the molecular mechanism involved in the exacerbation of liver pathology associated with HDV infection is still unknown. Some authors suggest a potential cytopathic effect of this virus according to data obtained in chimpanzees, particularly during an acute infection [95]. Work performed by other groups suggested the potential direct pathogenic role of HDV antigens. S-HDAs have been shown to have a cytotoxic effect when overexpressed in HepG2 or HeLa cells, inducing the necrosis of the cells [96]. Additionally, it has been postulated that the L-HDAg might play a role in HDV pathogenesis due to its capacity to activate many eukaryotic promoters and modulate different signaling pathways [62,73,74]. In order to elucidate the role of HDV antigens in the exacerbation of liver disease, the group of Dr. Frank Chisari at Scripps, La Jolla, CA, developed transgenic mice

for expression of SHDAg or L-HDAg in the liver [97]. These animals express HDAGs in hepatocyte nuclei, as observed in natural HDV infection. However, no obvious signs of biological or histopathological evidence of liver disease, cytotoxicity, or hepatitis were detectable during the mice's lifespan. Furthermore serum transaminase levels remained within the normal range, indicating that neither the large nor small form of HDAG are directly cytopathic to the hepatocyte *in vivo* [97]. Thus, contrary to expectations, HDAG *in vivo* does not seem have a pathological role.

Because HDV infection occurs mainly in the context of a coexisting HBV infection, the authors asked if the liver damage observed in patients with HDV infection might require the presence of both HDAGs and HBsAg. To answer this question, the authors crossed HDAG transgenic mice with HBsAg transgenic mice. Once again no histopathological or biochemical evidence of liver cell injury was observed, indicating that viral proteins are not directly cytopathic to the hepatocyte. The authors suggest that maybe the presence of other HBV proteins is required to promote hepatocyte damage [97]. However, the role of the immune response against viral antigens should not be forgotten. Transgenic animals' HDAG is expressed at fetal stages since the transgene is driven by an albumin promoter and the animals will recognize the viral antigen as a self-antigen, inducing a tolerogenic immune response. Moreover, liver injury associated with HDV infection could be a consequence of HDV and HBV protein and viral replication presence or the response of the host to the same factors.

After the transgenic animal model expressing HDAGs, a new transgenic mouse carrying a replication-competent HDV genomic dimer RNA was developed (HDVTg). HDVTg mice have been shown competent for studying HDV replication *in vivo* [98]. Surprisingly, despite the expression of HDV being under the control of the albumin promoter, HDV genomic and antigenomic sequences were detected in the liver, brain, testis, kidney, and particularly in skeletal muscle, where the amount of HDV RNA was 100-fold higher than in the liver. These results indicate that the transcriptional leakage associated with the albumin promoter allows HDV priming expression and consequently licenses HDV replication in several tissues. The presence of antigenomic HDV monomer RNA is possible only after processing and replication of the primary genomic dimer transcript; thus, the data in this transgenic animal model indicated that HDV can replicate in nearly all cell types. Interestingly, it is observed that HDV replicates more efficiently in muscle cells than in the hepatocytes, indicating that the hepatic specificity of HDV is due to the HBV-derived envelope. Moreover, analysis of HDV antigen expression showed a similar pattern, i.e., HDV small antigen was detected mainly in the muscles, and in lower amounts in the liver. However, no large HDV antigen was detected in any tissue, indicating that no efficient HDV RNA editing occurs in these animals. Finally, and in accordance with the results observed in HDAG transgenic animals, no evidence of pathology was seen in muscle, brain, or liver tissue without any manifestation of necrosis or inflammation. These data indicate that HDV RNA replication and delta small antigen expression did not appear to cause any evident pathology and consequently HBV presence might be required to induce hepatocyte damage. Unfortunately, there is no information about the potential immune response against viral antigens in transgenic animals that could help to understand the absence of liver damage and could determine if these animals could have any potential for analyzing HDV immune responses.

Although the NTCP gene is highly conserved between species, mouse NTCP does not contain molecular determinants required for viral entry [33]. Recent studies have shown that exogenous hNTCP expression in a mouse hepatoma cell line allows them to support HDV infection, but not HBV infection. Remarkably, *in vitro*

HDV infection was also achieved in cell lines originated from other species and tissues expressing exogenous hNTCP, confirming that HDV human hepatotropism is restricted by the presence of the hNTCP receptor [32,33]. Therefore, generation of transgenic animals expressing hNTCP or a chimeric mNTCP replaced with hNTCP 84 to 87 residues in mouse hepatocytes would be potentially susceptible to natural HDV infection. However, these animals would not be susceptible to HBV infection as mouse hepatocytes have been shown refractory to HBV infection and they will not support the complete HDV life cycle.

3.2.3. Mice with “Humanized” Livers

Another approach to study HDV virus replication requires the use of immunodeficient mice with human hepatocytes engrafted in their livers [20,55]. To generate mice with humanized livers, the investigators induced murine hepatocyte damage to create the space and the environment for engraftment and proliferation of human transplanted cells. The first model is based on the use of immunodeficient mice transgenic for the urokinase plasminogen activator (uPA-SCID), and the second model is based on Rag2-deficient mice and γ chain of interleukin 2 receptor (Il2rg) and lacking the the fumaryl acetoacetate hydrolase (Fah) gene. In both cases the animals suffer dramatic hepatocellular damage (death of a high percentage of mouse hepatocytes) and mice are rescued by transplantation of human hepatocytes [99]. The human cells residing in the mouse liver can proliferate and repopulate host liver tissue and they are susceptible to the establishment and maintenance of intrahepatic HDV mono-infection, increasing intrahepatic amounts of large HDAg; edited HDV RNA forms increased over time. Moreover, HBV superinfection of chimeric mice supporting HDV infection leads to the production of infective HDV virion in mice sera and an increase of HDAg-positive human hepatocytes, demonstrating intrahepatic HDV spreading [55]. Additionally, HDV infection reduces significantly the increase of HBV viremia and intrahepatic cccDNA loads in comparison with HBV mono-infected mice, as has been observed in patients. These mice have been used to show the ability of the NTCP inhibitor Myrcludex B to block HBV and HDV entry [20]. However, humanized mouse livers present several limitations:

1. The availability of primary human hepatocytes is limited and they cannot be propagated *in vitro*, which limits the number of available animals.
2. The susceptibility of primary human hepatocytes to HBV infection is highly variable and generally low, since these cells rapidly dedifferentiate, losing the expression of the NTCP receptor.
3. The engraftment of human hepatocytes in the liver of mice requires the use of immunodeficient mice, thus the interaction of the immune system and the virus is lost and consequently experiments are restricted to studies analyzing virus host–cell interactions.

3.2.4. Development of Gene Delivery Vectors to Deliver HDV Genomes into Mice

In vivo gene delivery has been widely used for elucidating gene function and for creating disease animal models. It is usually performed by a non-viral or viral approach. The former approach mainly depends on the use of recombinant DNA or RNA, whereas the latter approach depends on the use of viral vectors. The nonviral delivery has several advantages such as less toxicity, less immunogenicity, and safer and easier to prepare.

However, this approach has limited gene delivery efficiency and results in a short duration of transgene expression.

It has been observed that cloned plant viroids' cDNA copies are infectious when they are introduced in host cells [100]. Similarly, although HDV replication proceeds without DNA intermediates, multimeric forms of HDV cDNA transcribed or introduced in the cells are able to initiate the normal HDV replication pathway [101,102]. Accordingly, when an HBV-infected chimpanzee was inoculated by direct injection into the liver with a recombinant plasmid containing a full-length HDV genome and one expression vector allowing the translation of HDAg, it resulted in a productive infection with appearance of high levels of HDV RNA and long and short HDVAg in the liver [103]. HDV RNA and HDAg were also detected in serum following a similar kinetic to the one observed in an acute infection, generating virions with mature HDV particles characteristics and a marked transient suppression of the synthesis of HBV DNA replicative intermediates during the active phase of HDV, as is observed in HDV superinfection in both humans and chimpanzees [104,105]. These results suggest that transduction of animals with HDV expression vectors can recapitulate most of the HDV viral cycle.

As previously described, HDV transgenic animals have shown that viral replication *in vivo* is not restricted to the liver and is highly efficient in muscle cells [98]. Consequently, when cDNA dimers of HDV were inoculated intramuscularly into mice, HDV genomic RNA increased to substantial levels by week 7 post-injection; also, antigenomic sense HDV RNA and hepatitis delta antigen were present in myocytes' nuclei, confirming HDV ubiquitous replication competence, as has been observed in transgenic animals. Interestingly, sera from DNA injected mice contained antibodies specific for HDAg, indicating the induction of an immunological response to the intracellularly expressed antigen, similar to the one observed when mice are inoculated with an HDAg expression vector [106]. When HDV cDNA expression vector is hydrodynamically injected in the liver (a technique that allows the transduction of 10–30% of hepatocytes) there is an increase of genomic and antigenomic HDV RNA for two weeks, indicating the existence of HDV RNA replication [107]. Thereafter there is a decrease in HDV genomic RNA from day 15 to 30, in clear contrast to what is observed when the vector is inoculated intramuscularly. These differences can be caused by the use of different promoters for initial HDV RNA transcription or by the stronger HDV replication in muscle in comparison to hepatocytes, as has been previously observed in transgenic mice. However, we cannot exclude the possibility that this can also be due to the differences in the mouse strain used in each experiment. A similar situation was previously described for HBV replication: C57BL/6 mice develop robust HBV replication after hydrodynamic injection of HBV plasmids, whereas HBV replication is transient in BALB/c mice [108]. Interestingly, shortly after HDV hydrodynamic injection, small HDAg is highly expressed and is detected in nuclei and cytoplasm. S-HDAg expression becomes undetectable 15 days after DNA inoculation, indicating that HDAg decline precedes HDV RNA reduction. In this animal model, posttranscriptional RNA editing occurs, leading to the appearance of the large form of the large delta of HDV. However, L-HDAg protein represents just 3% of the accumulated delta protein in the hepatocytes, lower than the levels detected in transfected cells and indicating a deficient editing that can promote a suboptimal replication of the HDV genome, which results in the disappearance of the HDV genome and antigens. Therefore, it should be clarified whether transient HDV replication observed in mouse livers after the HDV-replicative vector is hydrodynamically delivered is due to the mouse strain used for the experiments or to liver characteristics.

As we already indicate several times, the HDV virions require for their formation the hepatitis B virus surface antigen subunits provided by HBV co-infection or by the administration of an HBsAg-expressing vector. When HBV transgenic mice that produce HBV virions are used as hosts for hydrodynamic injection of HDV cDNA, HDV viral particles are detected in the serum [23]. In these mice, HDV replicates in hepatocytes and close to 30% of hepatocytes display a characteristic nuclear staining observed in HDV-infected cells. There is a good correlation between the level of intrahepatic replication and HDV virions' RNA in the serum. However, as was observed in wild-type animals, HDV replication in hepatocytes that contain HBV-replicating virus do not promote an increase in ALT level, as is observed in humans and chimpanzees. Moreover, no anti-HDV antibodies were detected in the serum of these animals, which might be a consequence of the tolerogenic environment present in HBV transgenic mice livers. Very importantly, the majority of the HDV RNA was cleared by day 21 from the livers and serum. These animals were useful to demonstrate that pharmacologic prenylation inhibition can prevent the production of HDV virions *in vivo* [23].

Taking all these studies together, we can conclude that none of the murine models developed so far recapitulate all the features of chronic HDV infection.

In the last years several groups have developed HBV animal models using a recombinant virus carrying the HBV genome, like adenovirus (Ad) [109,110] or adenoassociated virus (AAV) [111,112], which acts as a shuttle vector for the delivery of the viral genome into the cells. In our laboratory we are currently working on the development of a similar strategy to create a model of HDV chronic infection; preliminary data indicates that by using this strategy, persistent HDV replication can be achieved in mice.

4. **Conclusions**

In conclusion, animal models are essential for the knowledge of HDV–host interactions as well as for the development of new therapeutic strategies (summarized in Table 1). Data obtained in cell culture are in clear contradiction with the data obtained in animal models. While overexpression of HDAGs in cells is associated with cytotoxicity, necrosis, and apoptosis, none of these effects are detected in transgenic animal models. In this review we showed that the animal models available nowadays that recapitulate HDV chronic infection are natural hosts susceptible to infection by members of the hepadnaviridae family that can be co-infected with human HDV. However, these animals present obvious ethical and experimental limitations. Murine models developed so far do not recapitulate all the characteristics of HDV infection, such as RNA editing, sustained viral load, or liver injury. Furthermore, several of them were developed in the context of immunosuppressed animals, precluding studies regarding the immune response against the virus. This review highlights the need for the development of new small animal models that better reflect the main feature of HDV chronic infection and that will allow a deeper analysis of HDV–host interaction as well as facilitate the development of new therapeutic agents and/or vaccines.

Table 1. Summary of the main characteristics of HDV animal models.

Animal model		Main characteristics	References
Natural animal model	chimpanzees	Chimpanzees can be efficiently infected by HDV, coinfection and superinfection experiments have been performed resulting in moderately severe and severe liver damage, respectively.	79–81
	woodchucks	Several laboratories have shown that woodchucks chronically infected with WHV can be infected by HDV and produce new HDV virions using WHV surface antigen to form the envelope. This animal model recapitulate many of the characterists of HDV infection in humans.	76–78
	bats	HDV pseudotyped with surface proteins of bat hepadnavirus TBHBV is able to infect both primary hepatocytes, a pattern similar to the pattern observed with HDV-HBV	83
WT mice	wild-type & immunodeficient mice	Mice injected with HDV virus obtained from woodchucks transiently infect and replicate in the liver	44
HDV-transgenic mice	S-HDAg transgenic mice	S-HDAg is expressed in hepatocytes and localized in the nucleus. No liver injury was observed, thus S-HDAg protein is not responsible for HDV inducing liver damage.	97
	L-HDAg transgenic mice	L-HDAg is expressed in hepatocytes an localized in the nucleus. No liver injury was observed, thus L-HDAg protein is not responsible for HDV inducing liver damage.	97
	HDV Ag x HBV sAg	The phenotype of these mice does not differ from the phenotype of the parents	97
	HDV genome under the control of the Albumin promoter	HDV replication and S-HDAg expression was detected in several organs including the liver, muscle, and brain. However, no large HDV large antigen were detected in any tissue, indicating that there was no efficient HDV RNA editing. Furthermore, no liver pathology was observed.	98
Humanized mouse models	Fah ^{-/-} RAG ^{-/-} IL-2Rg ^{-/-} + human hepatocytes	Establishment of HDV infection was highly efficient in both HBV-infected and naïve chimeric mice, representing an interesting animal model to study HDV-human hepatocyte interaction and new antivirals.	20,55,99
HDV-transfected mice	HDV plasmid hydrodynamic injection	In this animal model there is an increase of HDV genome and antigenome in the liver but only during the first two weeks after hydrodinamic injetion. There is no associated damage. Edition is observed in the liver.	107
HDV-transfected mice	HDV plasmid intramuscular injection	Sustained RNA accumulation at least for 7 weeks. HDAg antibody generation	106

Acknowledgements

Rafael Aldabe is supported by “Programa Torres Quevedo” Contract (PTQ-13-06466) from the Spanish Ministry of Economy and Competitiveness. Lester Suarez and Carla Usai are supported by FPU and FPI fellowships, respectively, from the Spanish Ministry of Science and Education.

Author Contributions

Rafael Aldabe, Lester Suárez-Amarán, and Gloria González-Aseguinolaza performed the literature research and wrote the manuscript. Carla Usai made the figures.

Conflicts of Interest

The authors declare no conflict of interest.

References

1. Rizzetto, M.; Ciancio, A. Epidemiology of hepatitis D. *Semin. Liver Dis.* **2012**, *32*, 211–219.
2. Rizzetto, M.; Canese, M.G.; Arico, S.; Crivelli, O.; Trepo, C.; Bonino, F.; Verme, G. Immunofluorescence detection of new antigen-antibody system (delta/anti-delta) associated to hepatitis B virus in liver and in serum of HBsAg carriers. *Gut* **1977**, *18*, 997–1003.
3. Rizzetto, M.; Hoyer, B.; Canese, M.G.; Shih, J.W.; Purcell, R.H.; Gerin, J.L. Delta agent: Association of delta antigen with hepatitis B surface antigen and RNA in serum of delta-infected chimpanzees. *Proc. Natl. Acad. Sci. USA* **1980**, *77*, 6124–6128
4. Lee, S.D.; Wang, J.Y.; Wu, J.C.; Tsai, Y.T.; Lo, K.J.; Lai, K.H.; Tsay, S.H.; Govindarajan, S. Hepatitis D virus (delta agent) superinfection in an endemic area of hepatitis B infection: Immunopathologic and serologic findings. *Scand. J. Infect. Dis.* **1987**, *19*, 173–177.
5. Lin, H.H.; Liaw, Y.F.; Chen, T.J.; Chu, C.M.; Huang, M.J. Natural course of patients with chronic type B hepatitis following acute hepatitis delta virus superinfection. *Liver* **1989**, *9*, 129–134.
6. Wedemeyer, H. Hepatitis D revival. *Liver Int.* **2011**, *31* (Suppl. 1), 140–144.
7. Rizzetto, M.; Alavian, S.M. Hepatitis delta: The rediscovery. *Clin. Liver Dis.* **2013**, *17*, 475–487.
8. Ciancio, A.; Rizzetto, M. Chronic hepatitis D at a standstill: Where do we go from here? *Nat. Rev. Gastroenterol. Hepatol.* **2014**, *11*, 68–71.
9. Gaeta, G.B.; Stroffolini, T.; Smedile, A.; Niro, G.; Mele, A. Hepatitis delta in Europe: Vanishing or refreshing? *Hepatology* **2007**, *46*, 1312–1313.
10. Heidrich, B.; Deterding, K.; Tillmann, H.L.; Raupach, R.; Manns, M.P.; Wedemeyer, H. Virological and clinical characteristics of delta hepatitis in central Europe. *J. Viral Hepat.* **2009**, *16*, 883–894.
11. Servant-Delmas, A.; Le Gal, F.; Gallian, P.; Gordien, E.; Laperche, S. Increasing prevalence of HDV/HBV infection over 15 years in France. *J. Clin. Virol.* **2014**, *59*, 126–128.
12. Abbas, Z.; Khan, M.A.; Salih, M.; Jafri, W. Interferon alpha for chronic hepatitis D. *Cochrane Database Syst. Rev.* **2011**, *12*, doi:10.1002/14651858.CD006002.pub2.
13. Abbas, Z.; Memon, M.S.; Mithani, H.; Jafri, W.; Hamid, S. Treatment of chronic hepatitis D patients with pegylated interferon: A real-world experience. *Antivir. Ther.* **2014**, *19*, 463–468.
14. Alvarado-Mora, M.V.; Locarnini, S.; Rizzetto, M.; Pinho, J.R. An update on HDV: Virology, pathogenesis and treatment. *Antivir. Ther.* **2013**, *18*, 541–548.
15. Chang, J.; Taylor, J.M. Susceptibility of human hepatitis delta virus RNAs to small interfering RNA action. *J. Virol.* **2003**, *77*, 9728–9731.
16. Singh, S.; Gupta, S.K.; Nischal, A.; Khattri, S.; Nath, R.; Pant, K.K.; Seth, P.K. Design of potential siRNA molecules for hepatitis delta virus gene silencing. *Bioinformation* **2012**, *8*, 749–757.

17. Abou-Jaoude, G.; Molina, S.; Maurel, P.; Sureau, C. Myristoylation signal transfer from the large to the middle or the small HBV envelope protein leads to a loss of HDV particles infectivity. *Virology* **2007**, *365*, 204–209.
18. Abou-Jaoude, G.; Sureau, C. Entry of hepatitis delta virus requires the conserved cysteine residues of the hepatitis B virus envelope protein antigenic loop and is blocked by inhibitors of thiol-disulfide exchange. *J. Virol.* **2007**, *81*, 13057–13066.
19. Blanchet, M.; Sureau, C.; Labonte, P. Use of FDA approved therapeutics with hNTCP metabolic inhibitory properties to impair the HDV lifecycle. *Antivir. Res.* **2014**, *106*, 111–115.
20. Lütgehetmann, M.; Mancke, L.V.; Volz, T.; Helbig, M.; Allweiss, L.; Bornscheuer, T.; Pollok, J.M.; Lohse, A.W.; Petersen, J.; Urban, S.; *et al.* Humanized chimeric uPA mouse model for the study of hepatitis B and D virus interactions and preclinical drug evaluation. *Hepatology* **2012**, *55*, 685–694.
21. Urban, S.; Bartenschlager, R.; Kubitz, R.; Zoulim, F. Strategies to inhibit entry of HBV and HDV into hepatocytes. *Gastroenterology* **2014**, *147*, 48–64.
22. Bordier, B.B.; Marion, P.L.; Ohashi, K.; Kay, M.A.; Greenberg, H.B.; Casey, J.L.; Glenn, J.S. A prenylation inhibitor prevents production of infectious hepatitis delta virus particles. *J. Virol.* **2002**, *76*, 10465–10472.
23. Bordier, B.B.; Ohkanda, J.; Liu, P.; Lee, S.Y.; Salazar, F.H.; Marion, P.L.; Ohashi, K.; Meuse, L.; Kay, M.A.; Cas, J.L.; *et al.* *In vivo* antiviral efficacy of prenylation inhibitors against hepatitis delta virus. *J. Clin. Investig.* **2003**, *112*, 407–414.
24. Taylor, J.M. Hepatitis delta virus. *Virology* **2006**, *344*, 71–76.
25. Kos, A.; Dijkema, R.; Arnberg, A.C.; van der Meide, P.H.; Schellekens, H. The hepatitis delta (delta) virus possesses a circular RNA. *Nature* **1986**, *323*, 558–560.
26. Taylor, J.M. Structure and replication of hepatitis delta virus RNA. *Curr. Top. Microbiol. Immunol.* **2006**, *307*, 1–23.
27. Makino, S.; Chang, M.F.; Shieh, C.K.; Kamahora, T.; Vannier, D.M.; Govindarajan, S.; Lai, M.M. Molecular cloning and sequencing of a human hepatitis delta (delta) virus RNA. *Nature* **1987**, *329*, 343–346.
28. Flores, R.; Grubb, D.; Elleuch, A.; Nohales, M.Á.; Delgado, S.; Gago, S. Rolling-circle replication of viroids, viroid-like satellite RNAs and hepatitis delta virus: Variations on a theme. *RNA Biol.* **2011**, *8*, 200–206.
29. Flores, R.; Ruiz-Ruiz, S.; Serra, P. Viroids and hepatitis delta virus. *Semin. Liver Dis.* **2012**, *32*, 201–210.
30. Ke, A.; Zhou, K.; Ding, F.; Cate, J.H.; Doudna, J.A. A conformational switch controls hepatitis delta virus ribozyme catalysis. *Nature* **2004**, *429*, 201–205.
31. Deny, P. Hepatitis delta virus genetic variability: From genotypes I, II, III to eight major clades? *Curr. Top. Microbiol. Immunol.* **2006**, *307*, 151–171.
32. Ni, Y.; Lempp, F.A.; Mehrle, S.; Nkongolo, S.; Kaufman, C.; Fälth, M.; Stindt, J.; Königer, C.; Nassal, M.; Kubitz, R.; *et al.* Hepatitis B and D viruses exploit sodium taurocholate co-transporting polypeptide for species-specific entry into hepatocytes. *Gastroenterology* **2014**, *146*, 1070–1083.
33. Yan, H.; Peng, B.; He, W.; Zhong, G.; Qi, Y.; Ren, B.; Gao, Z.; Jing, Z.; Song, M.; *et al.* Molecular determinants of hepatitis B and D virus entry restriction in mouse sodium taurocholate cotransporting polypeptide. *J. Virol.* **2013**, *87*, 7977–7991.

34. Yan, H.; Zhong, G.; Xu, G.; He, W.; Jing, Z.; Gao, Z.; Huang, Y.; Qi, Y.; Peng, B.; Wang, H.; *et al.* Sodium taurocholate cotransporting polypeptide is a functional receptor for human hepatitis B and D virus. *Elife* **2012**, *1*, e00049.
35. Pellicoro, A.; Faber, K.N. Review article: The function and regulation of proteins involved in bile salt biosynthesis and transport. *Aliment. Pharmacol. Ther.* **2007**, *26* (Suppl. 2), 149–160.
36. Xia, Y.P.; Yeh, C.T.; Ou, J.H.; Lai, M.M. Characterization of nuclear targeting signal of hepatitis delta antigen: Nuclear transport as a protein complex. *J. Virol.* **1992**, *66*, 914–921.
37. Chang, J.; Nie, X.; Chang, H.E.; Han, Z.; Taylor, J. Transcription of hepatitis delta virus RNA by RNA polymerase II. *J. Virol.* **2008**, *82*, 1118–1127.
38. Tseng, C.H.; Lai, M.M. Hepatitis delta virus RNA replication. *Viruses* **2009**, *1*, 818–831.
39. Taylor, J.M. Replication of the hepatitis delta virus RNA genome. *Adv. Virus Res.* **2009**, *74*, 103–121.
40. Lehmann, E.; Brueckner, F.; Cramer, P. Molecular basis of RNA-dependent RNA polymerase II activity. *Nature* **2007**, *450*, 445–449.
41. Greco-Stewart, V.S.; Schissel, E.; Pelchat, M. The hepatitis delta virus RNA genome interacts with the human RNA polymerases I and III. *Virology* **2009**, *386*, 12–15.
42. Cao, D.; Haussecker, D.; Huang, Y.; Kay, M.A. Combined proteomic-RNAi screen for host factors involved in human hepatitis delta virus replication. *RNA* **2009**, *15*, 1971–1979.
43. MacNaughton, T.B.; Gowans, E.J.; McNamara, S.P.; Burrell, C.J. Hepatitis delta antigen is necessary for access of hepatitis delta virus RNA to the cell transcriptional machinery but is not part of the transcriptional complex. *Virology* **1991**, *184*, 387–390.
44. Netter, H.J.; Kajino, K.; Taylor, J.M. Experimental transmission of human hepatitis delta virus to the laboratory mouse. *J. Virol.* **1993**, *67*, 3357–3362.
45. Lai, M.M. The molecular biology of hepatitis delta virus. *Annu. Rev. Biochem.* **1995**, *64*, 259–286.
46. Reid, C.E.; Lazinski, D.W. A host-specific function is required for ligation of a wide variety of ribozyme-processed RNAs. *Proc. Natl. Acad. Sci. USA* **2000**, *97*, 424–429.
47. Weiner, A.J.; Choo, Q.L.; Wang, K.S.; Govindarajan, S.; Redeker, A.G.; Gerin, J.L.; Houghton, M. A single antigenomic open reading frame of the hepatitis delta virus encodes the epitope(s) of both hepatitis delta antigen polypeptides p24 delta and p27 delta. *J. Virol.* **1988**, *62*, 594–599.
48. Chen, R.; Linnstaedt, S.D.; Casey, J.L. RNA editing and its control in hepatitis delta virus replication. *Viruses* **2010**, *2*, 131–146.
49. Hartwig, D.; Schütte, C.; Warnecke, J.; Dorn, I.; Hennig, H.; Kirchner, H.; Schlenke, P. The large form of ADAR 1 is responsible for enhanced hepatitis delta virus RNA editing in interferon-alpha-stimulated host cells. *J. Viral Hepat.* **2006**, *13*, 150–157.
50. Polson, A.G.; Bass, B.L.; Casey, J.L. RNA editing of hepatitis delta virus antigenome by dsRNA-adenosine deaminase. *Nature* **1996**, *380*, 454–456.
51. Wong, S.K.; Lazinski, D.W. Replicating hepatitis delta virus RNA is edited in the nucleus by the small form of ADAR1. *Proc. Natl. Acad. Sci. USA* **2002**, *99*, 15118–15123.
52. Macnaughton, T.B.; Lai, M.M. Genomic but not antigenomic hepatitis delta virus RNA is preferentially exported from the nucleus immediately after synthesis and processing. *J. Virol.* **2002**, *76*, 3928–3935.
53. Wang, C.J.; Chen, P.J.; Wu, J.C.; Patel, D.; Chen, D.S. Small-form hepatitis B surface antigen is sufficient to help in the assembly of hepatitis delta virus-like particles. *J. Virol.* **1991**, *65*, 6630–6636.

54. Freitas, N.; Salisse, J.; Cunha, C.; Toshkov, I.; Menne, S.; Gudima, S.O. Hepatitis delta virus infects the cells of hepadnavirus-induced hepatocellular carcinoma in woodchucks. *Hepatology* **2012**, *56*, 76–85.
55. Giersch, K.; Helbig, M.; Volz, T.; Allweiss, L.; Mancke, L.V.; Lohse, A.W.; Polywka, S.; Pollok, J.M.; Petersen, J.; Taylor, J.; *et al.* Persistent hepatitis D virus mono-infection in humanized mice is efficiently converted by hepatitis B virus to a productive co-infection. *J. Hepatol.* **2014**, *60*, 538–544.
56. Davies, S.E.; Lau, J.Y.; O’Grady, J.G.; Portmann, B.C.; Alexander, G.J.; Williams, R. Evidence that hepatitis D virus needs hepatitis B virus to cause hepatocellular damage. *Am. J. Clin. Pathol.* **1992**, *98*, 554–558.
57. Sheldon, J.; Ramos, B.; Toro, C.; Rios, P.; Martinez-Alarcon, J.; Bottecchia, M.; Romero, M.; Garcia-Samaniego, J.; Soriano, V.; *et al.* Does treatment of hepatitis B virus (HBV) infection reduce hepatitis delta virus (HDV) replication in HIV-HBV-HDV-coinfected patients? *Antivir. Ther.* **2008**, *13*, 97–102.
58. Babiker, Z.O.; Hogan, C.; Ustianowski, A.; Wilkins, E. Does interferon-sparing tenofovir disoproxil fumarate-based therapy have a role in the management of severe acute hepatitis delta superinfection? *J. Med. Microbiol.* **2012**, *61*, 1780–1783.
59. Sureau, C. The use of hepatocytes to investigate HDV infection: The HDV/HepaRG model. *Methods Mol. Biol.* **2010**, *640*, 463–473.
60. Brazas, R.; Ganem, D. A cellular homolog of hepatitis delta antigen: Implications for viral replication and evolution. *Science* **1996**, *274*, 90–94.
61. Wang, Y.H.; Chang, S.C.; Huang, C.; Li, Y.P.; Lee, C.H.; Chang, M.F. Novel nuclear export signal-interacting protein, NESI, critical for the assembly of hepatitis delta virus. *J. Virol.* **2005**, *79*, 8113–8120.
62. Mota, S.; Mendes, M.; Penque, D.; Coelho, A.V.; Cunha, C. Changes in the proteome of Huh7 cells induced by transient expression of hepatitis D virus RNA and antigens. *J. Proteomics* **2008**, *71*, 71–79.
63. Mota, S.; Mendes, M.; Freitas, N.; Penque, D.; Coelho, A.V.; Cunha, C. Proteome analysis of a human liver carcinoma cell line stably expressing hepatitis delta virus ribonucleoproteins. *J. Proteomics* **2009**, *72*, 616–627.
64. Greco-Stewart, V.S.; Thibault, C.S.; Pelchat, M. Binding of the polypyrimidine tract-binding protein-associated splicing factor (PSF) to the hepatitis delta virus RNA. *Virology* **2006**, *356*, 35–44.
65. Sikora, D.; Greco-Stewart, V.S.; Miron, P.; Pelchat, M. The hepatitis delta virus RNA genome interacts with eEF1A1, p54(nrb), hnRNP-L, GAPDH and ASF/SF2. *Virology* **2009**, *390*, 71–78.
66. Williams, V.; Brichtler, S.; Khan, E.; Chami, M.; Dény, P.; Kremsdorf, D.; Gordien, E. Large hepatitis delta antigen activates STAT-3 and NF-kappaB via oxidative stress. *J. Viral Hepat.* **2012**, *19*, 744–753.
67. Choi, S.H.; Jeong, S.H.; Hwang, S.B. Large hepatitis delta antigen modulates transforming growth factor-beta signaling cascades: Implication of hepatitis delta virus-induced liver fibrosis. *Gastroenterology* **2007**, *132*, 343–357.
68. Pugnale, P.; Paziienza, V.; Guilloux, K.; Negro, F. Hepatitis delta virus inhibits alpha interferon signaling. *Hepatology* **2009**, *49*, 398–406.
69. Goto, T.; Kato, N.; Yoshida, H.; Otsuka, M.; Moriyama, M.; Shiratori, Y.; Koike, K.; Matsumura M.; Omata, M. Synergistic activation of the serum response element-dependent pathway by hepatitis B virus x protein and large-isoform hepatitis delta antigen. *J. Infect. Dis.* **2003**, *187*, 820–828.
70. Lo, K.; Sheu, G.T.; Lai, M.M. Inhibition of Cellular RNA polymerase II transcription by delta antigen of hepatitis delta virus. *Virology* **1998**, *247*, 178–188.

71. Yamaguchi, Y.; Filipovska, J.; Yano, K.; Furuya, A.; Inukai, N.; Narita, T.; Wada, T.; Sugimoto, S.; Konarska, M.M.; Handa, H. Stimulation of RNA polymerase II elongation by hepatitis delta antigen. *Science* **2001**, *293*, 124–127.
72. Liao, F.T.; Lee, Y.J.; Ko, J.L.; Tsai, C.C.; Tseng, C.J.; Sheu, G.T. Hepatitis delta virus epigenetically enhances clusterin expression via histone acetylation in human hepatocellular carcinoma cells. *J. Gen. Virol.* **2009**, *90*, 1124–1134.
73. Mendes, M.; Perez-Hernandez, D.; Vazquez, J.; Coelho, A.V.; Cunha, C. Proteomic changes in HEK-293 cells induced by hepatitis delta virus replication. *J. Proteomics* **2013**, *89*, 24–38.
74. Wang, D.; Pearlberg, J.; Liu, Y.T.; Ganem, D. Deleterious effects of hepatitis delta virus replication on host cell proliferation. *J. Virol.* **2001**, *75*, 3600–3604.
75. Heinicke, L.A.; Bevilacqua, P.C. Activation of PKR by RNA misfolding: HDV ribozyme dimers activate PKR. *RNA* **2012**, *18*, 2157–2165.
76. Negro, F.; Korba, B.E.; Forzani, B.; Baroudy, B.M.; Brown, T.L.; Gerin, J.L.; Ponzetto, A. Hepatitis delta virus (HDV) and woodchuck hepatitis virus (WHV) nucleic acids in tissues of HDV-infected chronic WHV carrier woodchucks. *J. Virol.* **1989**, *63*, 1612–1618.
77. Casey, J.L.; Gerin, J.L. The woodchuck model of HDV infection. *Curr. Top. Microbiol. Immunol.* **2006**, *307*, 211–225.
78. Caselmann, W.H. HBV and HDV replication in experimental models: Effect of interferon. *Antivir. Res.* **1994**, *24*, 121–129.
79. Kos, T.; Molijn, A.; van Doorn, L.J.; van Belkum, A.; Dubbeld, M.; Schellekens, H. Hepatitis delta virus cDNA sequence from an acutely HBV-infected chimpanzee: Sequence conservation in experimental animals. *J. Med. Virol.* **1991**, *34*, 268–279.
80. Negro, F.; Bergmann, K.F.; Baroudy, B.M.; Satterfield, W.C.; Popper, H.; Purcell, R.H.; Gerin, J.L. Chronic hepatitis D virus (HDV) infection in hepatitis B virus carrier chimpanzees experimentally superinfected with HDV. *J. Infect. Dis.* **1988**, *158*, 151–159.
81. Gerin, J.L. Animal models of hepatitis delta virus infection and disease. *ILAR J.* **2001**, *42*, 103–106.
82. Engelke, M.; Mills, K.; Seitz, S.; Simon, P.; Gripon, P.; Schnölzer, M.; Urban, S. Characterization of a hepatitis B and hepatitis delta virus receptor binding site. *Hepatology* **2006**, *43*, 750–760.
83. Drexler, J.F.; Geipel, A.; König, A.; Corman, V.M.; van Riel, D.; Leijten, L.M.; Bremer, C.M.; Rasche, A.; Cottontail, V.M.; Maganga, G.D.; *et al.* Bats carry pathogenic hepadnaviruses antigenically related to hepatitis B virus and capable of infecting human hepatocytes. *Proc. Natl. Acad. Sci. USA* **2013**, *110*, 16151–16156.
84. Zhong, G.; Yan, H.; Wang, H.; He, W.; Jing, Z.; Qi, Y.; Fu, L.; Gao, Z.; Huang, Y.; Xu, G.; *et al.* Sodium taurocholate cotransporting polypeptide mediates woolly monkey hepatitis B virus infection of Tupaia hepatocytes. *J. Virol.* **2013**, *87*, 7176–7184.
85. Walter, E.; Keist, R.; Niederost, B.; Pult, I.; Blum, H.E. Hepatitis B virus infection of tupaia hepatocytes *in vitro* and *in vivo*. *Hepatology* **1996**, *24*, 1–5.
86. Li, Q.; Ding, M.; Wang, H. The infection of hepatitis D virus in adult tupaia. *Zhonghua Yi Xue Za Zhi* **1995**, *75*, 611–613, 639–640.
87. Ponzetto, A.; Hoyer, B.H.; Popper, H.; Engle, R.; Purcell, R.H.; Gerin, J.L. Titration of the infectivity of hepatitis D virus in chimpanzees. *J. Infect. Dis.* **1987**, *155*, 72–78.
88. Chen, P.J.; Yang, P.M.; Chen, C.R.; Chen, D.S. Characterization of the transcripts of hepatitis D and B viruses in infected human livers. *J. Infect. Dis.* **1989**, *160*, 944–947.

89. Karayiannis, P.; Goldin, R.; Luther, S.; Carman, W.F.; Monjardino, J.; Thomas, H.C. Effect of cyclosporin-A in woodchucks with chronic hepatitis delta virus infection. *J. Med. Virol.* **1992**, *36*, 316–321.
90. Karayiannis, P.; Saldanha, J.; Monjardino, J.; Jackson, A.; Luther, S.; Thomas, H.C. Immunisation of woodchucks with hepatitis delta antigen expressed by recombinant vaccinia and baculoviruses, controls HDV superinfection. *Prog. Clin. Biol. Res.* **1993**, *382*, 193–199.
91. Fiedler, M.; Lu, M.; Siegel, F.; Whipple, J.; Roggendorf, M. Immunization of woodchucks (*Marmota monax*) with hepatitis delta virus DNA vaccine. *Vaccine* **2001**, *19*, 4618–4626.
92. Fiedler, M.; Roggendorf, M. Vaccination against hepatitis delta virus infection: Studies in the woodchuck (*Marmota monax*) model. *Intervirology* **2001**, *44*, 154–161.
93. Fiedler, M.; Kosinska, A.; Schumann, A.; Brovko, O.; Walker, A.; Lu, M.; Johrden, L.; Mayer, A.; Wildner, O.; Roggendorf, M. Prime/boost immunization with DNA and adenoviral vectors protects from hepatitis D virus (HDV) infection after simultaneous infection with HDV and woodchuck hepatitis virus. *J. Virol.* **2013**, *87*, 7708–7716.
94. D’Ugo, E.; Paroli, M.; Palmieri, G.; Giuseppetti, R.; Argentini, C.; Tritarelli, E.; Bruni, R.; Barnaba, V.; Houghton, M.; Rapicetta, M. Immunization of woodchucks with adjuvanted sHDAg (p24): Immune response and outcome following challenge. *Vaccine* **2004**, *22*, 457–466.
95. Govindarajan, S.; Fields, H.A.; Humphrey, C.D.; Margolis, H.S. Pathologic and ultrastructural changes of acute and chronic delta hepatitis in an experimentally infected chimpanzee. *Am. J. Pathol.* **1986**, *122*, 315–322.
96. Cole, S.M.; Macnaughton, T.B.; Gowans, E.J. Differential roles for HDAg-p24 and -p27 in HDV pathogenesis. *Prog. Clin. Biol. Res.* **1993**, *382*, 131–138.
97. Guilhot, S.; Huang, S.N.; Xia, Y.P.; La Monica, N.; Lai, M.M.; Chisari, F.V. Expression of the hepatitis delta virus large and small antigens in transgenic mice. *J. Virol.* **1994**, *68*, 1052–1058.
98. Polo, J.M.; Jeng, K.S.; Lim, B.; Govindarajan, S.; Hofman, F.; Sangiorgi, F.; Lai, M.M. Transgenic mice support replication of hepatitis delta virus RNA in multiple tissues, particularly in skeletal muscle. *J. Virol.* **1995**, *69*, 4880–4887.
99. Grompe, M.; Strom, S. Mice with human livers. *Gastroenterology* **2013**, *145*, 1209–1214.
100. Navarro, B.; Gisel, A.; Rodio, M.E.; Delgado, S.; Flores, R.; Di Serio, F. Viroids: How to infect a host and cause disease without encoding proteins. *Biochimie* **2012**, *94*, 1474–1480.
101. Chen, P.J.; Kuo, M.Y.; Chen, M.L.; Tu, S.J.; Chiu, M.N.; Wu, H.L.; Hsu, H.C.; Chen, D.S. Continuous expression and replication of the hepatitis delta virus genome in Hep G2 hepatoblastoma cells transfected with cloned viral DNA. *Proc. Natl. Acad. Sci. USA* **1990**, *87*, 5253–5257.
102. Kuo, M.Y.; Chao, M.; Taylor, J. Initiation of replication of the human hepatitis delta virus genome from cloned DNA: Role of delta antigen. *J. Virol.* **1989**, *63*, 1945–1950.
103. Sureau, C.; Taylor, J.; Chao, M.; Eichberg, J.W.; Lanford, R.E. Cloned hepatitis delta virus cDNA is infectious in the chimpanzee. *J. Virol.* **1989**, *63*, 4292–4297.
104. Wu, J.C.; Chen, T.Z.; Huang, Y.S.; Yen, F.S.; Ting, L.T.; Sheng, W.Y.; Tsay, S.H.; Lee, S.D. Natural history of hepatitis D viral superinfection: Significance of viremia detected by polymerase chain reaction. *Gastroenterology* **1995**, *108*, 796–802.
105. Dienes, H.P.; Purcell, R.H.; Popper, H.; Ponzetto, A. The significance of infections with two types of viral hepatitis demonstrated by histologic features in chimpanzees. *J. Hepatol.* **1990**, *10*, 77–84.
106. Polo, J.M.; Lim, B.; Govindarajan, S.; Lai, M.M. Replication of hepatitis delta virus RNA in mice after intramuscular injection of plasmid DNA. *J. Virol.* **1995**, *69*, 5203–5207.

107. Chang, J.; Sigal, L.J.; Lerro, A.; Taylor, J. Replication of the human hepatitis delta virus genome is initiated in mouse hepatocytes following intravenous injection of naked DNA or RNA sequences. *J. Virol.* **2001**, *75*, 3469–3473.
108. Lin, Y.J.; Huang, L.R.; Yang, H.C.; Tzeng, H.T.; Hsu, P.N.; Wu, H.L.; Chen, P.J.; Chen, D.S. Hepatitis B virus core antigen determines viral persistence in a C57BL/6 mouse model. *Proc. Natl. Acad. Sci. USA* **2010**, *107*, 9340–9345.
109. Huang, L.R.; Gäbel, Y.A.; Graf, S.; Arzberger, S.; Kurts, C.; Heikenwalder, M.; Knolle, P.A.; Protzer, U. Transfer of HBV genomes using low doses of adenovirus vectors leads to persistent infection in immune competent mice. *Gastroenterology* **2012**, *142*, 1447–1450.
110. Xia, Y.; Zeng, D.; Yu, F.; He, J.; Zhou, Z.; Tu, W.; Deng, H.; Tian, D.A.; Liu, M. Role of autophagy in monokine induced by interferon gamma (Mig) production during adenovirus-hepatitis B virus infection. *Hepatogastroenterology* **2012**, *59*, 1245–1250.
111. Dion, S.; Bourguin, M.; Godon, O.; Levillayer, F.; Michel, M.L. Adeno-associated virus-mediated gene transfer leads to persistent hepatitis B virus replication in mice expressing HLA-A2 and HLA-DR1 molecules. *J. Virol.* **2013**, *87*, 5554–5563.
112. Huang, Y.H.; Fang, C.C.; Tsuneyama, K.; Chou, H.Y.; Pan, W.Y.; Shih, Y.M.; Wu, P.Y.; Chen, Y.; Leung, P.S.; Gershwin, M.E.; *et al.* A murine model of hepatitis B-associated hepatocellular carcinoma generated by adeno-associated virus-mediated gene delivery. *Int. J. Oncol.* **2011**, *39*, 1511–1519.

© 2015 by the authors; licensee MDPI, Basel, Switzerland. This article is an open access article distributed under the terms and conditions of the Creative Commons Attribution license (<http://creativecommons.org/licenses/by/4.0/>).